NTNU
Norwegian University of Science and Technology

Concrete Plates Designed with FEM

Prosjektering av betongplater med FEM

Marte Skibeli

Civil and Environmental Engineering
Submission date: June 2017
Supervisor: Jan Arve Øverli, KT

Norwegian University of Science and Technology
Department of Structural Engineering

Department of Structural Engineering
Faculty of Engineering
NTNU- Norwegian University of Science and Technology

MASTER THESIS 2017

SUBJECT AREA:	DATE:	NO. OF PAGES:
Concrete structures	6th of June, 2017	110+12 pages of appendices

TITLE:

Concrete Plates Designed with FEM

Prosjektering av betongplater med FEM

BY:

Marte Skibeli

SUMMARY:
Most engineering companies design plates by use of finite element programs that are entirely automated. The program decides the element type, the meshing, and performs all the calculations. Often, the automatic procedure is hidden for the user, and it's difficult for the engineer to verify that the analysis is done correctly. Therefore, the goal of this thesis is to describe how concrete plates should be modelled in commercial design software, and how a selection of design programs perform the automatic design procedure. The focus has been on plates subjected primarily to bending in both the Ultimate Limit State (ULS) and in the Serviceability Limit State (SLS).

It is normally recommended to model plates with the use of pinned support at the centre of columns or walls, because it avoids unintended rotational restraint. It is, however, also possible to model more realistically, with spring supports, if the stress distribution over the support is of interest, or the rotational restraint from the support is of importance for the stresses in the plate.

The main problem of plate design is that, in contrast to simple beam theory, plates also contain twisting moments. This causes the reinforcement and the principal moments to be in different directions.
An essential difference between the design procedures in the programs is the assumptions for the stress distribution in the cross section, and the internal lever arm. The programs are also separated by the way they define the crack angle.

In SLS, the programs differ in the way the stiffness reduction due to cracks is accounted for. One alternative is to reduce the stiffness locally in elements where the concrete is cracked. Another alternative is to give the whole plate a reduced stiffness to achieve a smooth deformation pattern. The crack width is controlled by either direct calculation of the crack width, or indirect calculation where the diameter and spacing of the reinforcement bars are controlled.

RESPONSIBLE TEACHER: Jan Arve Øverli

SUPERVISOR(S): Jan Arve Øverli

CARRIED OUT AT: Department of Structural Engineering, NTNU

Preface

This master thesis is written from January to June 2017 for the Department of Structural Engineering, NTNU, Trondheim.

Numerical calculations based on the finite-element method (FEM) have become a powerful tool for structural engineers when designing structures. Although the method can do complex calculations, it is important to remember that the results are no better than the input from the structural engineer. That is why this thesis will describe how to successfully model plates with FEM using various loads, boundary conditions, and geometry. The second part will focus on different methods that commercial software use in the automatic design of- and capacity control of concrete plates.

I would like to thank my supervisor Jan Arve Øverli for guidance and support, and also Ola Hansen and Trygve Skibeli for proofreading, and helpful comments.

Marte Skibeli

Marte Skibeli

Trondheim, 6th of June, 2017

Summary

Most engineering companies design plates by use of finite element programs that are entirely automated. The program decides the element type, the meshing, and performs all the calculations. Often, the automatic procedure is hidden for the user, and it's difficult for the engineer to verify that the analysis is done correctly. Therefore, the goal of this thesis is to describe how concrete plates should be modelled in commercial design software, and how a selection of design programs perform the automatic design procedure. The focus has been on plates subjected primarily to bending in both the Ultimate Limit State (ULS) and in the Serviceability Limit State (SLS).

When modelling a plate, the element type and mesh are often defined automatically by the software while the boundary conditions need to be specified by the user. It is normally recommended to use pinned support at the centre of columns or walls, because it avoids unintended rotational restraint. It is, however, also possible to model more realistically, with spring supports, if:

- The stress distribution over the support is of interest

- The rotational restraint from the support is of importance for the stresses in the plate.

The theory background and manuals for a chosen set of design programs were examined to figure out how the automatic design procedure for concrete plates can be carried out. The main problem of plate design is that, in contrast to simple beam theory, plates also contain twisting moments. This causes the reinforcement and the principal moments to be in different directions. The main steps of the design procedure in ULS are to rotate the stress resultants to the directions of the reinforcement, and then calculate either the

design moments, or imaginary in-plane forces. These forces are then used to find the required reinforcement for the upper and lower layer of the plate.

An essential difference between the programs is the assumptions for the stress distribution in the cross section, and the internal lever arm. The programs are also separated by the way they define the crack angle. Normally, the crack angle is assumed to be 45° in order to achieve a minimum amount of reinforcement. If, however, only one reinforcement direction is needed, the optimal crack angle is no longer 45°. In that case, some of the programs, like "FEM design", calculates a new optimal crack angle.

In SLS, the programs differ in the way the stiffness reduction due to cracks is accounted for. One alternative is to reduce the stiffness locally in elements where the concrete is cracked. Another alternative is to give the whole plate a reduced stiffness to achieve a smooth deformation pattern. The crack width is controlled by either of the following two approaches:

- Direct calculation of the crack width, and comparing this with the maximum allowed width

- Indirect calculation where the diameter and spacing of the reinforcement bars are controlled against tabulated maximum values

Sammendrag

Ved prosjektering av betongdekker blir som regel helautomatiserte elementmetodeprogrammer benyttet i utregningene. Ofte bestemmer programmene både elementtype og elementinndeling, og gjør hele utregningen. Hvordan denne prosessen foregår er ofte skjult for brukeren, og det blir vanskelig å verifisere at analysen er utført på rett måte. Målet med denne oppgaven er derfor å beskrive hvordan betongplater bør modelleres i dataprogrammer for prosjektering, og hvordan noen utvalgte programmer velger å løse den automatiske prosjekteringsprosessen. Fokuset i denne oppgaven er plater som hovedsakelig utsettes for bøyning både i brudd- og bruksgrensetilstand.

Når et betongdekke skal modelleres tilbyr som regel programmene automatisk valg av elementtype og elementinndeling, men opplagere må brukeren definere selv. For å unngå utilsiktet fastholdning mot rotasjon anbefales det vanligvis å bruke fritt opplager plassert midt på en søyle eller vegg. Det er også mulig å modellere mer realistisk, for eksempel ved bruk av fjærer, hvis:

- Den faktiske spenningsfordelingen i platen over søylen/veggen er av interesse

- Rotasjonsmotstanden fra opplageret gir store utslag på spenningene i platen

Hvordan programmene automatiserer prosjekteringsprosessen er studert gjennom å lese manualene og teorigrunnlaget bak de utvalgte prosjekteringsprogrammene. Hovedproblemet med å prosjektere plater, sammenlignet med bjelker, er at plater inneholder torsjonsmomenter. Det gjør at plater ikke får sammenfallende armerings- og hovedmomentsretninger. Hovedtrinnene i plateprosjektering går i grove trekk ut på å rotere spenningsresultantene til de gitte armeringsretningene, for deretter å finne dimensjonerende moment eller imaginære krefter i armeringsplanet. Til slutt beregnes nødvendig armeringsmengde i øvre og nedre lag i

platen.

En viktig forskjell mellom de ulike programmene er hvordan de antar trykkspenningsfordelingen i tverrsnittet, og dermed hva den indre momentarmen blir. I tillegg utgjør definisjonen av rissvinkelen en stor forskjell. Normalt sett gir en valgt rissvinkel på 45° minimal armeringsmengde, men dersom det kun er nødvendig med armering i én retning, så er ikke lenger 45° rissvinkel optimalt. Noen av programmene, som for eksempel "FEM design" beregner da en ny optimal rissvinkel.

I bruksgrensetilstand bruker programmene forskjellige metoder for å ta hensyn til reduksjon i stivheten på grunn av rissdannelse. Noen av programmene endrer stivheten lokalt i elementer der det er for høy spenning, mens andre gir hele platen redusert stivhet slik at nedbøyningen blir jevn over platen. Rissvidden blir kontrollert ved en av de to følgende metodene:

- Direkte utregning, og kontroll opp mot maksimal lovlig rissvidde

- Indirekte utregning hvor stangdiameteren og avstanden mellom armeringsstengene kontrolleres opp mot maksimalt tillate verdier fra tabell

Contents

List of Figures

Chapter 1

Introduction

Concrete plates are commonly used in structures such as bridges and buildings, from the smallest cabin to the tallest skyscraper. Figure 1.1 and Figure 1.2 show some examples of concrete structures.

Figure 1.1: Example of a bridge with concrete bridge decks [1]

Figure 1.2: Example of precast concrete slabs in a building [2]

Concrete plates can either be prefabricated, which makes the building process very effective, or cast-in-place, which makes it possible to create almost all the shapes that a creative architect may wish for. Consequently, concrete plates are appealing to use, and structural engineers need to know how to design these plates. The main focus of this thesis will be on design of concrete plates subjected primarily to bending, such as building floors and bridge decks. Design for shear will be commented briefly; however, punching shear has intentionally been left out.

The commercial design software packages available today offer almost endless possibilities for modelling, and good graphic design makes it intuitive for the structural engineer to model an arbitrary structure. However, since design software use the Finite Element Method (FEM), which is an approximate numerical method, it is important to know what assumptions are made and how they affect the results. Therefore, this master thesis will describe how to model a concrete plate to achieve proper stress resultants, and how design software automates the plate design.

The first part of the thesis discusses how to model plates to achieve accurate results for the internal forces, by correct choice of support conditions, material parameters, mesh fineness, element type and load application.

The second part of the thesis is about the design procedure for concrete plates. Some of the design alternatives that are useful for hand calculations are [7]:

- The strip method: A lower-bound design method, where it is assumed that the load on a plate is dispersed in a certain way in the plate such that the design can be obtained from a representative set of plate strips. The design forces in the strips can be calculated with beam theory, and the required reinforcement is found according to a design code.

- The equivalent frame method: For design of slabs supported by columns. Here, the plate strips, with center lines above the columns, are regarded as the frame system, and the maximum and minimum moments are found by calculating a strip in each

span direction according to beam theory. The strip width is normally assumed to be equal to the perpendicular span length. Then, the design moments are distributed in the perpendicular direction into field strips, outer column strips, and an inner column strip. Each of these sub-strips are designed separately according to codes.

- The yield line method: Suited for capacity control, in which plastic behaviour is assumed. The yield lines behave as hinges which carry the constant ultimate moment of resistance. By use of the virtual work method, the capacity of the different yield line patterns are found. The yield line pattern with the lowest capacity gives the dimensioning load capacity. This is an upper-bound approach to find the load capacity

Even though all the design methods mentioned above can be useful methods, they are not suited for automatic design in programs. The focus in this thesis will be on design methods which allow for automatic design performed by software. Chapter 3 will describe the theory of elasticity and the sandwich model because they are used as basis for the design in numerous design software. Then, in chapter 4, some commercially available FEM software will be examined to figure out what design procedure they operate with. Lastly, chapter 5 consists of a simple calculation example on a beam, in order to compare the different procedures.

Before discussing details about plate design, it is considered necessary to include information about the assumptions that are made for plates. Plates in general are planar, spatial structures that have sides that are at least five times greater than the plate thickness [8]. A plate can either be in the membrane state with only in-plane forces, or in the bending state with only out-of-plane forces [3]. A concrete plate in the bending state is called a slab, and normally the following assumptions are made [6]:

- Constant thickness

- The material is homogeneous and isotropic

- Only small vertical displacements (first order theory apply)

- No membrane forces

- Linear strain distribution over the section depth. The mid-plane remains strain-less after loading

- Plane sections normal to the mid-plane remain plane after loading

- Stresses in the normal direction, σ_{zz}, are zero

- The strain, ϵ_{zz}, is set to zero. Possible small differences in the displacement over the thickness of the slab are neglected

The stress resultants for slabs are bending moments in the x- and y-direction, twisting moments, and vertical shear forces in each direction, as can be seen in Figure 1.3. All of these internal forces are given per unit length. For thin plates, the shear deformation is neglected, hence the shear stresses, τ_{xz} and τ_{yz}, are set to zero. If that is the case, the shear forces must be derived from the moments rather than by integrating shear stresses.
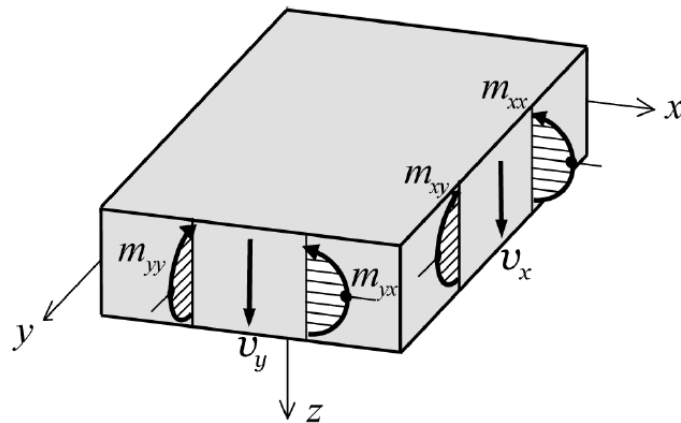
Figure 1.3: Stress resultants in a slab [3]

Chapter 2

FEM modelling of plates

2.1 General

Before going into details about finite-element modelling, a brief introduction will be given
to the basics of the Finite Element Method (FEM). The first step is to subdivide the
structure into a finite number of elements. Some of the standard elements that exists
in commercial software packages today are shown in Figure 2.1. Each element has a set
of nodes associated with them, in which you find generalized forces corresponding to the
Degrees Of Freedom (DOF) in the node. All elements are connected to the neighbouring
elements by enforcing compatibility and equilibrium in the shared nodes. For plates in
bending, it is common to use plane elements with three DOFs per node, one for vertical
displacement and two for rotation around the x- and y-axis respectively, as shown in
Figure 2.2.

Element type	Degrees of freedom	Representation
Mass	—	
2D bar	u, v	
2D beam	v, θ_z	
2D continuum plane stress plane strain axisymmetric	u, v	
2D interface	u, v	
Axisymmetric shell	u, v, θ_z	
3D bar	u, v, w	
3D beam	v, v, w $\theta_x, \theta_y, \theta_z$	
3D solid	u, v, w	
3D shell	u, v, w $\theta_x, \theta_y, \theta_z$	
3D interface	u, v, w	

Figure 2.1: Typical elements in commercial software packages [4]
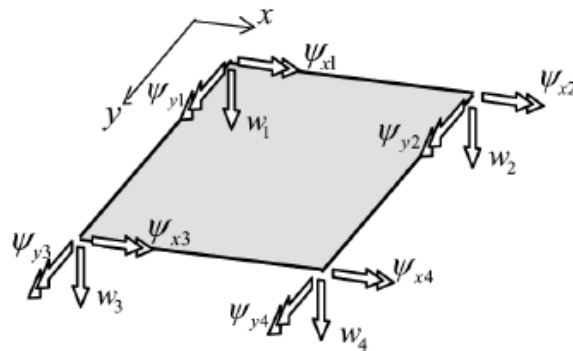
Figure 2.2: Degrees of freedom for a plate element [3]

The deformation field inside an element is determined by use of shape functions that connect the nodal deformations. To illustrate what shape functions may look like, a bar element with three nodes and the associated shape functions are showed in Figure 2.3. The shape function, N_1, is a function that is equal to 1 in node 1, and 0 in the other nodes. N_2 is 1 in node 2, and 0 in the other nodes, and so on [4].
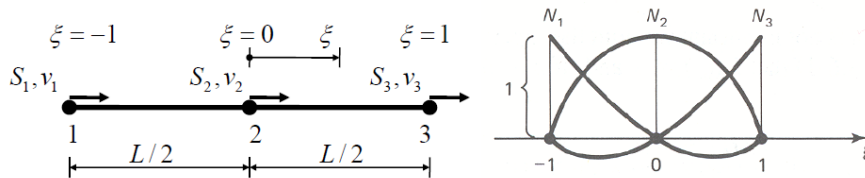
Figure 2.3: Example of shape functions for a bar element with three nodes [4]

The deformations are connected to the nodal forces by a stiffness matrix which helps predict the structural behaviour of the element. The stiffness matrix is found by performing a numerical integration with integration points inside the element. The integral is solved by summarizing the values at these integration points and giving each value a specific weight. For example, if an element has only one integration point, that value would be fully weighted, while with two integration points each value would get half the weight. Figure 2.4 illustrates the difference between analytical integration and numerical integration with two integration points.
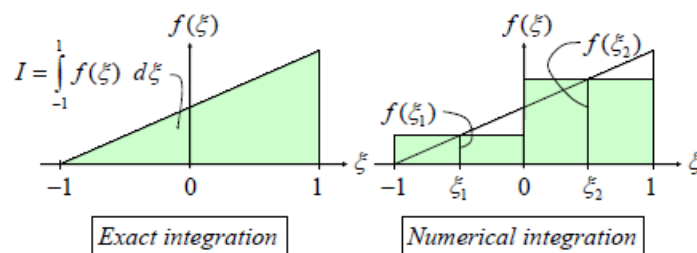
Figure 2.4: Analytical integration (left) and numerical integration with two integration points (right) [4]

The most common integration points to use are the Gaussian points. The location of each Gaussian point, and the weighing of the values can be found in tables; however, this operation is automatically done by the software. The reason why we use integration points inside the element instead of the values in the nodes, is that the stresses and strains are more accurate at the integration points. For more detailed information about the theory of FEM, see for example Hughes [13].

The recommendations for the modelling of plates (using FEM) is based on the recommendations presented by Rombach [5], and Pacoste, Plos, and Johansson [6].

2.2 Material behaviour

The response of concrete slabs in bending is highly non-linear due to the cracking and crushing of concrete and yielding of reinforcement. Nevertheless, it is normal to assume linear-elastic material behaviour in order to simplify the analysis, and to be able to use the superposition principle when evaluating the effects of different load cases [6]. The end result might, however, end up with unrealistic concentrations of moments and forces due to this simplification. It is therefore important to be aware of this effect in the design to avoid unnecessary high amounts of reinforcement.

According to the lower-bound theorem of plasticity, linear-elastic analysis can be justified for the Ultimate Limit State (ULS). The theorem states that if a load on a structure causes a stress distribution which is within the yield limits, and satisfies both the equilibrium and statical boundary conditions, then this stress distribution is called safe and statically admissible, and can't cause collapse of the body [14]. In linear-elastic analysis, all parts of the structure will always satisfy both equilibrium and statical boundary conditions; hence, linear-elastic assumption is always on the safe side when all the stresses present are below the yield stress.

Even though there are some cracks in the concrete which will lead to redistribution of forces, the assumption of linear-elasticity is considered acceptable in the Serviceability Limit State (SLS) because the redistribution of stresses is so limited that it can be neglected [6].

2.3   Material parameters

Based on the assumption that slabs have linear-elastic isotropic material behaviour, only two material parameters are necessary in the design. That is the modulus of elasticity, E, and the Poisson's ratio, ν. The modulus of elasticity, including creep effects, can be found either from tests, Eurocode 2 (EC2) [8], or other codes for concrete structures. The Poisson's ratio is defined as the ratio between the lateral and the axial strain, and varies between $\nu = 0.0$ and $\nu = 0.2$ for concrete. Figure 2.5 illustrates how deflection in one direction leads to deflection in the other for $\nu \neq 0.0$. The effect of Poisson's ratio on the curvature of an elementary block can be seen from Figure 2.6. The curvature, κ, in one direction will lead to an additional curvature in the transversal direction equal to $\nu \times \kappa$. Figure 2.7 shows a deformation model from the program "FEM design" where a plate is simply supported at the short edges and subjected to edge moments along the supports. It can clearly be observed that when $\nu > 0$, the plate gets an additional curvature in the transverse direction.
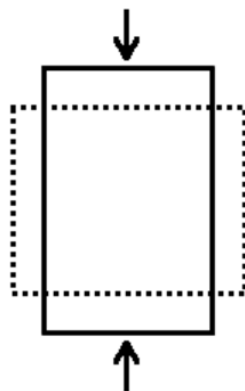
Figure 2.5: Effect of Poisson's ratio on an element in compression
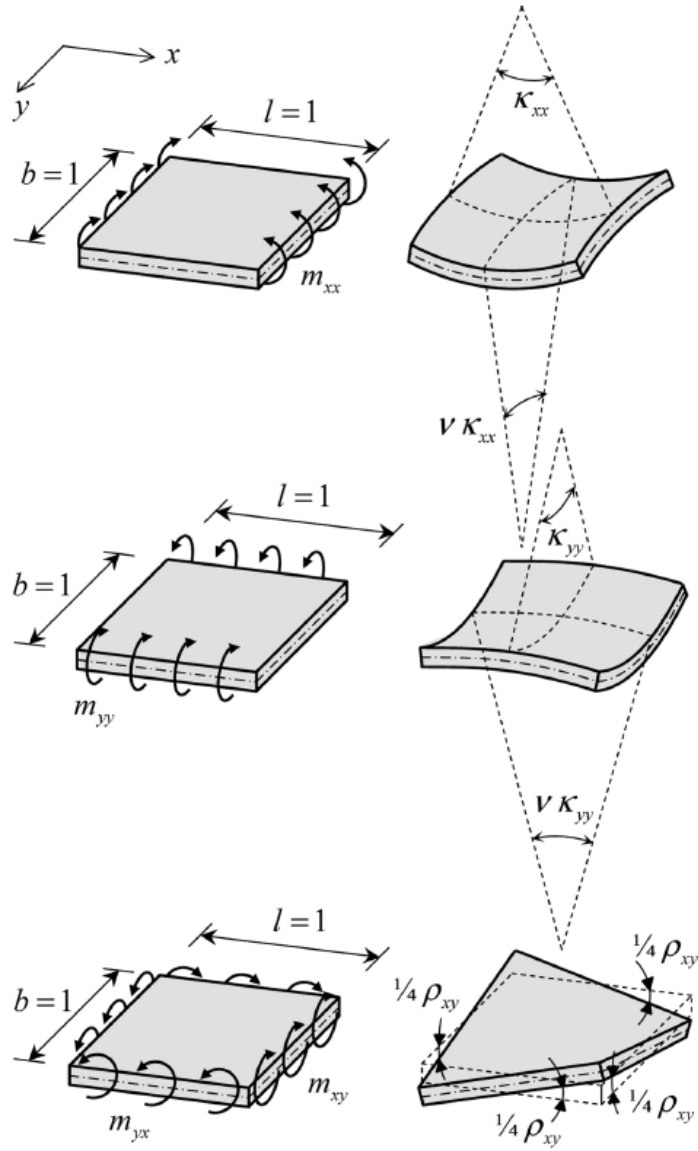
Figure 2.6: Moments and curvatures for non-zero Poisson's ratio [3]
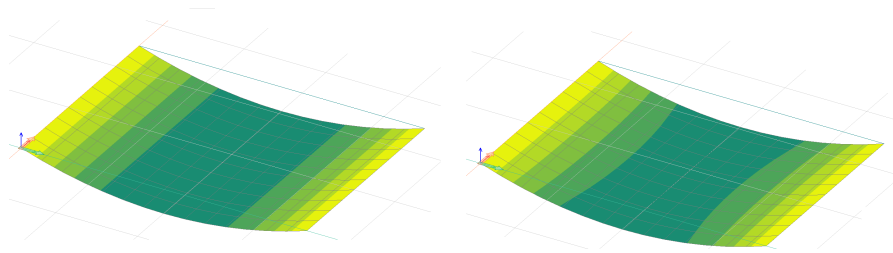
Figure 2.7: Deformation for $\nu=0$ (left) and $\nu > 0$ (right)

According to EC2 section 3.1.3(4), the Poisson's ratio should be set to 0.2 for uncracked concrete, and 0.0 for cracked concrete. The reason for the reduction in the Poisson's ratio when the concrete is cracked is that the tensile forces in the reinforcement can't be transmitted through the cracked concrete from one direction to another, so each direction works independently of each other.

An example of how Poisson's ratio can affect the results of the internal forces in a simply supported slab, with uniform loading, can be found in a parametric study done by Rombach [5]. The slab in the example has dimensions $l_x = 5.0$ m, $l_y = 5.0/7.5$ m, and h = 0.2 m. The results are shown in Figure 2.8 below.
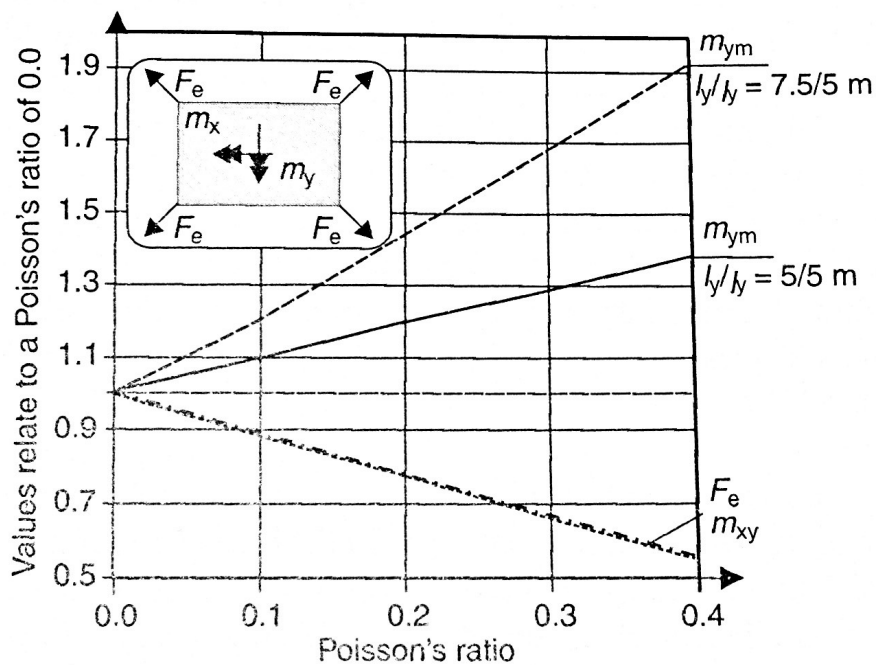
Figure 2.8: Bending moment, m_y, twisting moment, m_{xy}, and corner tie-down force, F_e, for different Poisson's ratios ν [5]

It can be seen from Figure 2.8, on the previous page, that the mid-span bending moment in the longitudinal direction of the plate, m_{ym}, increases almost linearly with increasing Poisson's ratio. The greater the l_y/l_x ratio is, the greater the effect of the Poisson's ratio is on the bending moment, m_{ym}. This can also be seen from the approximate formulations of the internal bending moments according to the Kirchhoff theory, shown in Eqs. (2.1) and (2.2). If one side of the plate is much longer than the other, the shorter direction is stiffer; hence, it will attract greater moment, and the contribution from this moment, $\nu \times m_x^{\nu=0}$, can be significant for the relatively low bending moment in the longitudinal direction, m_{ym}. Hence, the greater the l_y/l_x ratio is, the more the Poisson's ratio will affect the longitudinal bending moment.

$$m_x \approx m_x^{\nu=0} + \nu \times m_y^{\nu=0} \tag{2.1}$$

$$m_y \approx m_y^{\nu=0} + \nu \times m_x^{\nu=0} \tag{2.2}$$

Figure 2.8 also shows that with increased Poisson's ratio, the twisting moment, m_{xy}, and the corner tie-down force, F_e, will decrease linearly. This is also in accordance with Kirchhoff's theory formulation for m_{xy} and F_e shown in Eqs. (2.3) and (2.4) respectively, where K is the flexural rigidity of the slab, and w is the deflection of the slab.

$$m_{xy} = -K \times (1 - \nu) \times (\frac{\partial^2 w}{\partial xy^2}) \tag{2.3}$$

$$F_e = 2 \times m_{xy} \tag{2.4}$$

The bending moment in the transverse direction, and the shear forces are not included in Figure 2.8, because the Poisson's ratio have only limited effect on them [5].

In order to control the results presented by Rombach [5], the FEM design software "FEM design" is used to model a simply supported plate with the dimension 5x7 m being subjected to a surface load of 10 kN/m². The results are shown in Figure 2.9, where m_{xx} is the moment working in the longitudinal direction, and m_{yy} in the transverse direction.

As expected, the moment in the transverse direction, m_{yy}, is greater than the longitudinal moment, and it doesn't change much for different Poisson's ratio. The moment in the longitudinal direction, m_{xx}, on the other hand changes approximately 45% when the Poisson's ratio changes from $\nu = 0$ to $\nu = 0.2$. This result corresponds well with the graph in Figure 2.8.
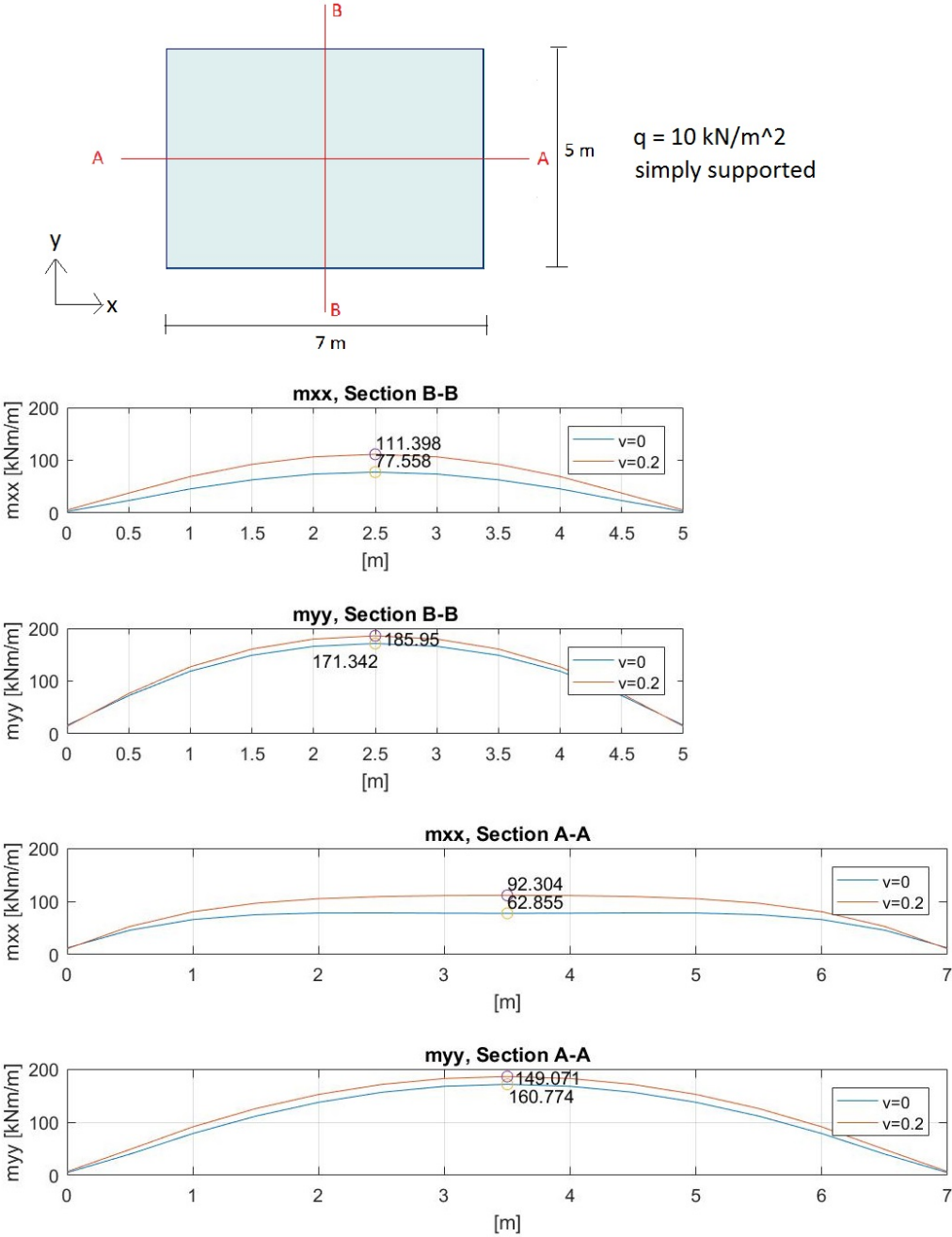
Figure 2.9: Bending moments, m_y and m_x, for different Poisson's ratios ν

2.4 Kirchhoff- and Mindlin-Reissner plates

When creating a FEM plate model, it is important to do a deliberate choice between the Kirchhoff theory and the Mindlin-Reissner theory. Although most commercial FEM software have one of these theories as default, it does not mean that this assumption is correct for all structural analysis. This chapter will point out the characteristics for both theories. Mindlin-Reissner theory is usually referred to as Mindlin theory in FE codes, and this shorter name will therefore be used hereafter.

Both theories follow the needle hypothesis which implies that if you have a straight needle perpendicular to the mid-plane of the plate, the needle will remain straight after loading. Moreover, if the shear force is neglected, the needle will also remain perpendicular to the mid-plane of the plate. The latter is true only for Kirchhoff theory. Mindlin theory accounts for shear deformations in the plate, and consequently the shear deformations might tilt the needle in the x- and/or the y-direction, see Figure 2.10 [3].
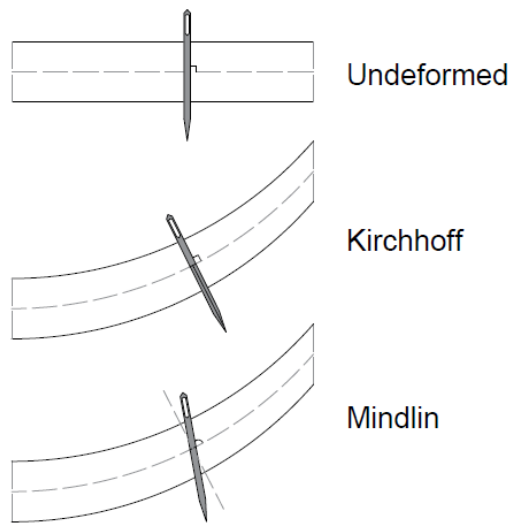
Figure 2.10: Comparison of Mindlin and Kirchhoff deformation

When the internal forces in a free- or simply supported edge is studied, an important difference between the two theories becomes clear. Figure 2.11 illustrates how the the shear force, v_x, and the twisting moment, m_{xy}, behaves on a free edge. In a distance approximately equal to the plate thickness, the twisting moment has to "turn around" as illustrated in the top section of Figure 2.11.

Kirchhoff theory handles this by keeping m_{xy} constant up to the edge, and then replacing all the vertical stresses with a concentrated shear force, V, at the very edge. The concentrated shear force will have the same numerical value as the twisting moment, m_{xy}.

Mindlin theory on the other hand, manage to achieve zero twisting moment at the edges (as it should be), by decomposing the shear stresses into decreasing horizontal stresses and increasing vertical forces. In order to detect this effect, the edge zone should be modelled with at least five elements over this short distance [3].
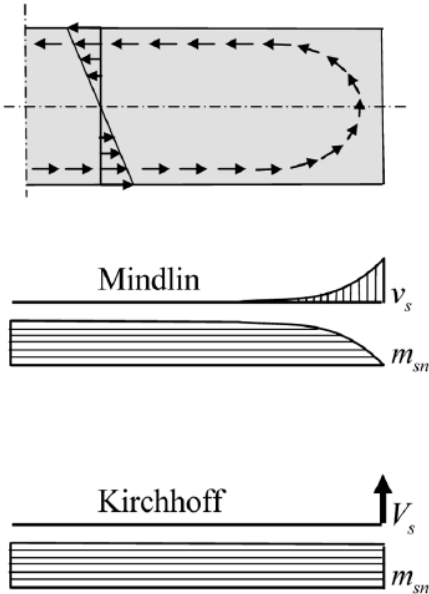
Figure 2.11: Comparison of Mindlin and Kirchhoff stresses on a free edge [3]

After this discussion, Mindlin theory might always seem like the correct choice. However, this is not the case for thin plates, where the edge zone is very small, because then Mindlin theory requires an unreasonably fine mesh to be able to get accurate results. Moreover, if Mindlin theory is used on thin plates, shear locking might be a problem. Shear locking is an error that occurs in linear, quadrilateral elements due to the fact that they fail to correctly model curvatures of elements, see Figure 2.12. Since the real curvature is restrained, spurious shear stresses will occur, and the plate will seem stiffer than it is in reality, and therefore underestimate the displacements. This is only a problem for Mindlin elements, because Kirchhoff elements ignore the spurious shear strains. The thinner the plate, the more curvature, and the more erroneous the results will be [4].
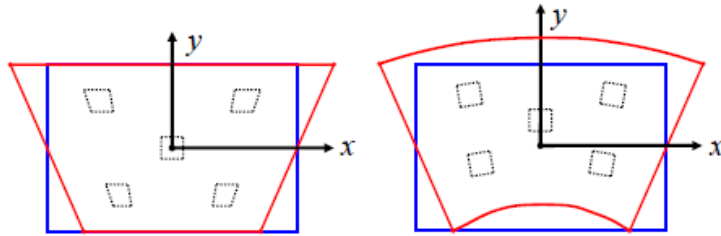
Figure 2.12: Linear element (left) and real curvature (right) [4]

Consequently, if the plate is thin enough to neglect shear deformations, one should use Kirchhoff theory. A span-thickness ratio l/t > 10 is sufficient to neglect the shear deformations [3].

2.5 Modelling of support conditions

Modelling of the support conditions for slabs should be done with great care as it has a significant effect on the results. How to model line supports and column supports correctly, for both hinged- and monolithic connections, is therefore discussed in detail in this chapter. The recommendations will be simplifications of the real structure, and it is important that the structural engineer is aware of this, and how it will affect the results.

2.5.1 Line supports

The connection between a slab and a continuous wall can be modelled in several ways depending on:

- The rotational stiffness of the connection

- The thickness of the slab

- The goal of the analysis

Figure 2.13 shows some of the modelling options that are most commonly used for hinged line supports [6].
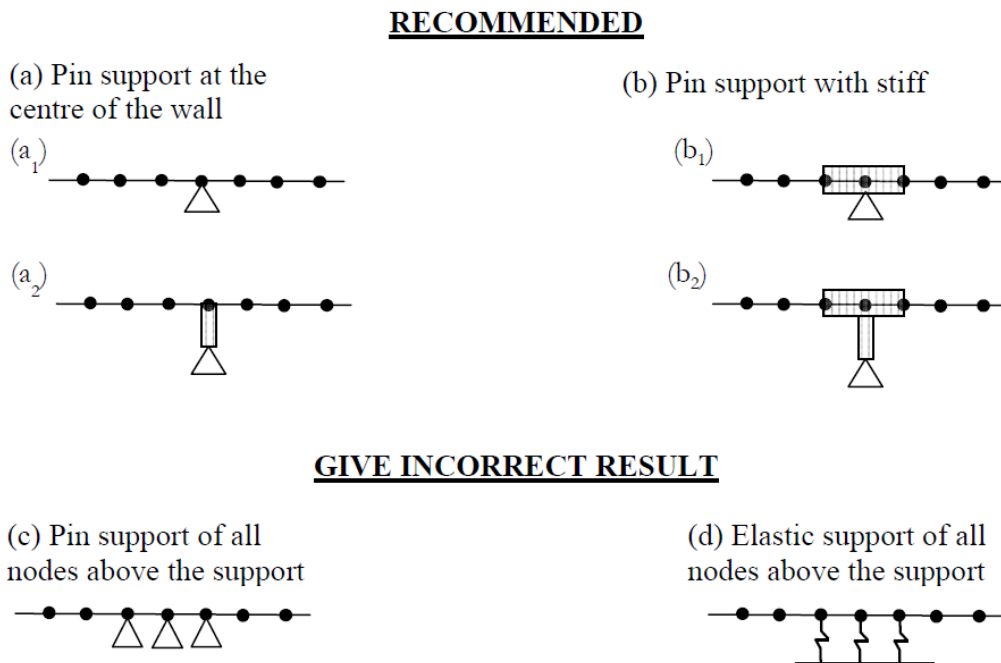
Figure 2.13: Different models for hinged line supports [6]

In alternative (a_1), the slab is pin-supported in a single node, and this connection is often called a knife-edge support. The only restraint in this case is the vertical displacement, at the centre of the support, which corresponds well with beam theory. This is a good alternative because unintended rotational restraints are avoided. In some cases, however, the rotational restraint from the wall might be of importance, and in such cases this model should be avoided. Alternative (a_2) is almost similar, with the addition of a rigid link from the mid-plane of the slab to the support. This option is useful if the plate is thick

17

(a Mindlin plate), and horizontal restraints are present [5].

Alternative (b_1) is also pin-supported, but in this case, all the nodes over the support are coupled to the master node in the middle to simulate an infinite stiff element that can rotate around the centre. It is important that only the out-of-plane deformation is restrained, and not the in-plane deformations, because that can cause overconstraining due to, for instance, temperature loads [6]. The coupling can be either hinged or rigid as illustrated in Figure 2.14. The rigid connection, shown on the right side of the figure has basically the same behaviour as alternative (c), and will therefore be discussed later. With a hinged coupling, the moment distribution corresponds well with beam theory when only one span is loaded. Figure 2.15 is an illustration presented by Rombach [5], where a one-way slab with two equal spans of 5 m is subjected to a uniform loading of $10\text{kN}/m^2$ at the left span only. The alternatives with only one pin support, with- and without hinge coupling, are almost equal, and close to what we would expect from beam theory.
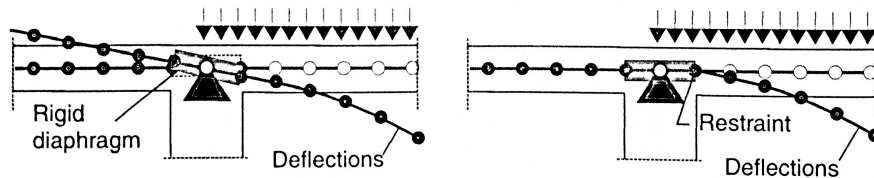
Figure 2.14: Hinge coupling (left), and rigid coupling (right) of nodes over the support [5]

18
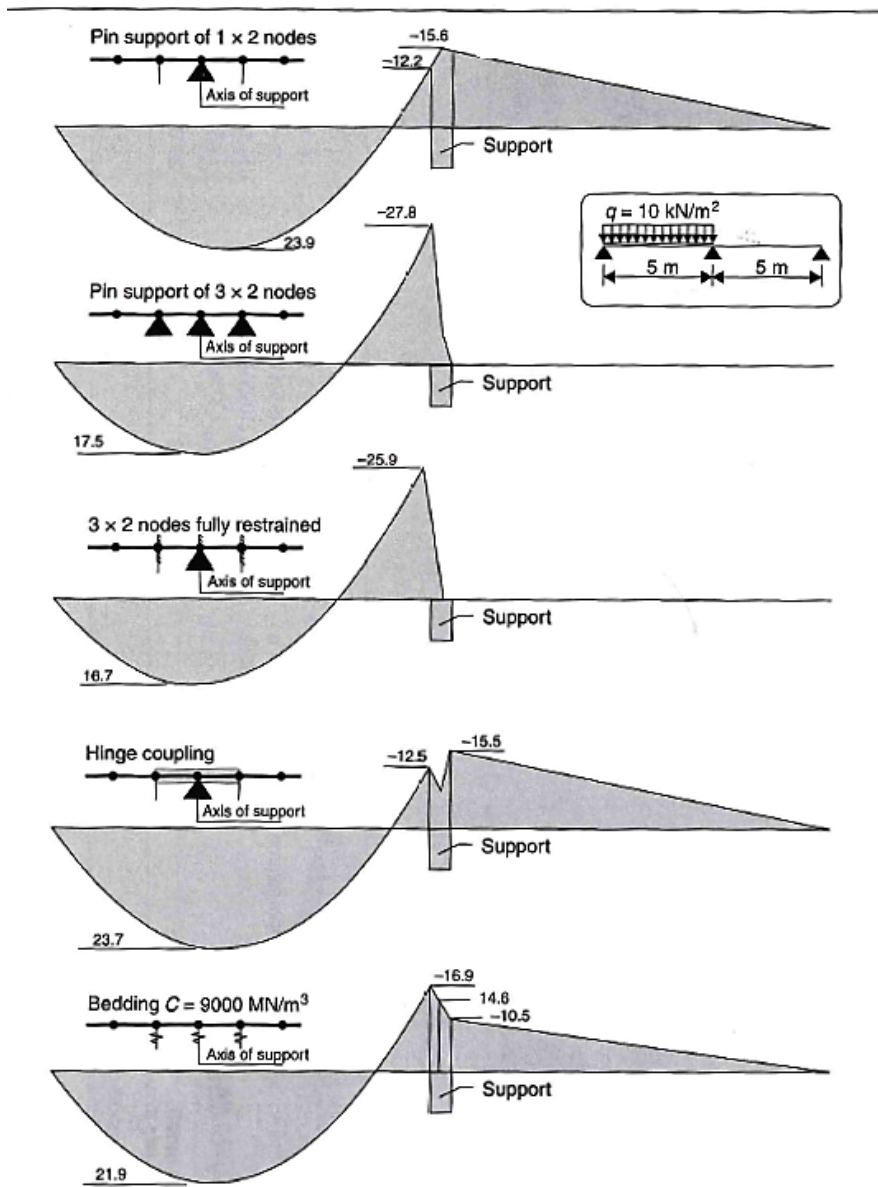
Figure 2.15: Bending moments for uniform loading at the left span [5]

Rombach [5] also argues that the same beam with hinged coupling, subjected to uniform load at both spans, gives almost similar results as beam theory. However, it is unclear how the hinged connection is modelled in a program in order to achieve such results since a very stiff coupling over the support would work as a fully restrained coupling when it is symmetrically loaded at both sides. To prove this, the same beam as shown in Figure 2.15 is modelled with "FEM design" for pinned support, hinged coupling, and fully restrained support in Figure 2.16. It can clearly be seen that the results with hinged coupling are much closer to the fully restrained model than the pinned support model. Consequently, the hinged coupling results in too much rotational restraint for uniform loading. For asymmetric load, however, the hinged coupling allows the beam to rotate more freely than the fully restrained connection. Similar to the (a_2) alternative, the (b_2) alternative applies only to thick plates [5].
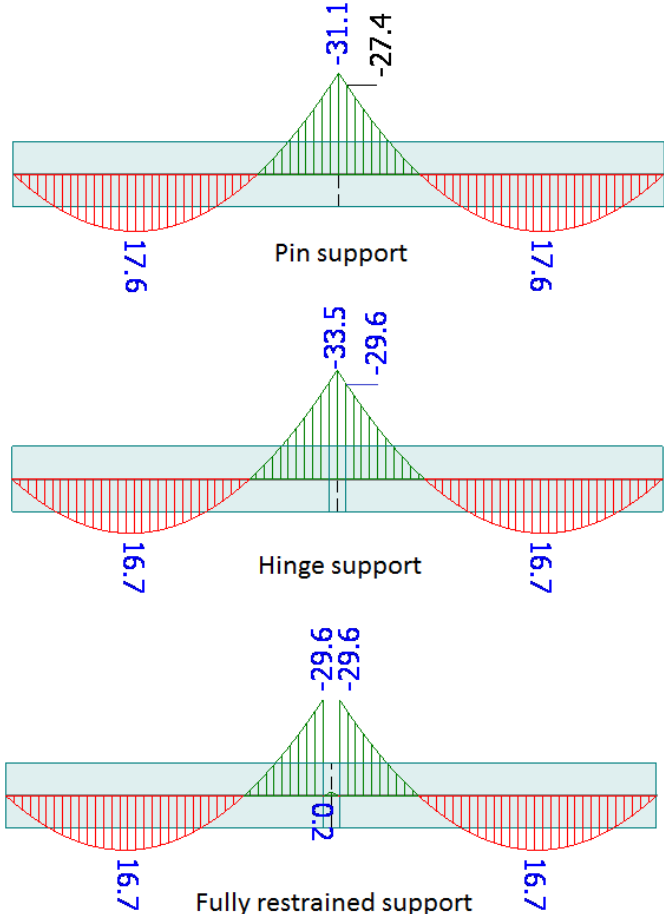
Figure 2.16: Bending moments for uniform loading at both spans (modelled with "FEM design")

20

Alternative (c) in Figure 2.13 (page 17) has pinned supports at all nodes over the support in order to consider the breadth of a very rigid wall. For uniform loading, the moment at the face of the support will be slightly underestimated, and if the load is asymmetric, the support moment will be highly overestimated. Alternative (d), with springs in all the nodes over the support, simulates a flexible, plane support. The results are highly dependent on the stiffness of the elastic supports which normally is derived from the stiffness of the wall. This model gives very erroneous results if the stiffness is wrong, and it is therefore normally recommended to rather simplify by using a simple pin support [5].

In some cases, the normal stiffness of the wall can be of importance for the results. If so, the entire wall should be included in the model, or alternatively the stiffness of the wall can be accounted for by translational springs along the centre line of the wall. This arrangement can be useful if the slab is supported on a wall with interruptions such as doors and windows [6].

If the slab and the wall are monolithically connected, the wall should preferably be included in the model because assuming either fixed or pinned support will be too coarse. If only the stresses in the slab is of interest, it is sufficient to model the bottom of the wall as either pinned or fixed. In Figure 2.17, two alternative models for monolithic connections are shown. Alternative (a) has a stiff coupling at the column top with a height corresponding to half the slab thickness, t. This can give accurate results if the slab thickness is at least half the size of the wall thickness, "a", and "a" is smaller than the distance from the wall centre to the nearest point of zero moment for permanent loads, l_0. If "a" $<< l_0$, the stiff coupling can be left out. Alternative (b) has a stiff coupling over the entire connection zone, including a rigid link on top of the column similar to alternative (a), and in addition a rigid link in the slab which connects all the nodes over the wall width. This connection is stiffer than alternative (a); therefore, the support moment will be greater, and the field moment will consequently decrease [6]. Another alternative is to simply increase the thickness of the slab locally over the support, and in that way considering the increased stiffness.
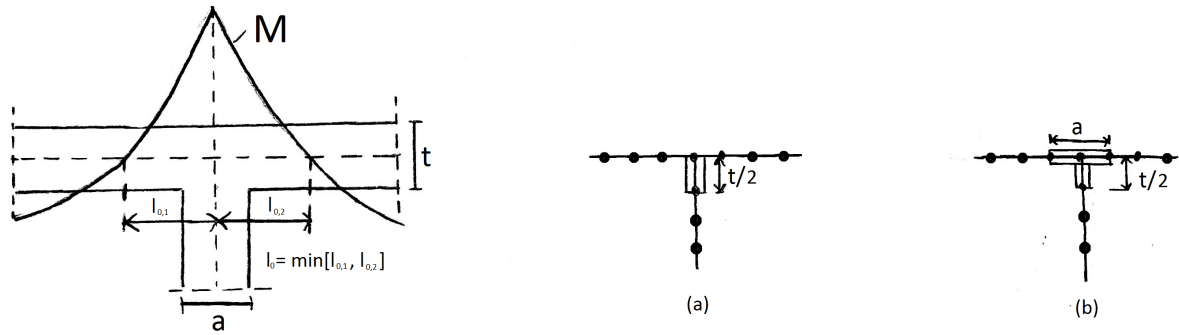
Figure 2.17: Different ways to model a monolithic connection between a slab and a supporting wall [6]

If a thin slab has supports with limited tensile restraint, there might be a problem with uplifting in the corners, due to twisting moments, as shown in Figure 2.18. This can happen in building floors if the weight from the wall above is insufficient. The uplifting force is the sum of the two concentrated Kirchhoff's shear forces from the meeting edges, as shown in Figure 2.19. The analysis of such a problem is highly non-linear, yet it can be solved with a linear-elastic program in an iterative way. First, all the nodes at the edge are restrained in the vertical direction, then one node after the other from the corners are released until the analysis show only compressive stresses at the edge. Such an analysis can be done with vertical springs or special boundary elements with no tensile stiffness. The uplifting effect results in reduced twisting moments at the corners at the cost of greater bending moment, greater mid-span deflection, and greater support reactions per unit length due to reduced supported length. It is wise to be aware of this phenomenon if tensile support reactions are limited [3].
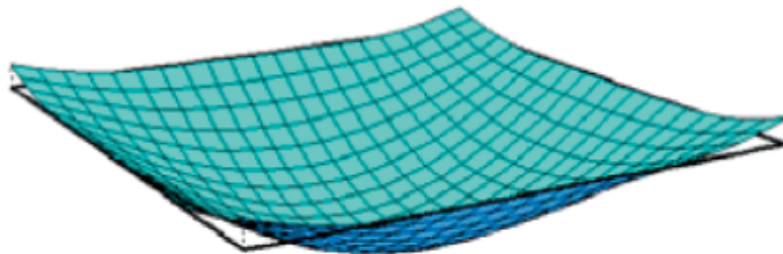
Figure 2.18: Uplifting of a simply supported slab subjected to uniformly distributed load [3]
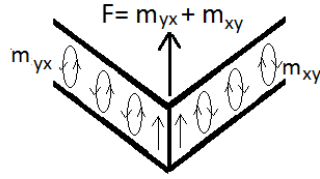
Figure 2.19: Uplifting force in a plate corner

If a line support is discontinuous, there will be numerical problems in the analysis due to the sudden change in boundary conditions. At the unsupported edges, both the shear force and the bending moment will apparently tend to infinity. However, in reality, the non-linear material behaviour of concrete will prevent this. Since such non-linear analysis are very complicated, there are some other alternatives for modelling discontinuous line supports, shown in Figure 2.20 [5].
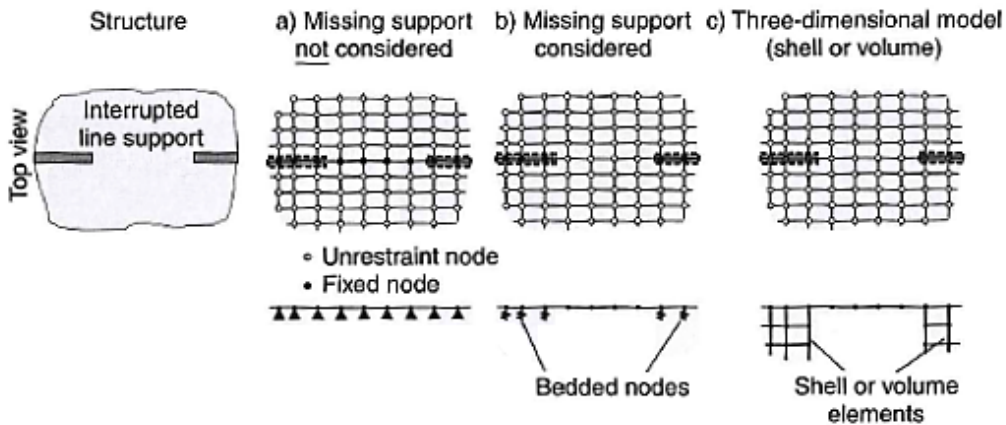
Figure 2.20: Modelling of discontinuous line supports [5]

One alternative is to ignore the missing supports and separately design a strip with sufficient reinforcement to behave as a rigid beam over the discontinuity. This solution is applicable if the length of the opening is less than 15 times the slab thickness. Another solution is to reduce the peak values at the unsupported edges by introducing elastic supports close to the opening. Both of these previous alternatives overcome the numerical problem of discontinuous line support, but only when looking at the overall behaviour of the slab. The complex stress and strain distribution at the unsupported edge can't be modelled with plain plate elements. A third alternative is to model the opening with shell or volume elements, but this is complicated and time consuming [5].

23

2.5.2   Column supports

Slabs supported on columns are called flat slabs, and are very commonly used. When flat slabs are subjected to uniformly distributed load, the load bearing behaviour is nearly axisymmetric around the supports [6]. The column supports can be modelled very similar to the line supports, shown previously in Figure 2.13 (page 17) for hinged connections, and Figure 2.17 (page 22) for monolithic connections. The only difference is that for column supports the load is carried in two directions. As for the line supports, it is recommended to model the column connection in single nodes in order to avoid unintended rotational restraints. Furthermore, for slender, interior columns, the moments from the column to the slab is negligible compared to the moments in the slab; hence, a pinned support is sufficient. It should be noted that pin supports in single nodes creates singularities. This is normally not of importance since one can use the results from critical sections outside of the singularity. However, the more slender the column is, the closer the critical section gets to the singularity point, and mesh refinement will just capture the singularity even more. Therefore, a pin support in a single point should be avoided if the column is very slender (width < 0.04 times the span) [5].

Sometimes, it is desired to describe the stress transfer from a slab to the support more realistic. This could be the case if the support width is large compared to either the slab thickness or the span length. If a more realistic model is used, the peak values over the support can be used for the design directly. Two such alternatives are shown in Figure 2.21 and 2.22. In Figure 2.21, the computed reaction force, R, is replaced by the equivalent surface loading, which will reduce the peak value. The reduction will be even greater if the reaction force is replaced by a line load over the perimeter of the column. Even though the reaction force from the support is replaced by distributed load, the mid node of the support still needs to be restrained for vertical displacement; however, the connected reaction force, R, will approximately be zero [3].
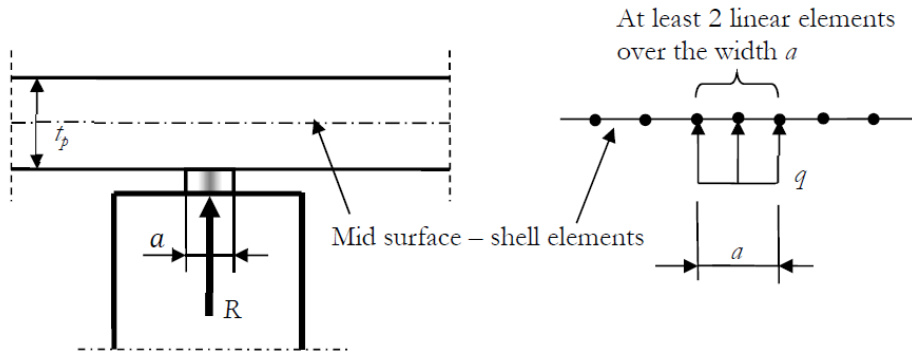
Figure 2.21: Point reaction replaced by surface loading [6]

Figure 2.22 shows a model with spring elements connecting the mid-surface of the slab to a stiff plate which can rotate around the support point. The stiffness of the different springs can be found from the stiffness properties of the real support. In the case of a monolithic connection, the column should be rigidly linked to the stiff plate [6].
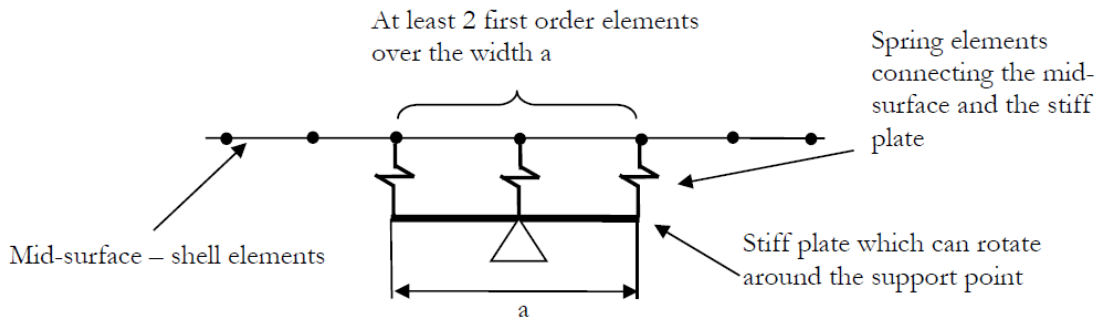
Figure 2.22: Bearing support modelled by spring elements [6]

In interior columns, the rotational stiffness can normally be neglected, but that is not the case for edge or corner columns. This is illustrated in Figure 2.23 with a 5x5 m plate supported by four corner columns. The plate is subjected to a uniformly distributed load of 10 kN/m^2. Due to symmetry, only a quarter of the plate is modelled. The differences in the moment, m_{yy}, both at the face of the column, and at mid-span for various modelling alternatives can be easily observed.
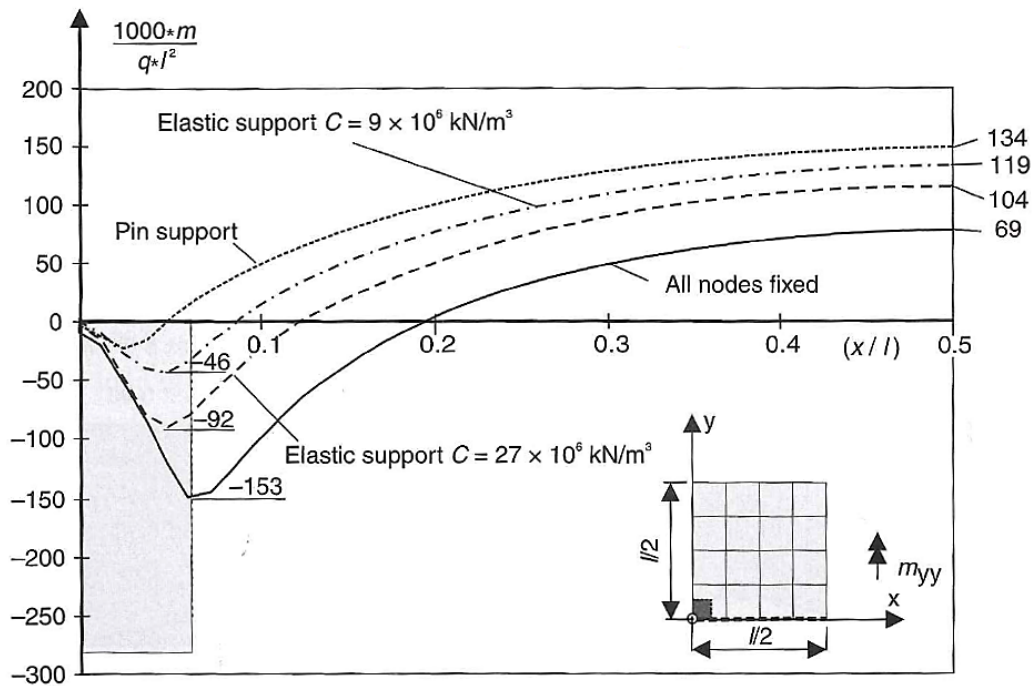
Figure 2.23: Bending moment, m_{yy}, in section y=0 of a slab supported by corner columns with different bedding moduli C [5]

If a pin support is used, the rotational stiffness of the column is not accounted for, and the moment at the column edge might be too low. If all nodes over the column is fixed on the other hand, the moment gets very high at the edge. To use fixed nodes in the model introduces high risk because a structure with fixed connections is difficult to construct in reality, and the resulting field moment in the model might be underestimated.

The bedded support model with c= 9×10^6 kN/m^3, in Figure 2.23, represents the normal stiffness of a 3.55 m high column with quadratic cross section (b=h= 25 cm). The bedded support model with c= 27×10^6 kN/m^3 includes the rotational stiffness of the same column with a pinned connection at the base [5]. Alternatively, one could use a torsional spring in the mid-node, but that approach won't take the width of the column into account.

The most precise results are achieved when the rotational stiffness of the columns is accounted for. It is, however, both difficult and time-consuming to determine the correct stiffness, and hence it might be more economical to use a conservative simplification. Another possibility is to model the edge and corner columns in the same way as monolithic connections where the entire column is included in the model [6]. However, as for the rotational stiffness, it might be beneficial to use a conservative simplification.

2.6   Modelling of load conditions

The loads in a FEM-analysis are always defined as point loads in the nodes. Even if the FEM software package allows the user to model an arbitrary load arrangement, the load will be automatically replaced by nodal loads. Nodal loads may in general be obtained by load lumping, or as work-equivalent consistent nodal loads. Load lumping is a term used for distributed loads getting discretized to the nearest nodes so that the nodal forces are statically equivalent to the applied force; however, load lumping should be restricted to linear elements with only corner nodes, otherwise it gives erroneous results [4].

Work-equivalent (consistent) nodal loads are also statically equivalent to applied load; furthermore, the work done by the nodal forces on the nodal displacements, equals the work done by the applied load over the entire displacement field. The consistent nodal loads are obtained by use of the same shape functions as was used for calculating the stiffness matrix. These methods won't be discussed in further details here, but it is important to be aware of the fact that uniformly distributed loads always get distributed to the nodes [4].

It is also worth noticing that many software packages neglect the load on restrained nodes since that load is transferred straight to the support without affecting the rest of the structure. Hence, the total support force is the sum of the forces on the unrestrained nodes only. It is important to be aware of this fact when the results for a structure component are used as loading for another structure component [4].

2.7   Singularities

Singularities are caused by simplifications in the numerical models. By assuming linear-elastic behaviour in disturbed regions, where the material in reality is highly non-linear, one achieves infinitely high stresses, which do not occur in real life. Typical regions of singularities are:

- Walls that end within a slab
- Discontinuous line supports
- Pin support
- Obtuse corners
- Openings
- Re-entrant corners ($\alpha \geq 90°$)
- Concentrated loads

In singularity zones, the stress will get higher with increasing fine mesh, as illustrated in Figure 2.24 for a simply supported slab (1x1 m) subjected to a point load of 1000 kN in the centre.
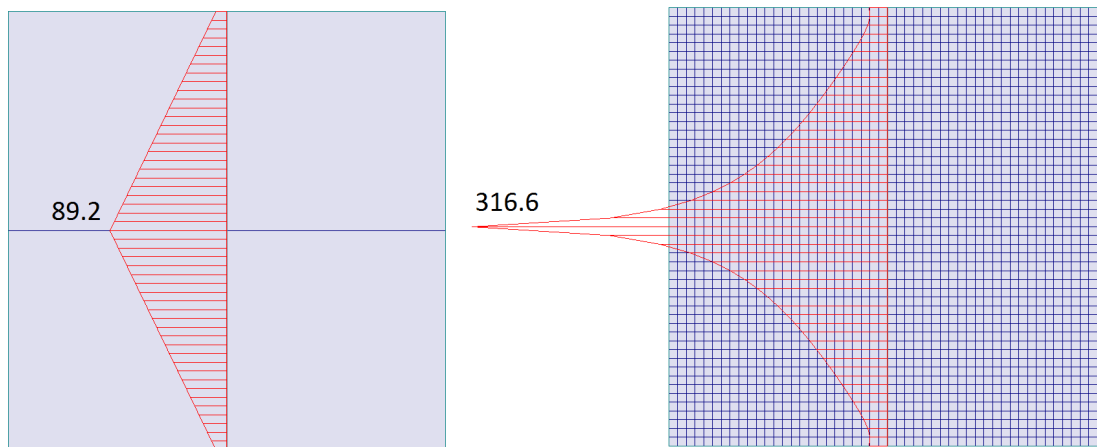
Figure 2.24: Stresses in a plate for element sizes 0.5 m (left) and 0.02 m (right) when subjected to a concentrated load (modelled in "FEM design")

In Figure 2.25, some typical singularity regions are marked in a typical building floor. As discussed in section 2.5 (about support conditions), singularities due to walls ending within a slab can be solved by either ignoring the missing support and design a fully restrained beam in the opening, or inserting bedded nodes at the edge of the support. Singularities due to pin supports, can be removed either by replacing the support with surface loading or by replacing the pin support with springs connected to a stiff plate which can rotate around the support point. However, it should be noted that it is usually unnecessary to remove singularities over supports, as the design forces can be found from critical sections outside the support centre [5].
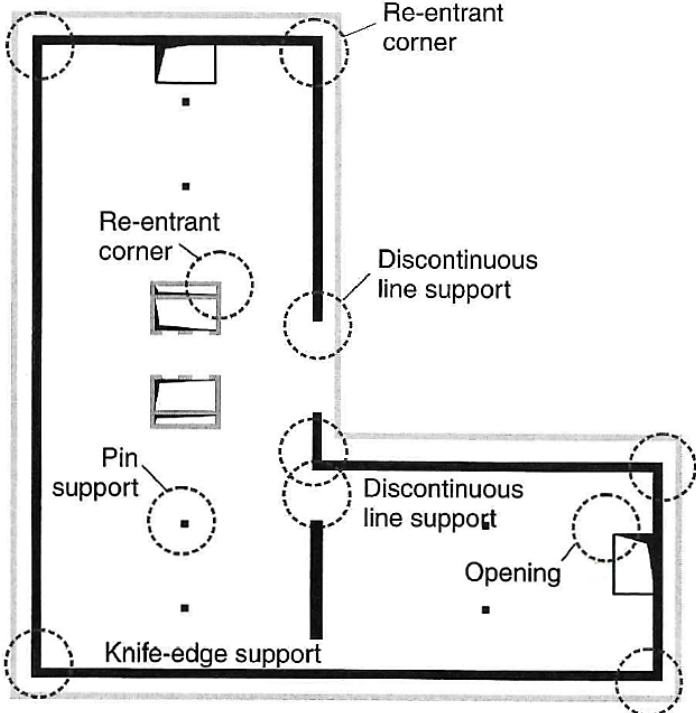
Figure 2.25: Singularity regions [5]

In re-entrant corners of an opening, singularities will arise because of inconsistency of the forces around the corners. While the bending moment on top and bottom of the opening approaches zero, the bending moment along the sides of the opening is non-zero, and hence there will be a jump in the moments at the corners, see Figure 2.26. This can be solved by rounding the corners in the model [5].
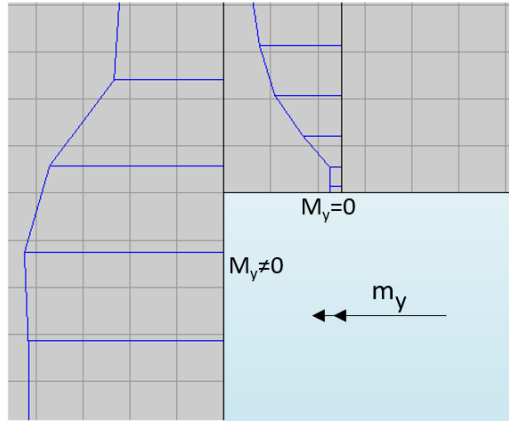
Figure 2.26: Moment distribution of m_y in sections near the corner of an opening (modelled with "DIANA")

When two walls meet in a re-entrant corner with an angle $\alpha \geq 90°$, as shown in Figure 2.27, the singularity can be clearly seen upon mesh refinement. The plate is simply supported and subjected to a uniformly distributed load of 10 kN/m². The coarse mesh to the left has a stress value in the re-entrant corner of 6950 kN/m², while the fine mesh to the right has a stress of 8910 kN/m², which is an increase of almost 30%. Further refinement of the mesh would produce stresses approaching infinity. The singularity can be avoided by including the stiffness of the walls in the model. This is shown in Figure 2.28, where the two sides, which makes up the re-entrant corner, are bedded instead of simply supported. When these supports are given a vertical stiffness of 1e+04 kN/m/m, the singularity is avoided at the cost of a slightly greater field moment.
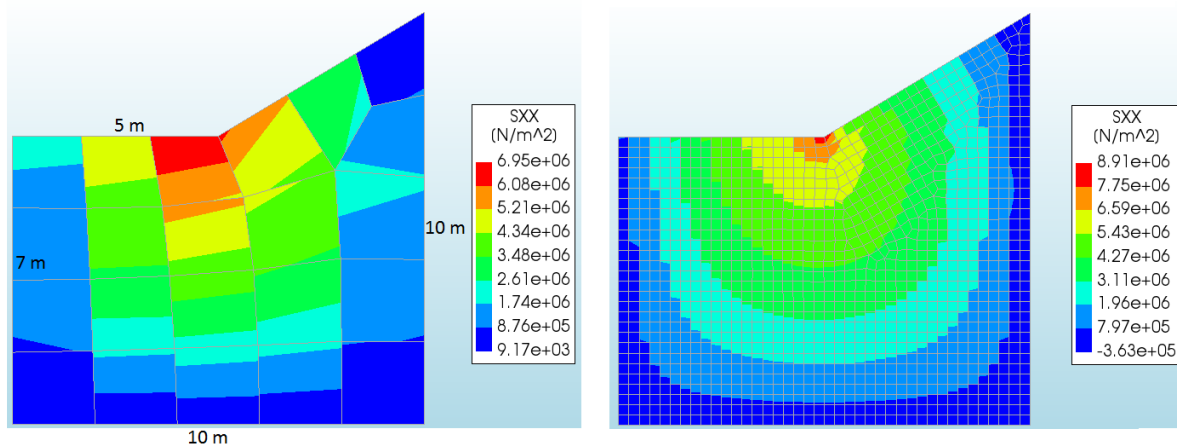
Figure 2.27: Stresses in a re-entrant corner for an element size of 2m (left) and 0.25m (right) (modelled with "DIANA")

a) all edges simply supported   b) k= 1e+05 kN/m/m   c) k= 1e+04 kN/m/m
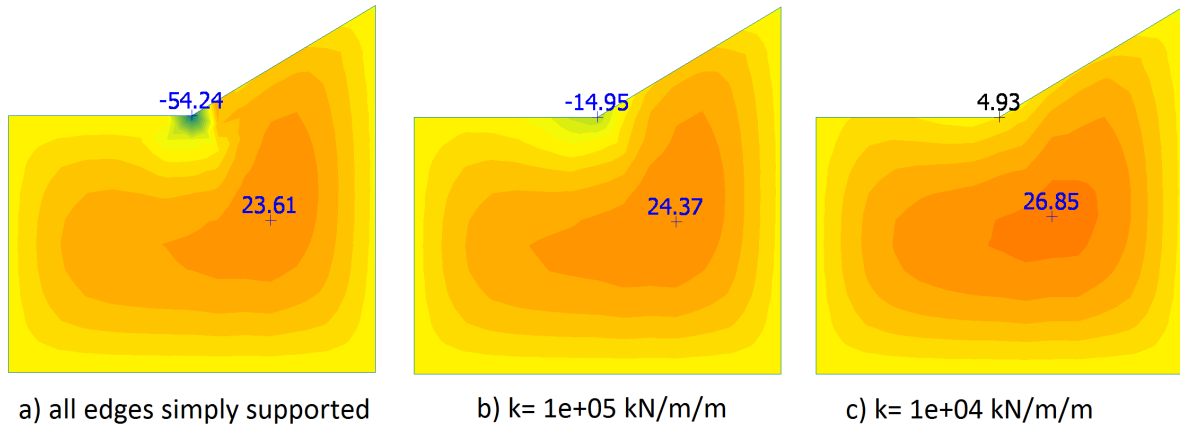
Figure 2.28: Bending moment, m_{xx} [kNm/m], in a plate with a re-entrant corner (modelled with "FEM design")

Singularities due to point loads can be avoided by dispersing the load down to the mid-plane of the slab, and hence get a greater loaded width in the analysis as illustrated in Figure 2.29 [5].
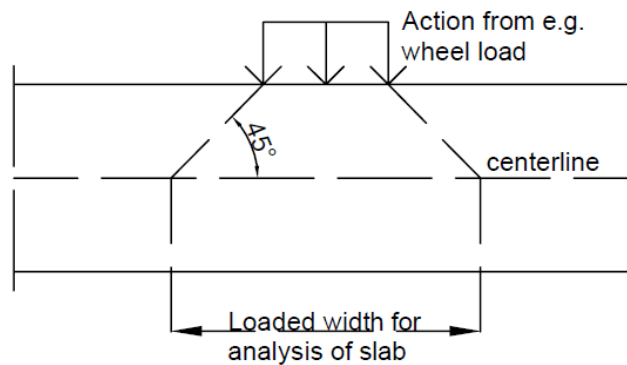
Figure 2.29: Dispersion of concentrated loads

2.8 Mesh refinement

The FEM programs available today are capable of dividing the structure into an almost infinite number of elements, but it's at the cost of longer computational time. The field moments are rarely affected by the mesh fineness, and there's no point in using more elements than necessary. However, in regions close to concentrated loads or supports, the results highly depend on the mesh fineness; the more elements, the better results. This can be seen, in Figure 2.30, for a simply supported one-way slab with two equal spans of 5 m and a uniformly distributed load. The field moments are almost independent of the mesh fineness, while the support moment deviates significantly when different number of elements are used. The shear force over the supports is also different for different number of elements, but since the design forces are found outside of the support, the result is rarely affected by the mesh [5].
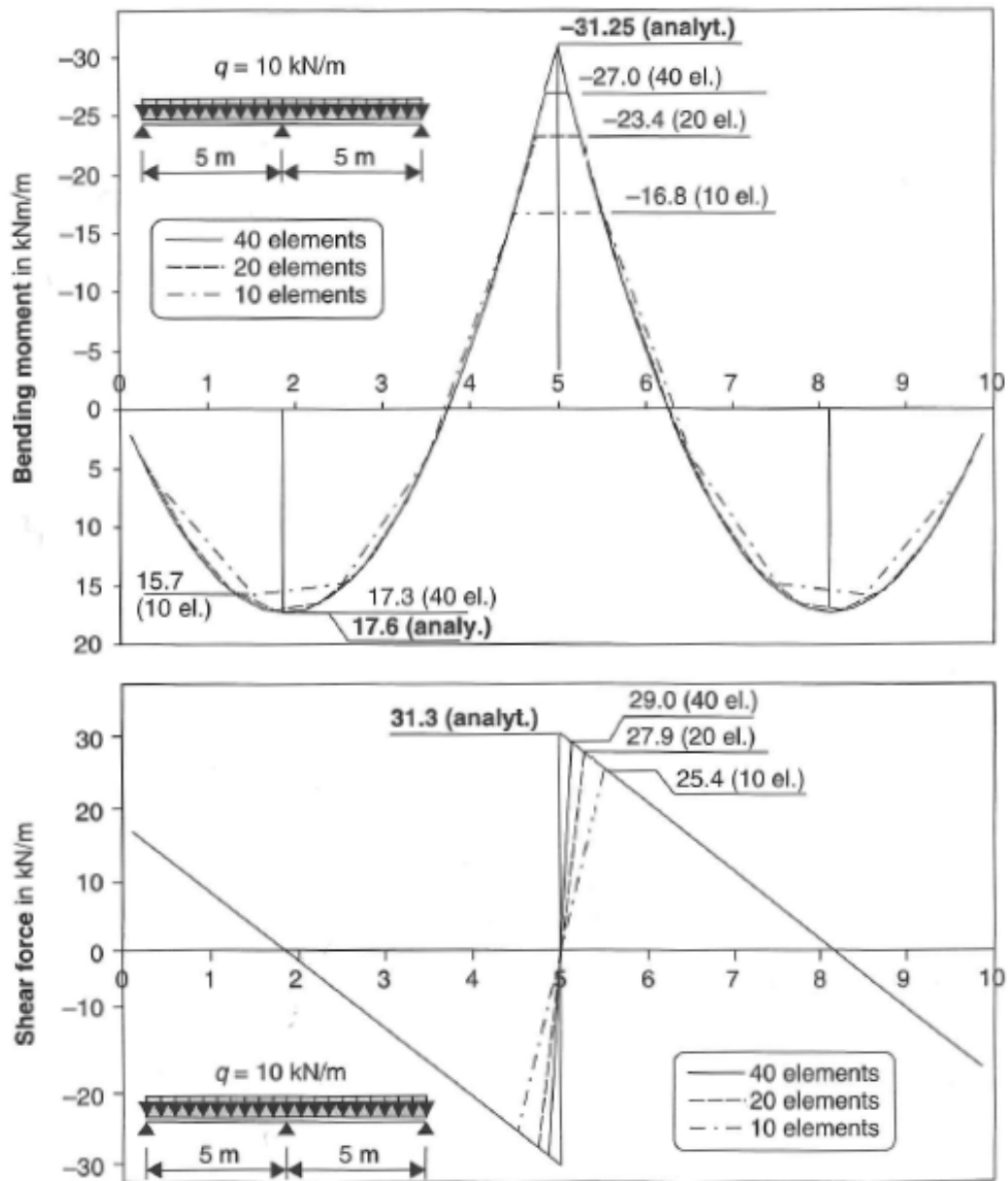
Figure 2.30: Member forces of a one-way slab for different numbers of finite elements [5]

The required number of elements are dependent on the polynomial order of the shape functions. When first order polynomials are used instead of second order polynomials, more elements are normally needed. This is illustrated in Figure 2.31, which compares axial deformation and axial stress for a 1D bar, of length $3 \times l$, with various number of elements and polynomial order. It can be seen that one quadratic element performs better than one linear element, but three linear elements give almost correct deformation. It's also worth noticing that the deformations are generally more accurate than the stresses, because the stresses are derived from the deformations [4].
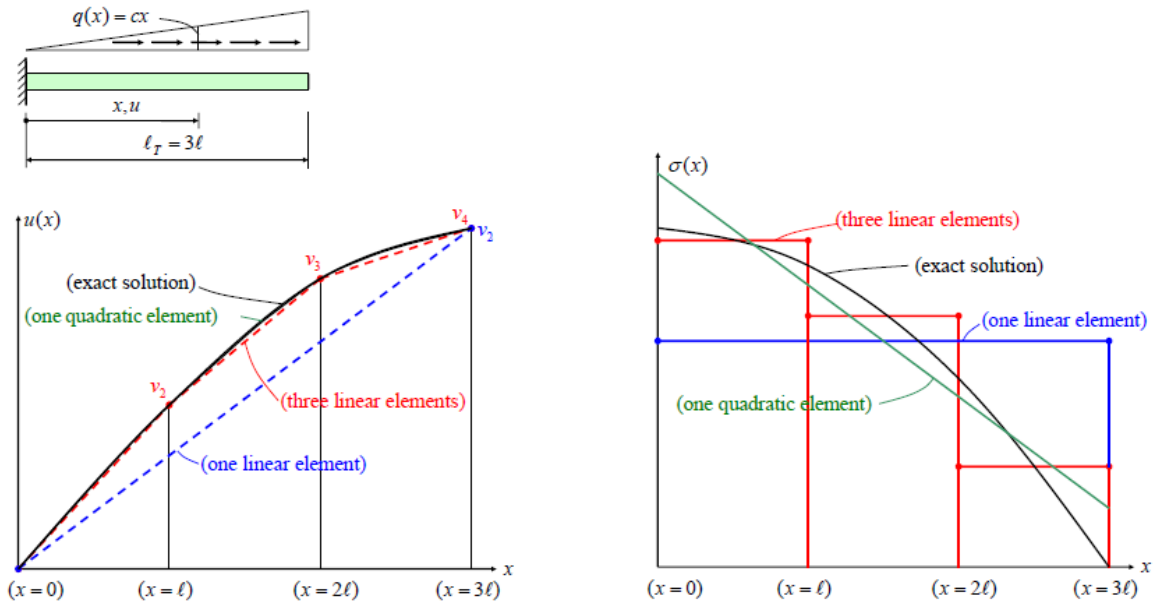
Figure 2.31: Axial deformation and axial stress for a 1D bar with elements of different polynomial order [4]

There are actually some exceptions to the claim that more elements always give better results. In singularity regions, as discussed in Section 2.7, the stresses increase to unrealistic levels when the mesh is (unreasonably) refined. However, even in singularity zones, the mesh should be fine enough to sufficiently model the forces at the support edge, where the design forces are found. In regions with high stress gradients, the maximum stress in the element can be greater than the stresses found from the integration points; therefore, the resulting design might become unsafe [5].

If the moment distribution found in the critical sections is smeared out in the perpendicular direction, as illustrated with dashed lines in Figure 2.32, the influence of the mesh density on the averaged moment is small. This is illustrated in Figure 2.33, where a plate with dimensions 20m x 10m x 0.6m, supported by four inner columns, is subjected to a uniformly distributed load of 10 kN/m^2. The distribution of the moment, m_{xx}, in the section above the two columns on the right-hand side is shown for three different meshes. The coarsest mesh is called 100%, and it can easily be seen that with a finer mesh the peak value increases. However, the moment integrated over the area of the section is almost

equal for the three different meshes [3]. If an average moment is used for the design, it is therefore sufficient to use two second order elements or one first order element from the centre of the support to the critical section [6].
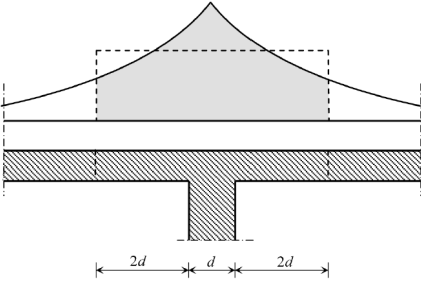
Figure 2.32: Smearing of moment peak [3]
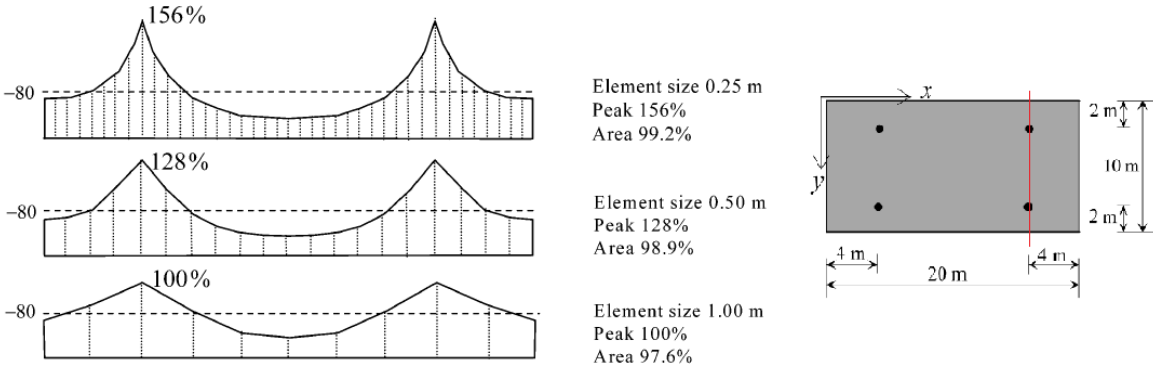
Figure 2.33: Moment distribution for different mesh fineness [3]

Most FEM software packages available today offer to automatically discretize the structure given an approximate size of the elements. However, in regions of great stress gradients or concentrated loads, the structural engineer has to manually insert a sufficient number of elements. It is also important to ensure that the nodes at the boundaries have been positioned accurately, especially at curved boundaries. Even a very small deviation from the correct coordinates can be critical. Curved boundaries will in general require a higher number of elements in order to model the real deformation and load-bearing behaviour [5]. It is also important to ensure that no elements cross interfaces. If, for example, there is a change in material, nodes should be placed along the interface line [15].

35

2.9 Choice of control sections

As mentioned previously, when modelling in single points or along a discrete line, the assumption of a linear-elastic material is a simplification that will produce too high values for the forces and moments. In reality, the concrete will crack and the reinforcement will yield, and the maximum values, which are used for design, are actually found in the result sections outside of the support centre. The exact location of the result sections will first be discussed for moments, and then for shear forces.

2.9.1 Result sections for moments

The location of the result section depends on the stiffness of the connection. For monolithic connections, the critical bending crack will develop no closer to the support than on the support edge, and hence it is safe to use the support surface as the result section. This is in accordance with the recommendation in EC2 5.3.2.2 [8]. Figure 2.34 shows the location of the result section for bending moment in a monolithic connection, where the width, "a", represents the length of a rectangular cross-section. In the case of a circular column with a diameter of ϕ, the equivalent value of "a" can be found from Eq. 2.5 [6].

$$a_{eqv} = \frac{\sqrt{\pi}\phi}{2} \qquad (2.5)$$
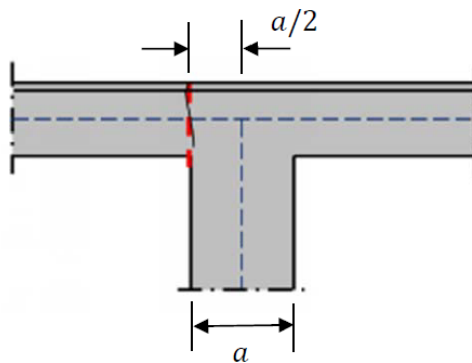
Figure 2.34: Result section for bending moment in a monolithic connection [6]

If the connection is hinged, and the support only transfers compression stresses, the location of the result section is dependent on the stiffness of the support. If the support is

stiff, the resultant force on each half side will be approximately at the support edge. If, on the other hand, the support is soft, the stress over the support will be almost uniformly distributed, which gives resultant forces at the middle of each half, see Figure 2.35 for an illustration of this. The stiffer the support, the more the resultant force will shift towards the edge. A column support will always shift the resultant force more towards the edge than a wall support. The result section of a simply supported slab can, as a conservative assumption, always be taken as the mid-section in between the centre and the edge of the support. This is applicable for walls, columns and bearings in agreement with EC2 5.3.2.2 [6, 8]. EC2 5.3.2.2 states that support moments, which are calculated with a span from centre to centre of supports, can be reduced with ΔM as shown in Eq. 2.6. This corresponds to shifting the resultant section a/4 out of the centre when the support load is uniformly distributed [8].

$$\Delta M = \frac{F_{Ed,sup}a}{8} \tag{2.6}$$
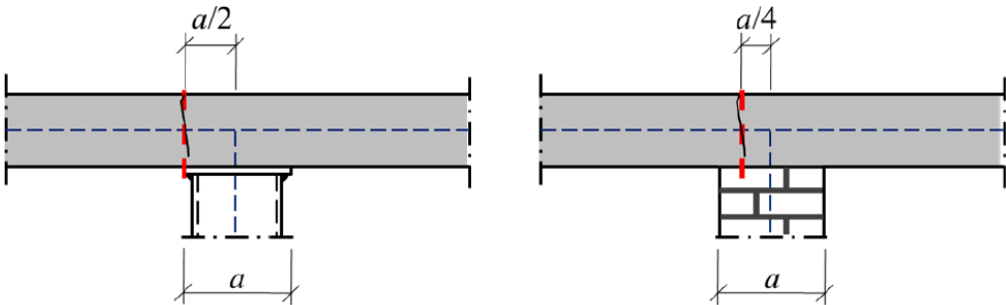
Figure 2.35: Result sections for bending moment in a hinged connection with a stiff support (left) and a soft support (right) [6]

2.9.2   Result sections for shear forces

Shear forces in a plate are due to the vertical forces which are transferred from the plate towards the supports. The result section for shear forces should be placed where the critical shear crack develops, which is where the crack can transfer the largest possible shear force. This will be no closer to the support than at the edge, because if it is any closer, the vertical force is transferred directly to the support. Hence, the critical result section should be placed at a distance of z×cotθ from the support edge, where z is the internal lever arm and θ is the crack angle as illustrated in Figure 2.36. Without shear reinforcement, the crack angle will be steeper than 45°, and z×cotθ is approximately equal to the effective height of the slab, d. When controlling shear compression failure, the full shear force at the support edge should be used [6].
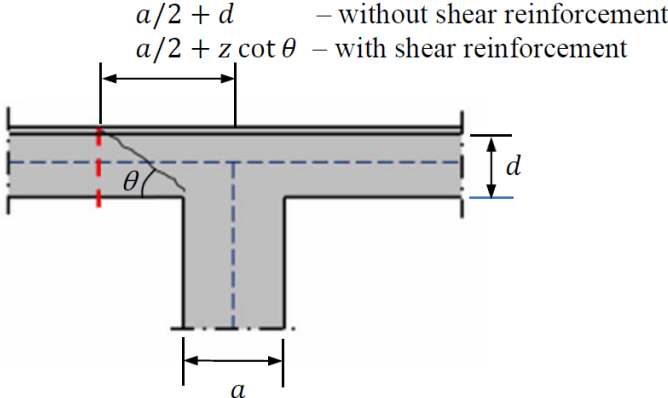
Figure 2.36: Result section for shear force [6]

2.10 Stress smoothing

As mentioned previously, the stresses in an element are found in integration points where the stresses are most accurate. However, it is desired to have the same accuracy for the stresses in the entire element, and to achieve this one can use element smoothing. Element smoothing involves extrapolating the element stresses from the integration points, σ_s^h, to the rest of the element by use of the same set of shape functions, $\mathbf{N}_u$, which were used to determine the displacement field. This can be seen in Eq. (2.7), where σ^* is the smoothed stress field [4]. An example on how an element smoothed stress field may look like is shown in Figure 2.37. It can be seen that the smoothed stress field looks relatively similar to the real stress field because of the smoothing of the discrete FEM stresses [4].

$$\sigma^* = \mathbf{N}_u \sigma_s^h \tag{2.7}$$
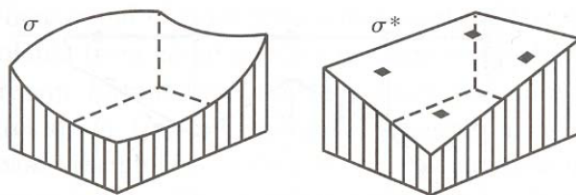
Figure 2.37: Element stress field σ (left), and element smoothed stress field σ^* (right) [4]

Even though element smoothing gives a continuous stress field inside the element, the stresses are still discontinuous over element borders. Unless there actually is a discontinuity in geometry or material in the structure, the stresses should be continuous over the element borders. This can be done by using nodal averaging, where the nodal stress becomes the average of the original nodal stresses in each of the surrounding elements. The nodal stress from each element is found either directly or by extrapolating from the integration points. When the averaged nodal stresses are found, continuity across element borders is achieved, and continuous stress field for each element can be found by interpolating the nodal average stresses with the use of the shape functions, $\mathbf{N}_u$. This can be seen in Eq. (2.8), where σ_n^* is a vector with the nodal stress averages in the element. [4].

$$\sigma^* = \mathbf{N}_u \sigma_n^* \tag{2.8}$$

Nodal averaging should only be used for low order elements, and only with meshes that have relatively uniform element sizes. A more accurate method to achieve improved stresses with continuity over element borders is by use of global smoothing. Global smoothing is a method which uses least-squares fit between the smoothed stress field, σ^*, and the finite element stress field, σ^h, to obtain the optimal nodal stresses, see Eq. (2.9), where N_{els} is the number of elements and σ^* is as described above in Eq. (2.8).

$$\frac{\partial}{\partial \sigma_n^*} \left(\sum_{e=1}^{N_{els}} \int_{V_e} (\sigma^* - \sigma^h)^2 dV \right) = 0 \tag{2.9}$$

Similar as for nodal averaging, the nodal stresses give the improved stress field for each element by interpolation. See Figure 2.38 for an illustration of global smoothing [4].
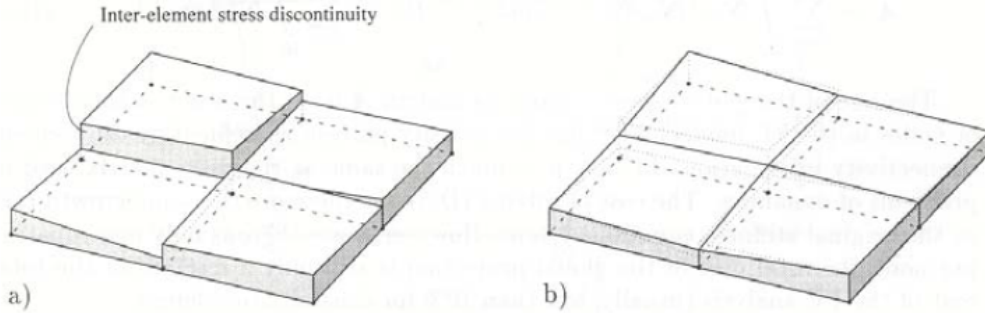
Figure 2.38: Finite element stress field σ (left), and global smoothed stress field σ^* (right) [4]

An even more accurate stress smoothing method is called Superconvergent Patch Recovery (SPR) or local smoothing. This method looks somewhat like global smoothing, but the smoothing is carried out on a patch of continuous elements surrounding the node where recovery is wanted. Some examples of patches are showed in Figure 2.39. The nodal values which are determined from the given patch is marked with black dots.
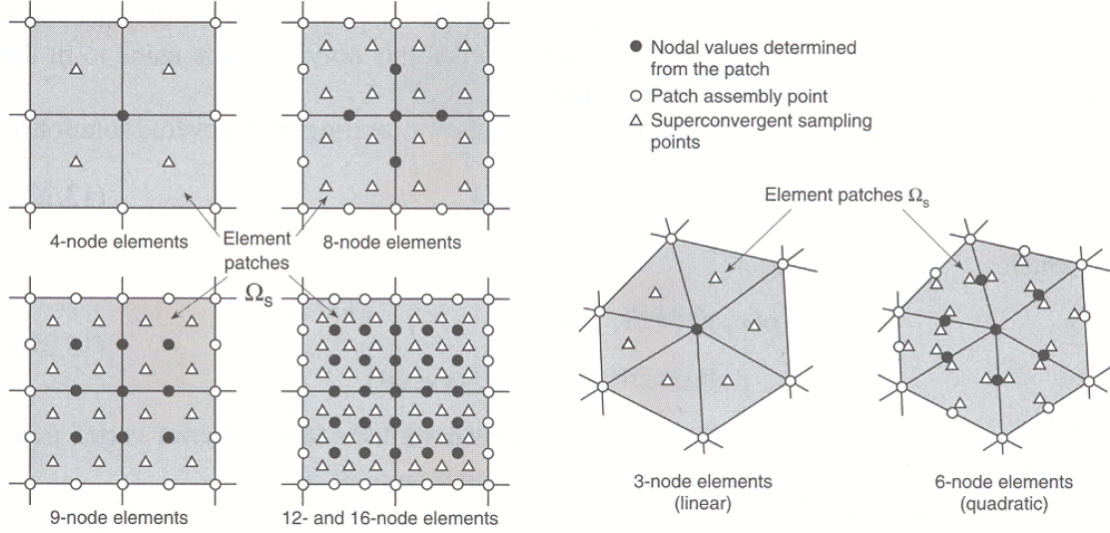
Figure 2.39: Examples of patches for lower and higher order elements [4]

The least-square fit method as described in Eq. (2.9) is still used, but the smoothed stress field, σ^*, is now described by a vector, $\mathbf{P}$, which contains polynomial terms in the Cartesian coordinates, and a vector, $\mathbf{a}$, containing unknown generalized coordinates for which the derivation should be solved with regard to, see Eq (2.10):

$$\sigma^* = \mathbf{Pa} \tag{2.10}$$

The summation inside the least-square fit is done over the number of sampling points in the patch, and not over the number of elements as in global smoothing. when $\mathbf{a}$ is found, the smoothed nodal values can be found with equation Eq. (2.10) where the Cartesian coordinates of the nodes are inserted in $\mathbf{P}$. Since the elements often are included in more than one patch, a unique solution for the stress field in an element can be found by multiplying the shape function for a node with the recovered stress found from SPR in that node, see Eq. (2.11), where N_{en} is the number of element nodes [4].

$$\sigma^* = \sum_{a=1}^{N_{en}} N_a \sigma_a^* \tag{2.11}$$

41

The user of a FEM design software should be conscious of what coordinate system is used to report the element stresses, what type of integration points is used, what techniques the program uses to extrapolate and interpolate, and what method is used for stress averaging. If all this is known, the user is more likely to interpret the output from the analysis correct. It might be useful to avoid stress smoothing, because the degree of stress discontinuity gives information about the accuracy of the finite element results [4].

All programs for FEM design use the stress resultants from the analysis as input in the design. The stress resultants are obtained by integrating the stresses over the thickness of the plate, see Eqs. (2.12)-(2.14), and Figure 2.40.

$$m_x = -\int_{-\frac{t}{2}}^{\frac{t}{2}} \sigma_x z\, dz \tag{2.12}$$

$$m_y = -\int_{-\frac{t}{2}}^{\frac{t}{2}} \sigma_y z\, dz \tag{2.13}$$

$$m_{xy} = -\int_{-\frac{t}{2}}^{\frac{t}{2}} \tau_{xy} z\, dz \tag{2.14}$$
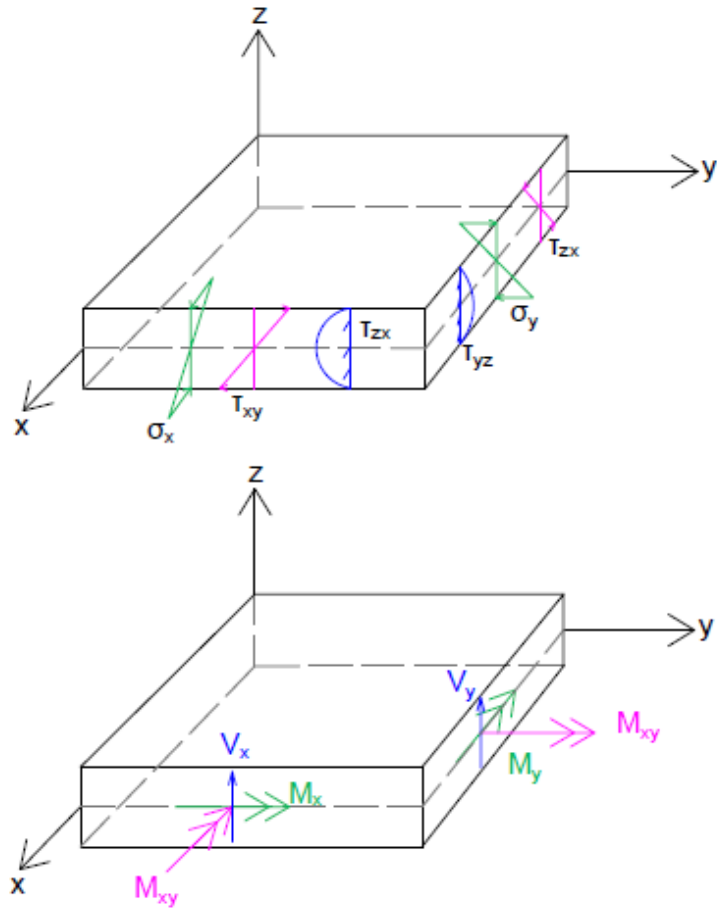
Figure 2.40: Stresses (top) and stress resultants (bottom) in a bending plate

Chapter 3

Design of plates

3.1 General

In this chapter, the theory of elasticity and the sandwich model will be described as they are the basis for numerous design programs.

The main difficulty with both these models are the fact that in general, plates don't have coinciding principal moment- and reinforcement directions. In beam theory, the principal moment always works in the load bearing direction. Plates on the other hand, have load bearing in two directions, and twisting moments that disturb the principal moment directions. It is almost impossible to place the reinforcement in the directions of the principal moments, because the directions may vary over the plate; moreover, a plate normally experience various load cases during a lifetime, which gives principal moments in varying directions.

3.2 Design based on theory of elasticity

The theory of elasticity is based on the equilibrium equation of an infinitesimal plate element subjected to distributed load in the normal direction, see Figure 3.1. M_x and M_y are bending moments, M_{xy} and M_{yx} are equal torsion moments, and V_x and V_y are shear forces.
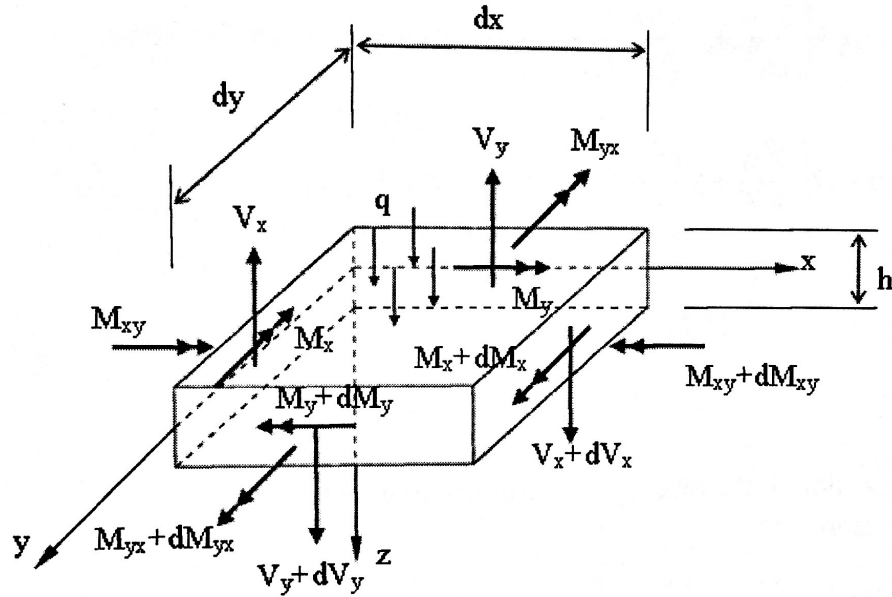
Figure 3.1: Forces in an infinitesimal plate element [7]

From equilibrium of the forces in the element, the result is Eq. (3.1) [7].

$$\frac{\delta^2 M_x}{\delta x^2} + \frac{\delta^2 M_{xy}}{\delta x \delta y} + \frac{\delta^2 M_y}{\delta y^2} = -q \tag{3.1}$$

This equation holds for all infinitesimal plate elements. In the theory of elasticity, however, it is further assumed that the material is linear-elastic and isotropic, the vertical deformation is small compared to the thickness of the plate, Kirchhoff's theory is valid, and that there is plane stress in the xy-plane. By use of these assumptions in the constitutive and kinematic relations, the results are Eqs. (3.2)-(3.4), where w represents the vertical deformations, and D is the plate flexural stiffness.

$$M_x = -D \left(\frac{\partial^2 w}{\partial x^2} + \nu \frac{\partial^2 w}{\partial y^2} \right) \tag{3.2}$$

$$M_y = -D \left(\frac{\partial^2 w}{\partial y^2} + \nu \frac{\partial^2 w}{\partial x^2} \right) \tag{3.3}$$

$$M_{xy} = -\frac{\partial^2 w}{\partial x \partial y} D(1 - \nu) \tag{3.4}$$

When Eq. (3.2)-(3.4) are inserted into Eq. (3.1), the fourth order partial differential equation for elastic bending of isotropic plates is achieved [7]:

$$\frac{\partial^4 w}{\partial x^4} + 2 \frac{\partial^4 w}{\partial x^2 \partial y^2} + \frac{\partial^4 w}{\partial y^4} = \frac{q}{D} \tag{3.5}$$

This equation can be solved analytically as long as the plate is rectangular and has ideal boundary conditions. Several tables with results for moments and deflections exists for different span ratios, boundary conditions, and Poisson's ratios [7].

When the design moments are found, the next step in the design of a concrete plate is to calculate the moment capacity of the compression zone, which is done with moment equilibrium according to Eq. (3.6), where α is the relative height of the compression zone [16]:

$$M_{Rd} = 0,8\alpha(1 - 0.4\alpha)f_{cd}bd^2 \tag{3.6}$$

Then, an approximation of the internal lever arm can be found dependent on the compression zone utilization according to Eq. (3.7) [16]:

$$z = \left(1 - 0.17 \frac{M_{Ed}}{M_{Rd}} \right) d_x \leq 0.95d \tag{3.7}$$

Finally, the required reinforcement for the Ultimate Limit State (ULS) can be found according to Eq (3.8):

$$A_s = \frac{M_{Ed}}{z \times f_{yd}} \tag{3.8}$$

This procedure is performed for each reinforcement direction independently. If torsion moment is present, the required cross section area of anchoring reinforcement is:

$$A_{anchoring} = \frac{2M_{xy}}{f_{yd}} \tag{3.9}$$

For the Serviceability Limit State (SLS), the vertical deformation, w, is found from tables. Reduced bending stiffness should be used due to cracking of concrete.

3.3 The sandwich model

One widely used model for calculating the required reinforcement is the sandwich model. The sandwich model method is a general procedure for design of shells, but it is also applicable for plates since the only difference between plates and shells is that shells include membrane forces.

The first step in the sandwich model method is to divide the plate into three layers, and then translating the stress resultants into in-plane forces in the layers. The shear forces are handled by the middle layer, and the outer layers handle the bending moments and in-plane forces. The outer layers also help support the middle layer. The thickness of the outer layers depend on whether the concrete is cracked or not. If the concrete is cracked, the thickness of the layer is assumed to be two times the distance from the surface to the reinforcement gravity centre. If the concrete is uncracked the thickness of the layer is assumed to be half the plate thickness. When the thickness of the top and bottom layer is found, the middle layer is simply the remaining thickness of the plate. In bending, we assume cracked concrete as a conservative approach because it gives the largest lever arm, and hence the highest utilization of the reinforcement. Figure 3.2 illustrates the imaginary in-plane forces in the three layers of a sandwich model [7].
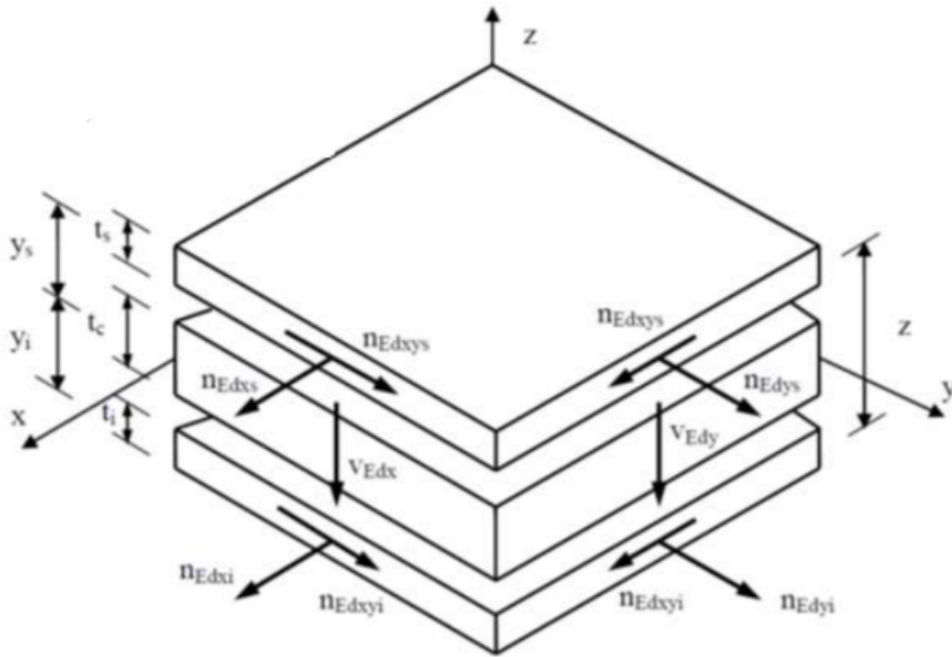
Figure 3.2: The layers of a sandwich model for a shell element [7]

The second step in the sandwich model method is to control whether shear reinforcement is necessary or not. This is done by finding the principal shear force, v_0, and the associated shear angle, φ_0, according to Eqs. (3.10) and (3.11), and control that v_0 is smaller than the shear compressive capacity and the shear tensile capacity which both are given in EC2, chapter 6 [7].

$$v_0 = \sqrt{v_x^2 + v_y^2} \tag{3.10}$$

$$\varphi_0 = tan^{-1}\left(\frac{v_y}{v_x}\right) \tag{3.11}$$

If the shear capacity is insufficient, shear reinforcement is needed, and can be calculated using EC2. By adding shear reinforcement, there will be extra contributions to the in-plane forces in the outer layers with a value of Δn, see Eqs. (3.12)-(3.14). Cotθ is the angle to the compression strut in the concrete (see Figure 3.3), and can be chosen between 1< $cot\theta$ <2.5 [7].

$$\Delta n_x = \frac{1}{2}\frac{v_x^2}{v_0}cot\theta \tag{3.12}$$

$$\Delta n_y = \frac{1}{2}\frac{v_y^2}{v_0}cot\theta \tag{3.13}$$

$$\Delta n_{xy} = \frac{1}{2}\frac{v_x v_y}{v_0}cot\theta \tag{3.14}$$
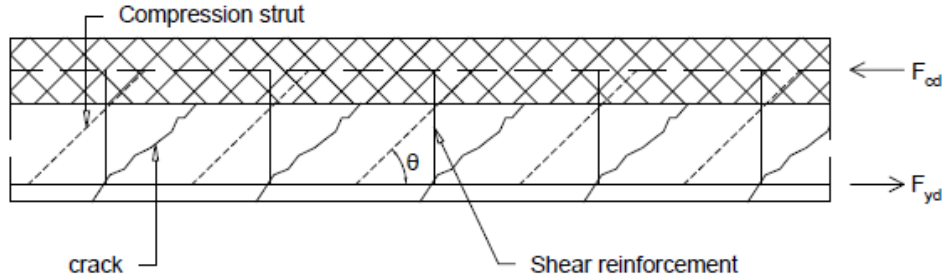
Figure 3.3: Compression struts and the angle θ [8]

In the third step, the total value of the in-plane forces in the top and bottom layers are calculated. It is assumed orthogonal reinforcement in the directions corresponding to the local axis. The contributions from the internal moments are simply the moment divided by the internal lever arm which goes from the middle of the top layer to the middle of the bottom layer. In the next step, the maximum principal in-plane force in each of the outer layers is calculated according to Eq. (3.15). This is done to control whether the concrete is cracked or not [7].

$$n_{11} = \frac{n_x + n_y}{n_{xy}} + \sqrt{\left(\frac{n_x - n_y}{n_{xy}}\right)^2 + n_{xy}^2} \tag{3.15}$$

If the principal force, n_{11}, is below zero, the concrete is uncracked; hence, minimum reinforcement is sufficient as long as the compression stress is below the design compressive

strength, f_{cd}. If the concrete is cracked, however, the design of the layer is done according to compression field theory (CFT). CFT implies that there is equilibrium between the fictitious in-plane forces, and the reinforcement- and compression strut forces. The equilibrium conditions of the theory are illustrated in Figure 3.4 [7].
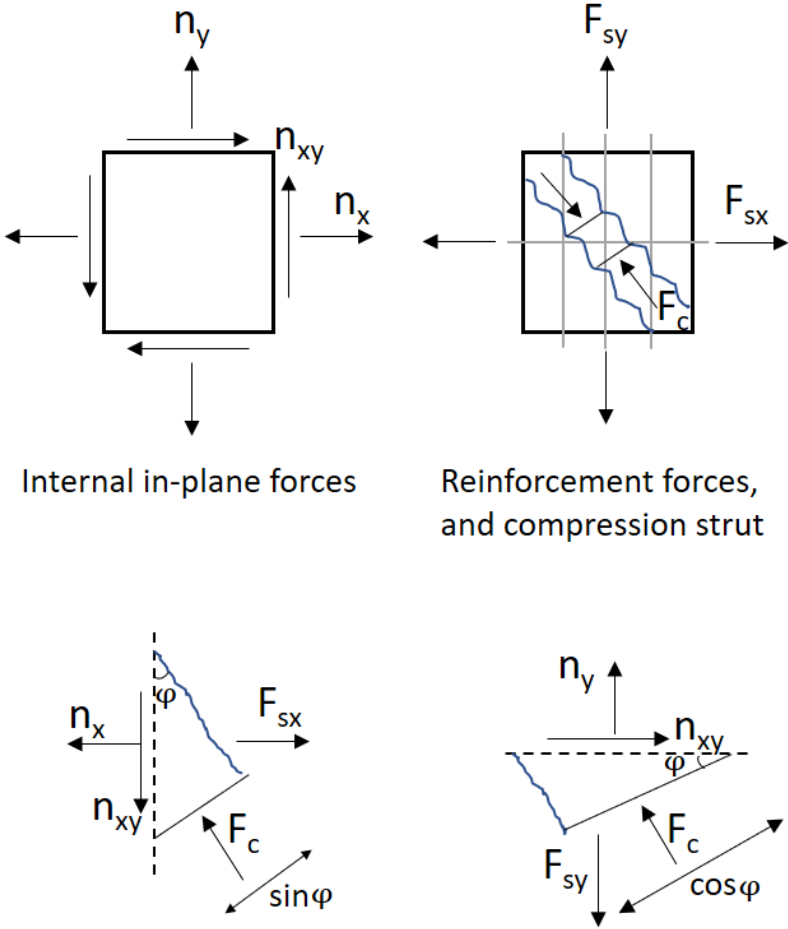
Figure 3.4: Equilibrium conditions in the compression field theory

The resulting expressions for the reinforcement forces in each direction, F_{sx} and F_{sy}, as well as the concrete compression force, F_c are all shown in Eqs. (3.16)-(3.18) [7].

$$F_c = \frac{n_{xy}}{sin\phi cos\phi} \tag{3.16}$$

$$F_{sx} = n_x + n_{xy}tan\phi \tag{3.17}$$

$$F_{sy} = n_y + n_{xy}cot\phi \tag{3.18}$$

The compression force has to be checked against the dimensioning maximum compression stress, $\sigma_{Rd,max}$, from EC2 6.5.2, see Eq (3.19):

$$\sigma_{Rd,max} = 0.6 \left(1 - \frac{f_{ck}}{250} \right) f_{cd} \qquad (3.19)$$

The concrete compression capacity is reduced compared to pure compression capacity, f_{cd}, due to the effect of the transverse tensile stress. In the theory of elasticity, this reduction in capacity is neglected since each direction is calculated independently.

If the compression capacity is insufficient, there are several possibilities to solve the problem. Three options are illustrated in Figure 3.5 [7].

a) Account for the compression capacity in the reinforcement

b) Increase the concrete cover locally

c) Increase the thickness of the layer
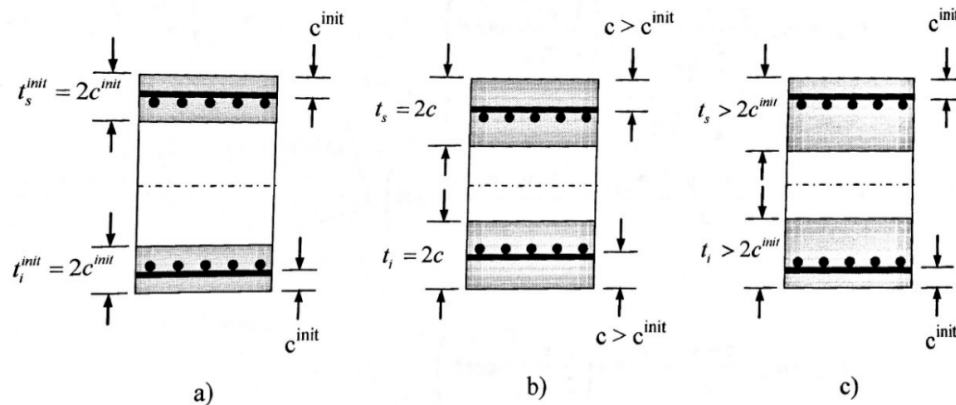
Figure 3.5: Different ways to solve a problem of too low concrete compression capacity [7]

Alternative a) might lead to buckling of the reinforcement, and hence a brittle failure mode which is undesirable. Alternative b) is not a practical approach at the building site. The most practical option is alternative c) where the thickness of the layer is increased while the reinforcement stays at its original position. In that case, the forces due to the eccentricity have to be recalculated [7].

Finally, the required reinforcement amount is found from Eqs. (3.20) and (3.21), where f_{yd} is the yield strength of the reinforcement [7].

$$A_{sx} = \frac{F_{sx}}{f_{yd}} \tag{3.20}$$

$$A_{sy} = \frac{F_{sy}}{f_{yd}} \tag{3.21}$$

This is a quick and simple method, but it has some disadvantages. It assumes constant stress and strain in the outer layers, which is inaccurate, and cracking is only controlled in the mid-plane of the membrane [7].

Chapter 4

Commercial FEM design software

4.1 Introduction

This chapter will show some examples on how automatic design of concrete plates can be done with reference to some of the commercial design software packages available today.

In all of the automatic procedures for design described in this thesis, it is assumed that the concrete only supports compressive forces, while the reinforcement supports all the tensile forces.

Some of the programs offer both calculation of necessary reinforcement, and capacity control for applied reinforcement. A description of how the design and/or control is done for both Ultimate Limit State (ULS) and Serviceability Limit State (SLS) is included for each of the selected software packages. Due to variable access to the theory behind the calculations, the focus for each software package will be different.

The notations in this chapter changes for each subsection in order to use the same notation as in the given programs.

4.2 Design with "FEM design"

4.2.1 Ultimate limit state (ULS)

The "FEM design" software package from StruSoft is an advanced design tool for concrete, steel, and timber. The primary source of information for this chapter is "FEM-Design, Applied Theory and Design" [9].

When deciding the mesh density, one should be aware of the fact that "FEM design" only uses Mindlin plates. If the plate is thin, the mesh near edges needs to be very fine to capture the effect of the decreasing twisting moment. It is also worth noticing that "FEM design" uses an average value for the nodal forces between elements of the same kind. This is done to avoid discontinuities generated from the FEM calculation. The "FEM design" theory background does, unfortunately, not document what method is used for the stress smoothing.

"FEM design" can calculate the necessary reinforcement in either the whole structure or in selected parts. It is also possible to manually edit the reinforcement lay-out by deleting or adding reinforcement bars, and then let the program calculate utilization factors for the bars. The reinforcement bars can be placed in two arbitrary directions, and they don't have to be perpendicular to each other. The directions of the reinforcement are called ξ and η, and the angles between the reinforcement directions and the global x-axis are called α and β, respectively. The various directions and angles are shown in Figure 4.1 [9].
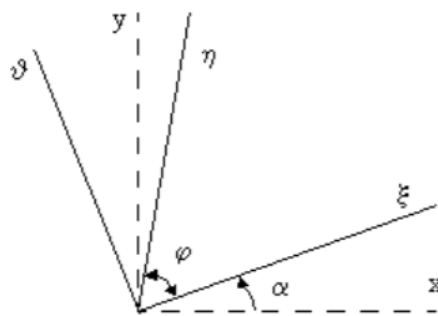
Figure 4.1: Coordinate system in "FEM design" [9]

The first step of the automatic design procedure is to translate the moments from the x-y coordinate system to the ξ-ϑ coordinate system, with the use of the rotation matrix, R_α, see Eq.(4.1). The results are the formulas given in Eqs. (4.2) - (4.4). Notice that the ϑ-direction is perpendicular to the ξ-direction, and not necessarily equal to the second reinforcement direction, η [9].

$$M'_{\xi\vartheta} = R_\alpha M R_\alpha^T$$

$$M'_{\xi\vartheta} = \begin{bmatrix} m_\xi & m_{\xi\vartheta} \\ m_{\xi\vartheta} & m_\vartheta \end{bmatrix}, R_\alpha = \begin{bmatrix} cos\alpha & sin\alpha \\ -sin\alpha & cos\alpha \end{bmatrix}, M = \begin{bmatrix} m_{xx} & m_{xy} \\ m_{xy} & m_{yy} \end{bmatrix} \tag{4.1}$$

$$m_\xi = \frac{m_x + m_y}{2} + \frac{m_x - m_y}{2}cos2\alpha + m_{xy}sin2\alpha \tag{4.2}$$

$$m_\vartheta = \frac{m_x + m_y}{2} - \frac{m_x - m_y}{2}cos2\alpha - m_{xy}sin2\alpha \tag{4.3}$$

$$m_{\xi\vartheta} = -\frac{m_x - m_y}{2}sin2\alpha + m_{xy}cos2\alpha \tag{4.4}$$

Secondly, the moments are rotated to the ξ-η-coordinate system by use of the R_φ matrix, see Eq. (4.5).

$$M'_{\xi\eta} = R_\varphi M'_{\xi\vartheta} R_\varphi^T$$

$$M'_{\xi\eta} = \begin{bmatrix} m_\xi & m_{\xi\eta} \\ m_{\xi\eta} & m_\eta \end{bmatrix}, R_\varphi = \begin{bmatrix} sin\varphi & -cos\varphi \\ 0 & 1 \end{bmatrix}, \tag{4.5}$$

When the moments in the reinforcement directions are found, the program calculates four cases of possible design moment pairs, which are called case a), b), ξ), and η). Reinforcement in both directions are needed in the cases a) and b), and the design moments are basically just the moments perpendicular to the reinforcement axes, see Figure 4.2. These design moments can be written as Eqs. (4.6) and (4.7), where x' and y' represent the reinforcement directions (ξ and η).

$$m_1' = m_{xx}' \pm m_{xy}' \tag{4.6}$$

$$m_2' = m_{yy}' \pm m_{xy}' \tag{4.7}$$
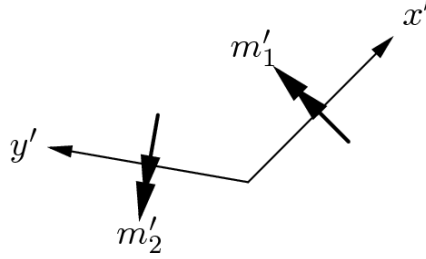
Figure 4.2: Design moments normal to the reinforcement directions [10]

In Cases ξ) and η) on the other hand, one of the reinforcement moments are set to zero because only reinforcement in one direction is needed. The other reinforcement moment is found from optimal reinforcement amount consideration.

The four cases as they are written in "FEM design", with respect to moments in the ξ-ϑ-coordinate system, are listed in Eqs. (4.8)-(4.15). A case is valid if the signs of m_ξ and m_η are equal, and $\overline{m}_\eta + \overline{m}_\xi > m_x + m_y$. If a valid moment pair is positive, then these are the design moments for the bottom reinforcement. If, however, the valid moment pair is negative, these moments should be used for design of the top reinforcement.

Case a)

$$\overline{\mathrm{m}}_\xi = m_\xi - m_\vartheta \frac{\cos\varphi}{1 + \cos\varphi} + m_{\xi\vartheta} \frac{1 - 2\cos\varphi}{\sin\varphi} \tag{4.8}$$

$$\overline{\mathrm{m}}_\eta = m_\vartheta \frac{1}{1 + \cos\varphi} + m_{\xi\vartheta} \frac{1}{\sin\varphi} \tag{4.9}$$

Case b)

$$\overline{\mathrm{m}}_\xi = m_\xi + m_\vartheta \frac{\cos\varphi}{1 - \cos\varphi} - m_{\xi\vartheta} \frac{1 + 2\cos\varphi}{\sin\varphi} \tag{4.10}$$

$$\overline{\mathrm{m}}_\eta = m_\vartheta \frac{1}{1 - \cos\varphi} - m_{\xi\vartheta} \frac{1}{\sin\varphi} \tag{4.11}$$

case ξ)

$$\overline{m}_\xi = m_\xi - \frac{m_{\xi\vartheta}^2}{m_\vartheta} \tag{4.12}$$

$$\overline{m}_\eta = 0 \tag{4.13}$$

case η)

$$\overline{m}_\xi = 0 \tag{4.14}$$

$$\overline{m}_\eta = \frac{m_\xi m_\vartheta - m_{\xi\vartheta}^2}{m_\xi(sin\varphi)^2 + m_\vartheta(cos\varphi)^2 - m_{\xi\vartheta}sin2\,\varphi} \tag{4.15}$$

When the design moments are calculated, the last step is to find the necessary reinforcement amount for each direction in the top and bottom layer. This is done with a simplified stress distribution from EC2 as illustrated in Figure 4.3. It is assumed that the compressive stress is rectangular distributed with a value of ηf_{cd} over a depth of λx. The values of λ and η depends on the concrete strength, and are in accordance with EC2 3.1.7 [8].
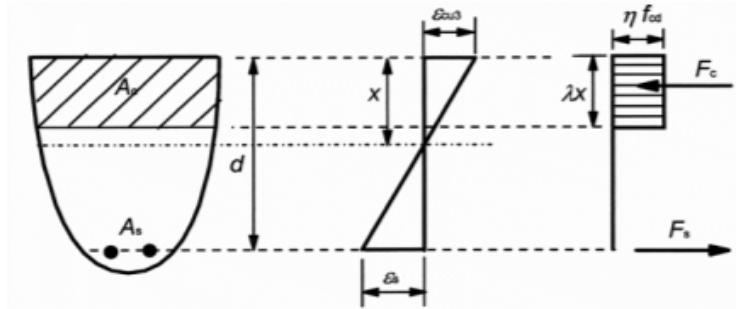
Figure 4.3: Rectangular stress distribution [8]

Moment equilibrium of the cross section gives λx, see Eq. (4.16):

$$\overline{m}_{\xi/\eta} = F_c * (d - \frac{\lambda x}{2}) \tag{4.16}$$

The necessary reinforcement can be found from equilibrium between the stress resultants, see Eqs. (4.17)-(4.19), where a_s is the necessary reinforcement amount per length and f_{yd} is the steel yield strength of the steel [8].

$$F_c = F_s \tag{4.17}$$

$$\lambda x * \eta * f_{cd} = a_s * f_{yd} \tag{4.18}$$

$$a_s = \frac{\lambda x * \eta * f_{cd}}{f_{yd}} \tag{4.19}$$

The result can be displayed like in Figure 4.4. The figure shows the required reinforcement in mm^2/m for a quadratic plate with sides equal to 10 m, and thickness of 0.2 m. The plate is simply supported on all edges, and has a uniformly distributed surface load of 10 kN/m. The element borders are shown with blue lines, and the nodes are illustrated with circles. It can be seen that "FEM design" uses 9-node plate elements in this case, but 6-node triangular elements are also available for bending plates.
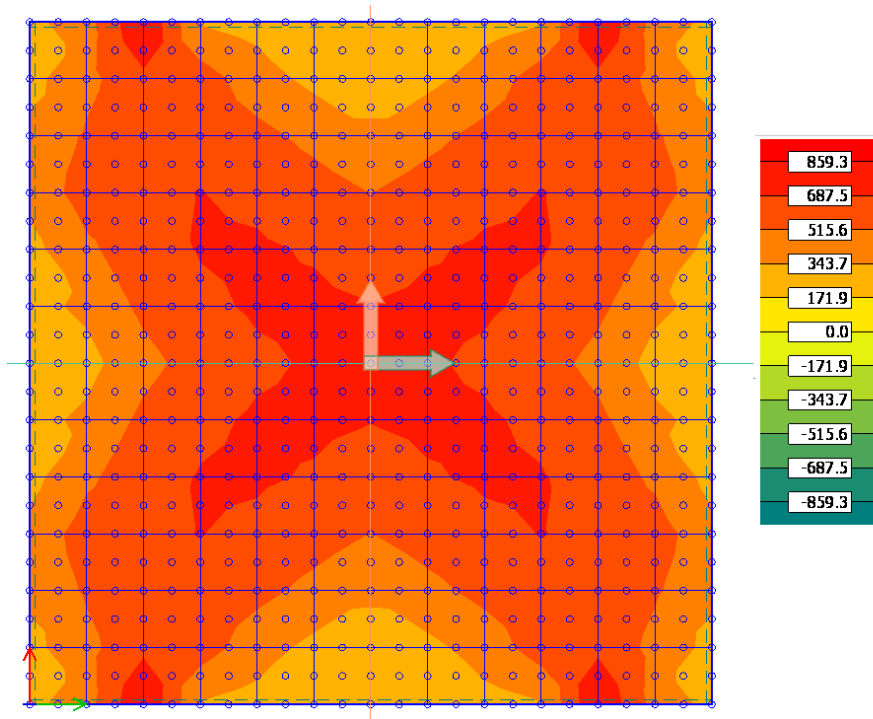
Figure 4.4: Example of design output from "FEM design" [mm^2/m]

The "FEM design" software supports peak smoothing over singularity regions. this means that the program calculates an average moment over a chosen distribution region. Figure 4.5 shows how smoothing over a column peak can look like in the program.
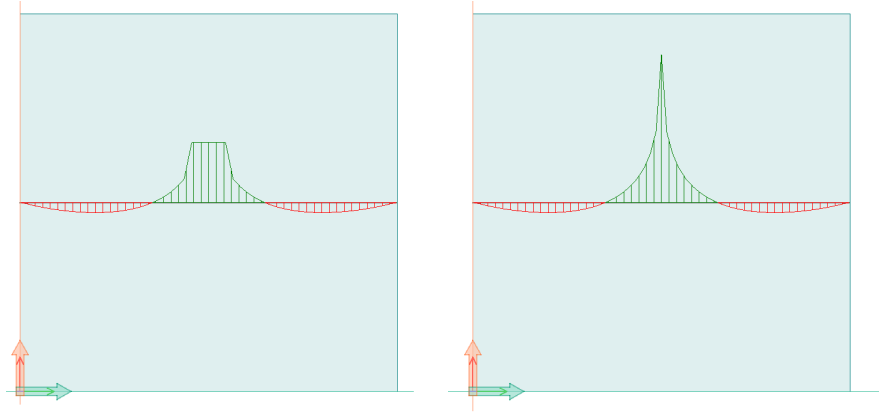
Figure 4.5: Example of peak smoothing with "FEM design"

4.2.2 Serviceability Limit State (SLS)

"FEM design" can perform crack- and deflection control of the structure. This is done according to EC2 7.3.4 and 7.4.3, respectively [8]. The user can do the control assuming either cracked or uncracked concrete. If the concrete is uncracked, the full stiffness of the structure will be used. If the concrete is cracked, however, the stiffness will be reduced to somewhere in between the stiffness of an uncracked and fully cracked structure. The correct stiffness is found by iterations according to the workflow illustrated in Figure 4.6 until the deflection from two consecutive calculations differ with less than a chosen percentage, or the maximum allowed number of iterations is reached. The calculations are based on either the applied or the required reinforcement. If it is based on the required reinforcement, the reinforcement in each element is the maximum required reinforcement calculated from all load cases.
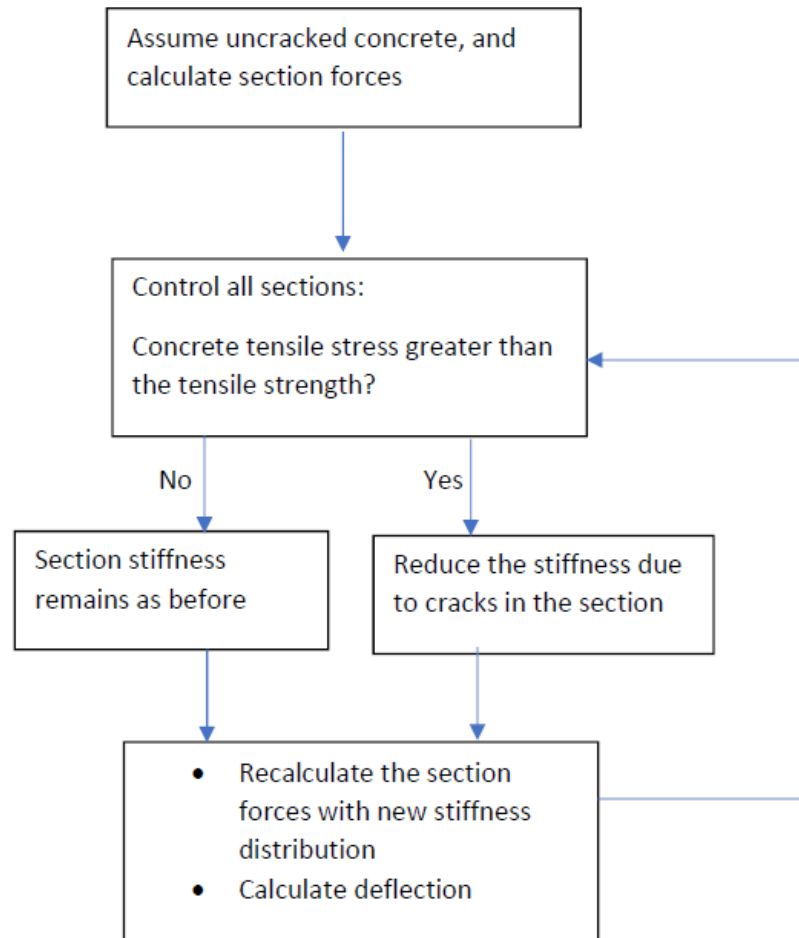
Figure 4.6: The workflow of the stiffness iteration in "FEM design"

4.2.3 Verification

In order to verify the automatic design method in "FEM design", a plate element subjected to constant moments are designed both by hand, and in the program. The input parameters are:

Concrete C30/37

h = 200 mm

f_{cd} = 17 MPa

E_s = 200 GPa

f_{yd} = 434.8 MPa

Ø = 10 mm (reinforcement diameter)

$c_x = 20$ mm; $c_y = 30$ mm (concrete cover)

$d_x = 175$ mm; $d_y = 165$ mm (effective heights)

The plate element is loaded with edge moments as illustrated in Figure 4.7, and is supported by spring supports in each corner with negligible small stiffness in order to achieve constant moments.
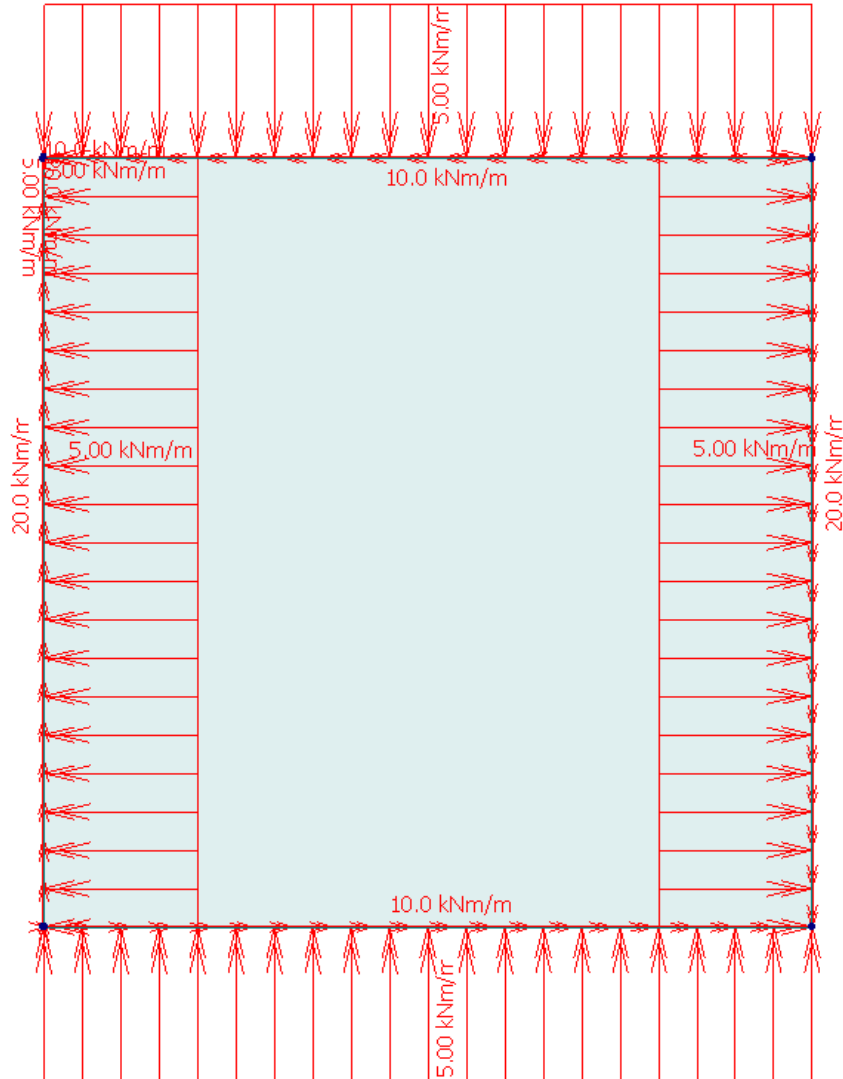
Figure 4.7: Applied edge moments on the plate

For orthogonal reinforcement where ξ corresponds with the global x-direction, and η corresponds with the y-direction ($\varphi=90°$):

$$m_x = m_\xi = 20\,kNm/m \tag{4.20}$$

$$m_y = m_\vartheta = m_\eta = -10\,kNm/m \tag{4.21}$$

$$m_{xy} = m_{\xi\vartheta} = m_{\xi\eta} = 5kNm/m \tag{4.22}$$

The four possible design moment pairs are then:

Case a)

$$\overline{m}_\xi = m_\xi - m_\vartheta \frac{cos\varphi}{1+cos\varphi} + m_{\xi\vartheta}\frac{1-2\,cos\varphi}{sin\varphi} = m_\xi + m_{\xi\vartheta} = 25\,kNm/m \tag{4.23}$$

$$\overline{m}_\eta = m_\vartheta \frac{1}{1+cos\varphi} + m_{\xi\vartheta}\frac{1}{sin\varphi} = m_\vartheta + m_{\xi\vartheta} = -5\,kNm/m \tag{4.24}$$

Case b)

$$\overline{m}_\xi = m_\xi + m_\vartheta \frac{cos\varphi}{1-cos\varphi} - m_{\xi\vartheta}\frac{1+2\,cos\varphi}{sin\varphi} = m_\xi - m_{\xi\vartheta} = 15\,kNm/m \tag{4.25}$$

$$\overline{m}_\eta = m_\vartheta \frac{1}{1-cos\varphi} - m_{\xi\vartheta}\frac{1}{sin\varphi} = m_\vartheta - m_{\xi\vartheta} = -15kNm/m \tag{4.26}$$

Case ξ)

$$\overline{m}_\xi = m_\xi - \frac{m_{\xi\vartheta}^2}{m_\vartheta} = 22.5\,kNm/m \tag{4.27}$$

$$\overline{m}_\eta = 0 \tag{4.28}$$

Case η)

$$\overline{m}_\xi = 0 \tag{4.29}$$

$$\overline{m}_\eta = \frac{m_\xi m_\vartheta - m_{\xi\vartheta}^2}{m_\xi(sin\varphi)^2 + m_\vartheta(cos\varphi)^2 - m_{\xi\vartheta}sin2\,\varphi} = \frac{m_\xi m_\vartheta - m_{\xi\vartheta}^2}{m_\xi} = -11.25\,kNm/m \tag{4.30}$$

The cases a) and b) are invalid solutions because $\overline{m}_\eta$ and $\overline{m}_\xi$ have different signs. Cases ξ) and η) on the other hand, are valid solutions, because the signs are equal, and $\overline{m}_\eta + \overline{m}_\xi$

$\geq m_x + m_y$. Case ξ) will be used to calculate the bottom reinforcement since the moment is positive, and case η) will be used to calculate the top reinforcement. An overview of the design moments are shown in Figure 4.8.
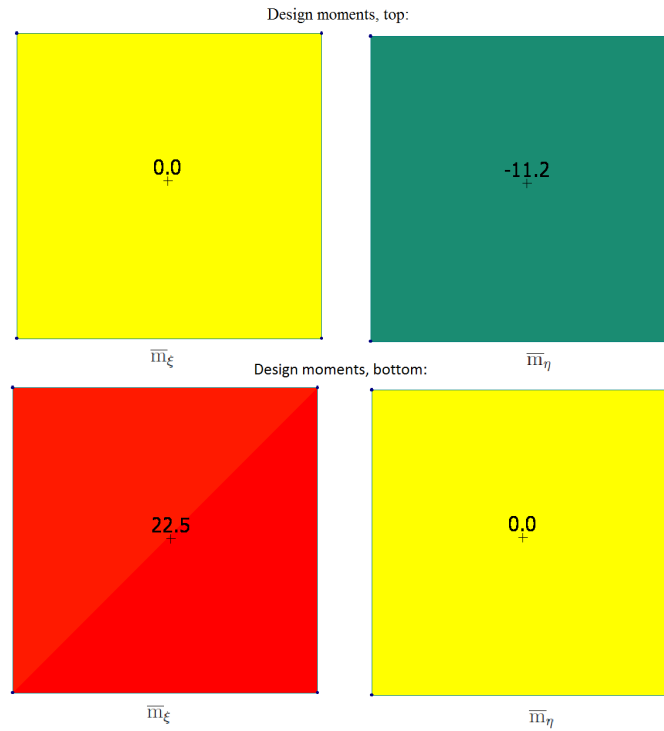
Figure 4.8: The design moments for hyperbolic bending with orthogonal reinforcement [kNm/m]

Calculation of the required bottom reinforcement in the ξ-direction:

$$\overline{m}_\xi = f_{cd} \times \lambda x (d - \frac{\lambda x}{2}) \tag{4.31}$$

$$22500 \frac{Nmm}{mm} = 17 \frac{N}{mm^2} \times \lambda x (175mm - \frac{\lambda x}{2}) \tag{4.32}$$

$$\lambda x = 7.73\, mm \tag{4.33}$$

$$a_{s\xi} = \frac{\lambda x \times \eta * \times f_{cd}}{f_{yd}} \tag{4.34}$$

$$a_{s\xi} = \frac{7.73mm \times 1.0 \times 17N/mm^2}{434.8N/mm^2} \tag{4.35}$$

$$a_{s\xi} = 0.3022\, mm^2/mm = \underline{302.2\, mm^2/m} \tag{4.36}$$

The top reinforcement in the η-direction is calculated in the same way, and gives $a_{s\eta} = 158.7mm^2/m$, see Eqs (4.37)-(4.40). Figure 4.9 shows the required reinforcement results from "FEM design" which correlates very well with the values calculated by hand. The small deviations are due to rounding errors.

$$11250\frac{Nmm}{mm} = 17\frac{N}{mm^2} \times \lambda x(165mm - \frac{\lambda x}{2}) \tag{4.37}$$

$$\lambda x = 4.06\,mm \tag{4.38}$$

$$a_{s\eta} = \frac{4.06mm \times 1.0 \times 17N/mm^2}{434.8N/mm^2} \tag{4.39}$$

$$a_{s\eta} = 0.1587\,mm^2/mm = 158.7\,mm^2/m \tag{4.40}$$
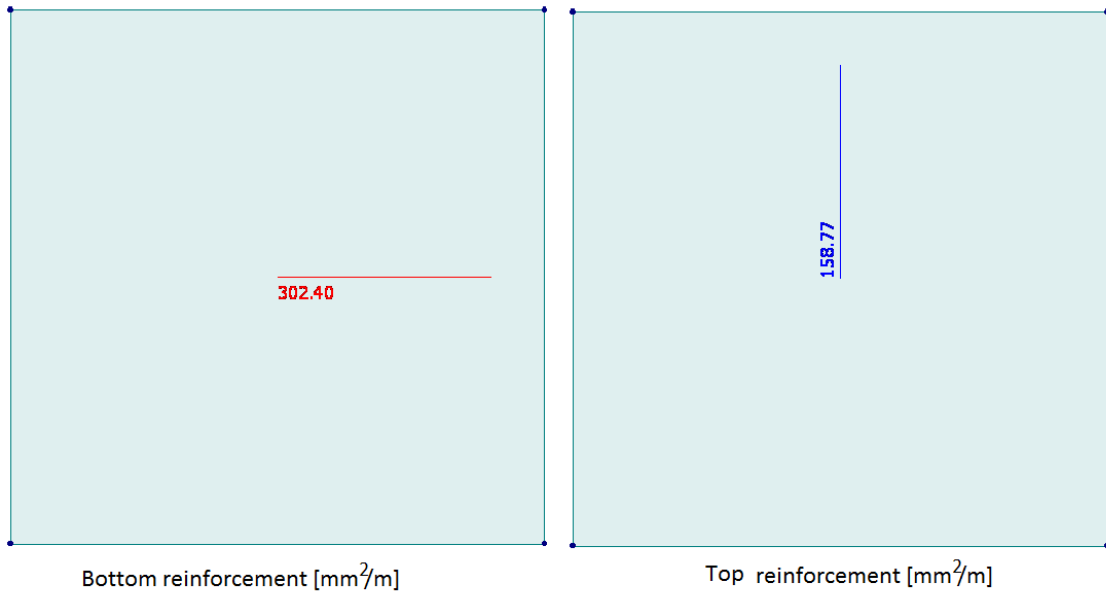
Figure 4.9: The required reinforcement for hyperbolic bending with orthogonal reinforcement in "FEM design" $[mm^2/\mathrm{m}]$

If the reinforcement is non-orthogonal, the calculation will appear slightly different than for the orthogonal case. Even though it is unpractical to use non-orthogonal reinforcement, it might be necessary because of the geometry of the structure. Therefore, a new verification is done for an angle of $\vartheta = 75°$ between ξ and η, where ξ corresponds with the global x-axis, as illustrated in Figure 4.10. The moment input is as shown in Eqs. (4.41)-(4.43).

$$m_x = m_\xi = 20 \, kNm/m \tag{4.41}$$

$$m_y = m_\vartheta = -10 \, kNm/m \tag{4.42}$$

$$m_{xy} = m_{\xi\vartheta} = 5 \, kNm/m \tag{4.43}$$
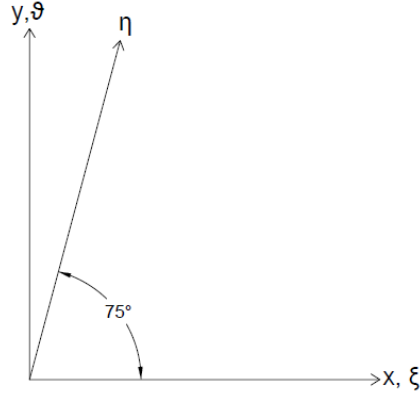
Figure 4.10: Coordinate-system for calculation with non-orthogonal reinforcement

The four possible design moment pairs are then:

Case a)

$$\overline{m}_\xi = m_\xi - m_\vartheta \frac{\cos(75°)}{1 + \cos(75°)} + m_{\xi\vartheta} \frac{1 - 2\cos(75°)}{\sin(75°)} = 24.55 \, kNm/m \tag{4.44}$$

$$\overline{m}_\eta = m_\vartheta \frac{1}{1 + \cos(75°)} + m_{\xi\vartheta} \frac{1}{\sin(75°)} = -2.76 \, kNm/m \tag{4.45}$$

Case b)

$$\overline{m}_\xi = m_\xi + m_\vartheta \frac{\cos(75°)}{1 - \cos(75°)} - m_{\xi\vartheta} \frac{1 + 2\cos(75°)}{\sin(75°)} = 8.65 \, kNm/m \tag{4.46}$$

$$\overline{m}_\eta = m_\vartheta \frac{1}{1 - \cos(75°)} - m_{\xi\vartheta} \frac{1}{\sin(75°)} = -18.67 \, kNm/m \tag{4.47}$$

Case ξ)

$$\overline{m}_\xi = m_\xi - \frac{m_{\xi\vartheta}^2}{m_\vartheta} = 22.5 \, kNm/m \tag{4.48}$$

$$\overline{m}_\eta = 0 \tag{4.49}$$

Case η)

$$\overline{m}_\xi = 0 \tag{4.50}$$

$$\overline{m}_\eta = \frac{m_\xi m_\vartheta - m_{\xi\vartheta}^2}{m_\xi(sin^2(75°)) + m_\vartheta(cos^2(75°)) - m_{\xi\vartheta}sin(2 \times 75°)} = -14.53\,kNm/m \tag{4.51}$$

The cases a) and b) are, as discussed earlier, not valid because the signs of the moment pairs are unequal. Case ξ) will give the same amount of required bottom reinforcement as for the previous example with orthogonal reinforcement ($a_{s\xi} = 302.2\,mm^2/m$). The top reinforcement, however, has to be re-calculated:

$$\overline{m}_\eta = f_{cd} \times \lambda x(d - \frac{\lambda x}{2}) \tag{4.52}$$

$$14530\frac{Nmm}{mm} = 17\frac{N}{mm^2} \times \lambda x(165mm - \frac{\lambda x}{2}) \tag{4.53}$$

$$\lambda x = 5.26\,mm \tag{4.54}$$

$$a_{s\eta} = \frac{\lambda x \times \eta \times f_{cd}}{f_{yd}} \tag{4.55}$$

$$a_{s\eta} = \frac{5.26mm \times 1.0 \times 17N/mm^2}{434.8N/mm^2} \tag{4.56}$$

$$a_{s\eta} = 0.2057\,mm^2/mm = 205.7\,mm^2/m \tag{4.57}$$

The required reinforcement calculated in "FEM design" is shown in Figure 4.11, and the small deviation from the values calculated by hand are only due to rounding errors.
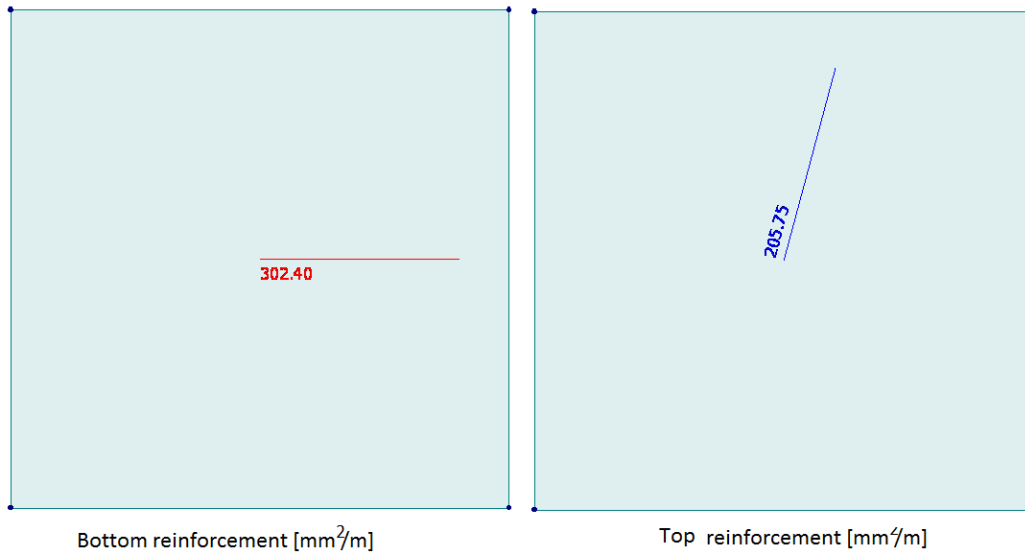
Figure 4.11: The required reinforcement for hyperbolic bending with non-orthogonal reinforcement $[mm^2/\text{m}]$

The top-reinforcement is increased with almost 30% compared to the solution with orthogonal reinforcement. This is due to the fact that the reinforcement direction, η, is further away from the principal moment direction. The directions of the principal moments are shown in Figure 4.12; it is rotated 9.2° anticlockwise relative to the global coordinate system, see Eq. (4.58).

$$\alpha_0 = arctan\left(\frac{m_1 - m_x}{m_{xy}}\right) = arctan\left(\frac{20.81 - 20}{5}\right) = 9.2° \qquad (4.58)$$
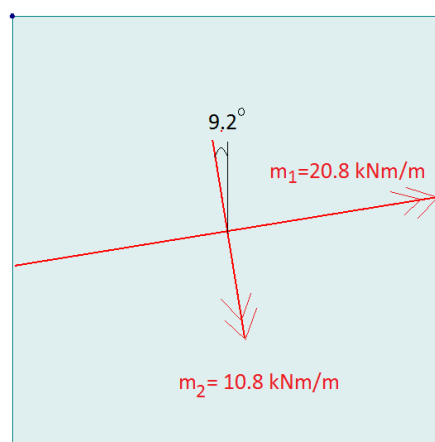
Figure 4.12: The principal moments in the plate [kNm/m]

69

4.3 Design with "Robot Structural Analysis Professional"

4.3.1 Ultimate Limit State (ULS)

"Robot Structural Analysis Professional" ("Robot") is a program from Autodesk. "Robot" supports analysis and design of several different structure components, including concrete slabs. Most of the information presented in this chapter has been found in Robot's "User's Guide" [11].

For plane elements in bending state, discrete Kirchhoff-Mindlin triangles or quadrilaterals are used with a one or four point Gaussian quadrature, respectively. Similar to Mindlin plate elements, these elements include shear strain fields. However, contrary to Mindlin elements, they prevent the problem with shear locking for thin plates [17].

The internal forces can be displayed with either global smoothing, local smoothing, averaged values in element centres or without any stress smoothing. How the stresses from the integration points are extrapolated to the nodes is unclear in the "User's Guide".

"Robot" has three different methods for determining required reinforcement in plates and shells:

- Analytical method
- Equivalent moment method (Wood & Armer) [18]
- Equivalent moment method according to the Netherlands Standardization Institute (NEN)

The NEN- and the Wood & Armer method are both simplified methods which enable faster calculations, and normally sufficiently accurate results for plates in pure bending or bending with only small membrane forces. For shell structures with both bending and membrane forces, the analytical method must be used. Because these scenarios are not relevant for this thesis, it won't be described further.

The workflow of the Wood & Armer method is showed in Figure 4.13, where x and y are the chosen directions of the reinforcement.
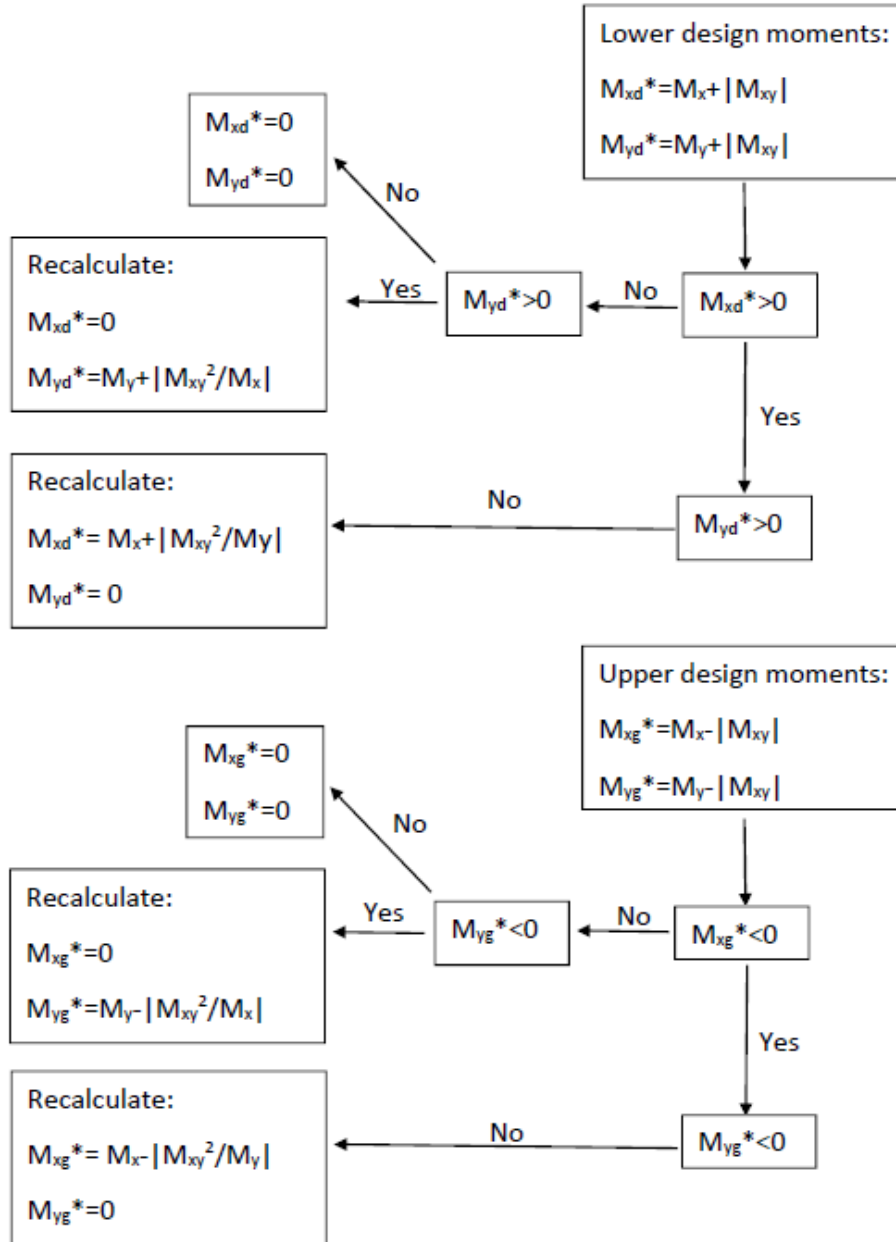
Figure 4.13: Dimensioning of slabs according to Wood & Armer

A positive moment gives tension at the bottom of the plate, while a negative moment gives tension at the top. The formulas for design moments are found from the compression field theory described for the sandwich model method in Section 3.3, see Eqs.(4.59) and (4.60).

$$M_{xd}^* = M_x + |M_{xy}| \tan\theta \qquad (4.59)$$

$$M_{yd}^* = M_y + |M_{xy}| \cot\theta \qquad (4.60)$$

If the design moment $M_{xd}^* \geq 0$, the angle to the compression strut in the concrete, θ, can be assumed to be $\pm\frac{\pi}{4}$, which gives the minimum total amount of reinforcement. If, however, the design moment $M_{xd}^* \leq 0$, there is no tension at the bottom in the x-direction, so M_{xd}^* is set to zero. The design moment in the y-direction should therefore be recalculated with a new θ for optimal reinforcement amount. This is found by inserting $M_{xd}^*{=}0$ in Eq. (4.59), resulting in $\cot\theta = M_{xy}/|M_x|$, and then use this in Eq (4.60). The same procedure is followed for the y-direction [11].

Correspondingly, if the design moment $M_{xg}^* \geq 0$, there is no tension at the top of the plate in the x-direction, and M_{xg}^* is set to zero, while M_{yg}^* is recalculated with a new θ [11]. When the reinforcement is orthogonal, this method equals the method from "FEM design". Another commonality is the fact that the internal lever arm is found by assuming a rectangular stress distribution in the cross section.

The NEN method is a simplification of the Wood & Armer method, where it is assumed that the compression strut angle always is $\pm\frac{\pi}{4}$. Hence, the design moments are simply given as in Eqs. (4.61) and (4.62) for both the upper and lower reinforcement [11].

$$M_x^* = M_x \pm |M_{xy}| \qquad (4.61)$$

$$M_y^* = M_y \pm |M_{xy}| \qquad (4.62)$$

If this method is used, the required reinforcement amount increases compared to the Wood & Armer method. This can be illustrated with the same example as was used in the verification of the "FEM design" program where a plate element was loaded with constant moments, and given orthogonal reinforcement:

$$m_x = 20kNm/m \tag{4.63}$$

$$m_y = -10kNm/m \tag{4.64}$$

$$m_{xy} = 5kNm/m \tag{4.65}$$

With the NEN-method, this results in a bottom reinforcement in the x-direction of 337.0 mm^2/m, and an upper reinforcement in the y-direction of 212.7 mm^2/m, see Eqs. (4.66)-(4.79). The increase in the reinforcement amount, is as much as 11% and 34%, respectively, compared to the values from the more complex Wood & Armer method. The values for the Wood & Armer method are the same as the values calculated in Section 4.2.3 for "FEM design".

$$M_{xd}^* = 20 + 5 = 25\,kNm/m\,(lower) \tag{4.66}$$

$$M_{yg}^* = -10 - 5 = -15\,kNm/m\,(upper) \tag{4.67}$$

$$M_{xd}^* = f_{cd} \times \lambda x(d - \frac{\lambda x}{2}) \tag{4.68}$$

$$25000\frac{Nmm}{mm} = 17\frac{N}{mm^2} \times \lambda x(175mm - \frac{\lambda x}{2}) \tag{4.69}$$

$$\lambda x = 8.62\,mm \tag{4.70}$$

$$a_{sx} = \frac{\lambda x \times \eta \times f_{cd}}{f_{yd}} \tag{4.71}$$

$$a_{sx} = \frac{8.62mm \times 1.0 \times 17N/mm^2}{434.8N/mm^2} \tag{4.72}$$

$$a_{sx} = 0.3370\,mm^2/mm = \underline{337.0\,mm^2/m} \tag{4.73}$$

$$M_{yg}^* = f_{cd} \times \lambda x(d - \frac{\lambda x}{2}) \tag{4.74}$$

$$15000\frac{Nmm}{mm} = 17\frac{N}{mm^2} \times \lambda x(165mm - \frac{\lambda x}{2}) \tag{4.75}$$

$$\lambda x = 5.44\,mm \tag{4.76}$$

$$a_{sy} = \frac{\lambda x \times \eta \times f_{cd}}{f_{yd}} \tag{4.77}$$

$$a_{sy} = \frac{5.44mm \times 1.0 \times 17N/mm^2}{434.8N/mm^2} \tag{4.78}$$

$$a_{sy} = 0.2127\, mm^2/mm = \underline{212.7\, mm^2/m} \tag{4.79}$$

4.3.2 Serviceability Limit State (SLS)

The SLS deformation calculation in "Robot" is based on the elastic deformation, but it is linearly scaled to compensate for cracking and applied reinforcement, see Eqs. (4.80) and (4.81) [11].

$$u_R^i = u^i * \frac{D}{B} \tag{4.80}$$

$$D = E * \frac{1[m] * h^3}{12} \tag{4.81}$$

u_R^i: The real displacement in point i in the plate

u^i: The elastic displacement in point i

D: Elastic stiffness of the plate

B: Equivalent stiffness of the reinforced slab

The equivalent stiffness, B, is an averaged value of the equivalent stiffness in each reinforcement direction, B_x and B_y. The averaging is done according to Eq. (4.82) [11].

$$B_{x,y}^i = c_f * B_x + (1 - c_f) * B_y \tag{4.82}$$

The coefficient, c_f, is a weight coefficient which depends on the moment ratio, and is calculated according to Eq. (4.83). If the ratio between the moments in the two directions of the reinforcement is more than four, the equivalent stiffness in the direction of the greatest moment will be decisive.

$$c_f = 1,0 \qquad\qquad for \quad \frac{|M_{xx}|}{|M_{yy}|} > 4$$

$$c_f = 0,5 + \frac{2}{3} * \frac{|M_{xx}| - |M_{yy}|}{max(|M_{xx}|; |M_{yy}|)} \qquad for \quad 0.25 \le \frac{|M_{xx}|}{|M_{yy}|} \le 4 \qquad (4.83)$$

$$c_f = 0,0 \qquad\qquad for \quad \frac{|M_{xx}|}{|M_{yy}|} < 0.25$$

The next step is to calculate the average stiffness ratio, D/B, by using the formula shown below, where $B(M_{max})$ is the equivalent stiffness of the element containing the maximum moment in any direction.

$$\frac{D}{B} = 0,25 * \left(\frac{D}{B_{xy}^i}\right) + 0,75 * \left(\frac{D}{B(M_{max})}\right) \qquad (4.84)$$

The equivalent stiffness (elastic) method, described above, averages the stiffness for all finite elements, so that the whole plate is assigned the same stiffness. The resulting deflection is therefore the elastic deflection times the average stiffness ratio, as illustrated in the left part of Figure 4.14. However, if a method with stiffness update is used (inelastic method), the stiffness is calculated independently for each element and each direction, resulting in an anisotropic plate of varying rigidity, as illustrated to the right of Figure 4.14 [11].
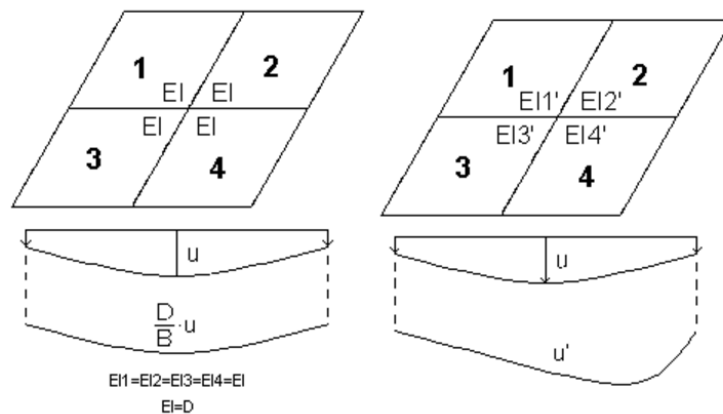
Figure 4.14: Left: Stiffness averaged for all elements. Right: Different stiffness for all elements [11]

The crack control in "Robot" is done by direct calculation of the crack width, according to Eurocode 2, based on the equivalent moments in the two reinforcement directions. For both the crack calculation and the deflection calculation, "Robot" offers to automatically increase the tension reinforcement if the crack width or the deflection is too high [11].

4.4   Design with "DIANA"

4.4.1   Ultimate Limit State (ULS)

"DIANA" (DIsplacement ANAlyzer) is a finite element software package, developed by DIANA FEA BV, which is able to both find the required reinforcement, and to calculate the utilization of the applied reinforcement. The reinforcement bars can be applied in two directions which don't necessarily have to be orthogonal. "DIANA" can design both thick and thin plates since both Kirchhoff and Mindlin plates are offered. The information source for major parts of this chapter is "DIANA User's Manual" [10].

The first step of the plate design in "DIANA" is to rotate the calculated internal forces, m_x, m_y, and m_{xy} to the chosen direction of the reinforcement. This is done similarly to what was described previously for "FEM design" in Section 4.2.1.

Like in the sandwich model, "DIANA" transforms the internal forces to in-plane forces in a top- and a bottom layer. As discussed in Chapter 3.3, the sandwich model assumes the layer thicknesses to be two times the concrete cover, and the lever arm to be the distance between the midpoints. "DIANA", however, sets the lever arm as the effective depth of the plate, d, times a relative lever arm, z_r, as illustrated in Figure 4.15. The value of z_r depends on the ratio between the bending moments and the membrane forces, and is by default set to 0.9 [10].
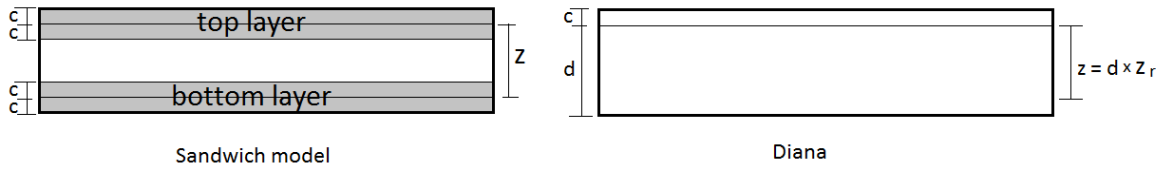
Figure 4.15: Different internal lever arms [7]

The next step is to calculate the reinforcement forces. This is similar to F_{sx} and F_{sy} in the sandwich model, except for the fact that "DIANA" assumes the crack angle to always be 45° which normally gives the smallest amount of reinforcement. This method is similar to the previously described NEN-method in Section 4.3.1, except for the fact that "DIANA" works with equivalent in-plane forces instead of design moments. The reinforcement forces in "DIANA" are called $n_1^{\prime c}$ and $n_2^{\prime c}$, and are given in Eqs. (4.85) and (4.86) for the upper layer, and correspondingly for the bottom layer [10].

$$n_{1,up}^{\prime c} = n_{xx,up}^{\prime c} + n_{xy,up}^{\prime c} \ (= F_{sx'}) \tag{4.85}$$

$$n_{2,up}^{\prime c} = n_{yy,up}^{\prime c} + n_{xy,up}^{\prime c} \ (= F_{sy'}) \tag{4.86}$$

The required reinforcement per unit length is then calculated with Eqs. (4.87) and (4.88):

$$A_{req,x} = \frac{n_1^{\prime c}}{f_{yd}} \tag{4.87}$$

$$A_{req,y} = \frac{n_2^{\prime c}}{f_{yd}} \tag{4.88}$$

"DIANA" offers to check the utilization of applied reinforcement in the structure compared to the required amount. In addition, "DIANA" automatically does a unity check on the applied reinforcement related to the maximum and minimum reinforcement areas according to EC2.

Before the design check in "DIANA", the user has to specify the bar diameter and spacing for the reinforcement in both directions. However, the stiffness off the reinforcement grid is not accounted for as long as the grid is labelled for design check. If it is desired to account for the stiffness, "DIANA" either applies the reinforcement stiffness directly or automatically calculates and applies the equivalent thickness for the reinforcement grids [10].

Since the concrete compression capacity is reduced if a lateral tensile force is present, "DIANA" has several model options to calculate the reduction factor. This thesis won't go into detail about the models, but some of the available options are mentioned below. They all have in common that they depend on the cracking of the concrete due to the lateral tensile force.

- No reduction of the compressive strength

- Model of Vecchio and Collins 1993 [19]

- Model of Japan Society of Civil Engineers (JSCE) 2012 [20]

- Model with a multi-linear diagram

The shear capacity is controlled by calculating the principal shear force, referred to as q' in "DIANA", with Eq.(4.89). As long as q' is smaller than the shear compressive capacity and the shear tensile capacity, given in EC2 chapter 6, the capacity is sufficient [10].

$$q' = \sqrt{q_x^2 + q_y^2} \tag{4.89}$$

After the analysis are performed in "DIANA", there are many output options for the various results. Even though the results may look different with different output options, they are all based on the same results from the integration points. The available ways of displaying the stress, strain, etc. are listed below [10]:

- Constant per reinforcement (uses the maximum integration point value inside the grid)

- Constant per element (uses the maximum integration point value inside the element)

- Different for every integration point

- Extrapolated from the integration points to the nodes of the element

- Averaged in the direction normal to the reinforcement bars over a user defined length, which is related to the thickness of the plate. The average results over the reinforcement particles that are intersected by this line are calculated and displayed in the integration points.

4.4.2 Serviceability Limit State (SLS)

Since reinforced concrete is a non-linear material, but linear-elastic analysis is preferable, "DIANA" has an iterative method for calculating load distributions, deformations, crack patterns, and crack openings in the structure. The first step in the procedure is to calculate the stress distribution for an initial Young's modulus and a Poisson's ratio. The program then controls whether the stresses at all integration points are below a user-specified uniaxial stress-strain curve. If that is not the case, the concrete will crack, and the local stiffness will be reduced. This is illustrated in Figure 4.16, where the stress σ_0 is outside the stress-strain curve, and the stiffness is therefore changed from E_0 to E_1. The stress distribution is then re-calculated, and new stresses are found at the integration points. This procedure is repeated until all stresses are inside the curve, or the maximum allowable number of iterations is reached. The stiffness adaption analysis can be performed for various number of load steps. With large load increments, many integration points will reach too high stresses, and a widely spread area will obtain reduced stiffness. With small load increments, however, the cracks will be much more localized [10].
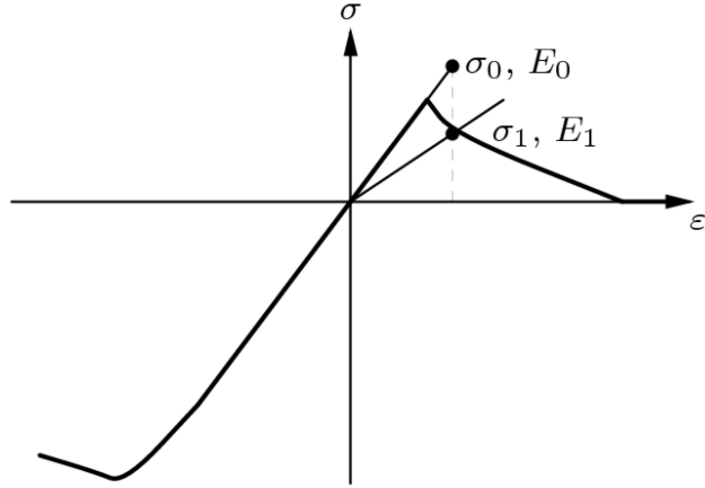
Figure 4.16: Uniaxial stress-strain curve with stress and stiffness reduction [10]

Whereas "FEM design" and "Robot" perform the crack control by direct calculation of the crack width, "DIANA" controls cracking without direct calculations, but instead restricts the bar diameter and spacing according to tabulated values in EC2 7.3.3. This is a simplified control used for slabs in buildings subjected to bending with limited tension, and overall thickness ≤200 mm. In order to use the simplified control, the requirements for minimum reinforcement and the structural rules for plates, given in EC2 9.3, should be fulfilled [8].

4.4.3 Verification

In order to verify the design procedure in "DIANA", the same example with a plate element subjected to a constant moment as was used for "FEM design" will be used here. Since "DIANA" has defined that positive moments give tension in the top of the plate, the bending moments have opposite signs of the "FEM design" example:

$$m'_{xx} = -20\,kNm/m \tag{4.90}$$

$$m'_{yy} = 10\,kNm/m \tag{4.91}$$

$$m'_{xy} = 5\,kNm/m \tag{4.92}$$

It is used an average value for the effective height in the x- and the y-direction, so that the internal lever arm, for both directions, is:

$$z_d = 0.9 * d = 0.9 * 170\,mm = 153\,mm \tag{4.93}$$

The imaginary in-plane forces in the top layer of the plate is then:

$$n'_{xx,up} = \frac{m'_{xx}}{z_d} = \frac{-20 * 10^6\,Nmm/m}{153\,mm} = -130718.95\,N/m \tag{4.94}$$

$$n'_{yy,up} = \frac{m'_{yy}}{z_d} = \frac{10 * 10^6\,Nmm/m}{153\,mm} = 65359.48\,N/m \tag{4.95}$$

$$n'_{xy,up} = \left| \frac{m'_{xy}}{z_d} \right| = \frac{5 * 10^6\,Nmm/m}{153\,mm} = 32679.74\,N/m \tag{4.96}$$

The imaginary in-plane forces in the bottom layer of the plate will be equal, except that the normal forces have opposite signs. Consequently, the design in-plane forces are:

$$n'^c_{1,up} = n'^c_{xx,up} + n'^c_{xy,up} = -98039.21\,N/m \tag{4.97}$$

$$n'^c_{1,low} = n'^c_{xx,low} + n'^c_{xy,low} = 163398.69\,N/m \tag{4.98}$$

$$n'^c_{2,up} = n'^c_{yy,up} + n'^c_{xy,up} = 98039.22\,N/m \tag{4.99}$$

$$n'^c_{2,low} = n'^c_{yy,low} + n'^c_{xy,low} = -32679.74\,N/m \tag{4.100}$$

Reinforcement is only required for positive values of the design forces. Consequently, reinforcement is only needed in the x-direction in the bottom layer, and in the y-direction in the top layer.

The calculated required reinforcement is then 375.8 mm^2 in the bottom layer, and 225.5 mm^2 in the top layer, see Eqs. (4.101) and (4.102):

$$A_{req,x} = \frac{n'^c_{1,low}}{f_{yd}} = \frac{163398.69\,N/m}{434.8\,MPa} = \underline{375.80\,mm^2/m} \tag{4.101}$$

$$A_{req,y} = \frac{n'^c_{2,up}}{f_{yd}} = \frac{98039.21\,N/m}{434.8\,MPa} = \underline{225.48\,mm^2/m} \tag{4.102}$$

The required reinforcement calculated in "DIANA" is shown in Figure 4.17, and the values correspond well with the values calculated by hand.
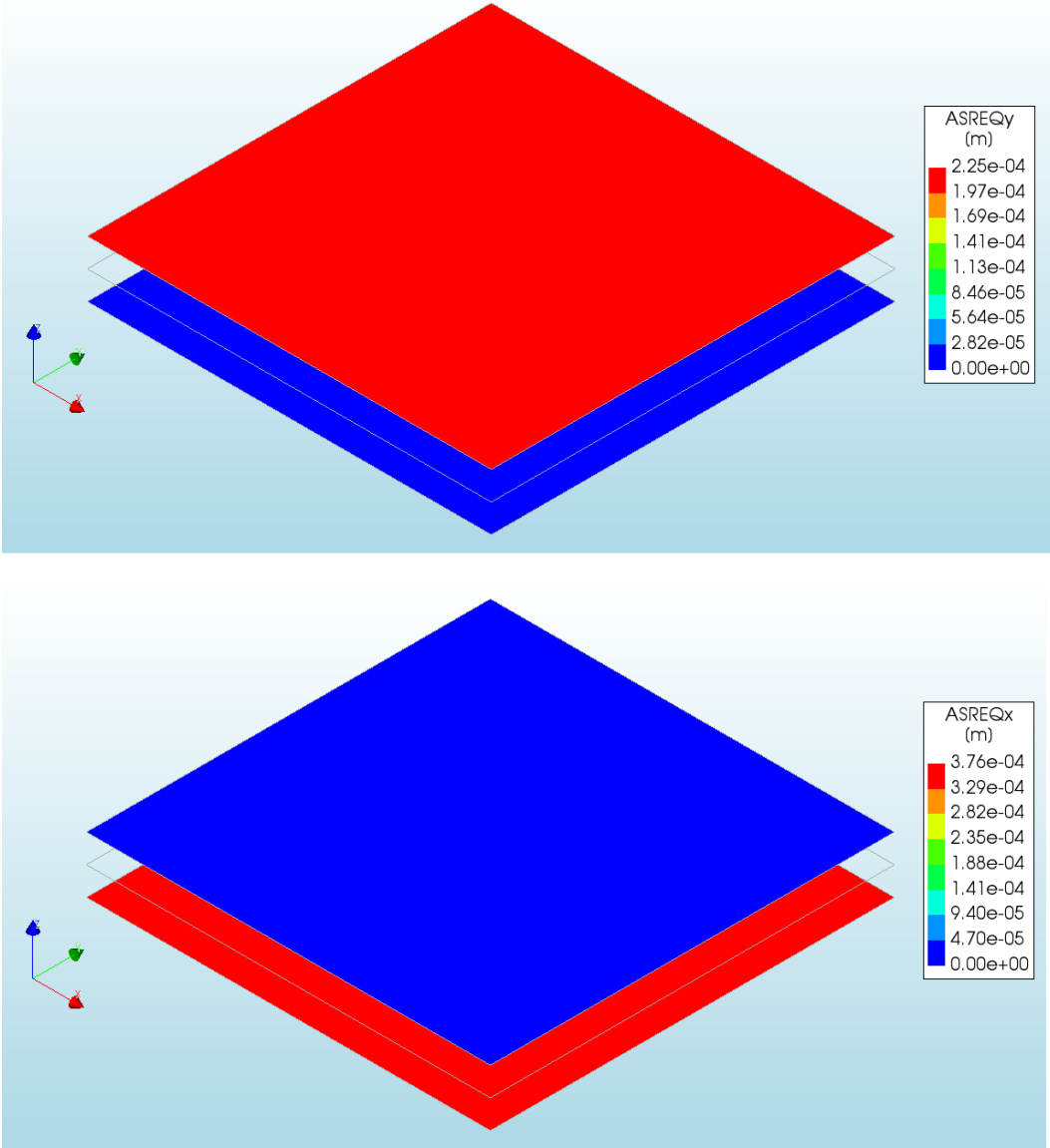

Figure 4.17: Required reinforcement in the y-direction (upper) and in the x-direction (lower)

4.5 Design with "SOFiSTiK"

4.5.1 Ultimate Limit State (ULS)

The software "SOFiSTiK" developed by SOFiSTiK AG offers several different FEM
packages which include all the necessary programs needed to analyse and design different
structures. The internal forces and moments are calculated with the program "ASE-General
Static Analysis of Finite Element Structures" (ASE). ASE makes use of Mindlin theory
in plate calculations. The program used for design is called "BEMESS", and it is the
focus of this chapter. Most of the information is found in the manual "BEMESS- Design
of Plates and Shells" [12].

"BEMESS" distinguishes between three different design cases:

- Disks

- Plates

- Shells

If disk is chosen, the structure is designed as a disk, even though out-of-plane forces might
actually be present in the structure [12].

An orthogonal reinforcement grid is in most cases the most effective solution, but "BEMESS"
also offers a two-course oblique reinforcement for slightly skew constructions, and three-course
oblique reinforcement for higher skewness than 60°. A radial and a tangential orthogonal
reinforcement is available for circular plates [12].

The principals of the plate design are similar to that of "DIANA". The moments are
initially transformed to the direction of the applied or calculated reinforcement directions.
Then, the internal lever arm is determined from the compression zone utilization, as
illustrated in Figure 4.18. The more utilized the compression zone is, the smaller the lever
arm; however, it is unclear which formula "BEMESS" uses in this calculation. The fictive
in-plane forces are calculated using the lever arm. Finally, the necessary reinforcement is
calculated according to the selected code [12].
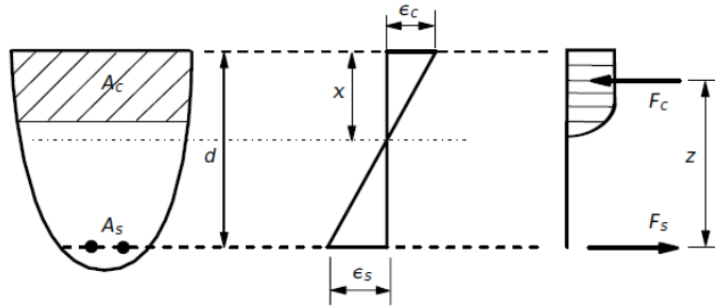
Figure 4.18: Stress and strain distributions in the cross-sections [12]

In "BEMESS", the shell design is very similar to the sandwich model, and can also be used for plate design. The plate thickness is divided into three layers, where the outer layers are given a thickness of 35% each of the total thickness. The lever arm is, in contrast to plate design, calculated assuming full utilization of the compressive zone. The average concrete cover between the two reinforcement directions is applied as concrete cover. An illustration of the different layers and the internal lever arm is shown in Figure 4.19.
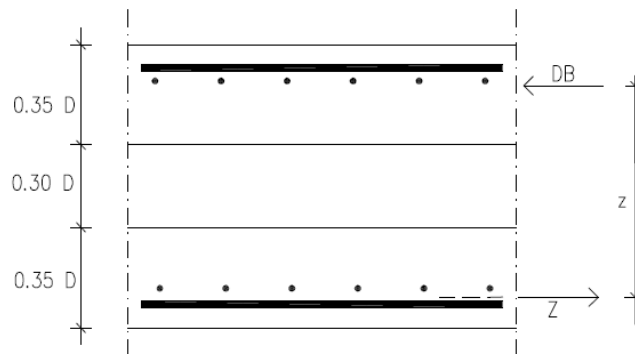
Figure 4.19: Fictitious disks and lever arm for shells [12]

Secondly, the fictive in-plane forces are calculated as half the membrane forces summed up with the moment forces divided by the lever arm, z. As the next step, the principal forces in each layer are calculated together with the angle, α, between the principal forces and the applied reinforcement directions. Then α is used to transform the in-plane forces to equivalent forces in the direction of the reinforcement. The required amount of tensile reinforcement is found by dividing the in-plane forces with f_{yd}.

As the final step, the concrete compression is controlled. In the case of compressive stress in the concrete together with transverse tensile stress, the compression capacity of the concrete is reduced according to the chosen design code. If the concrete can't resist the principal compressive force alone, "BEMESS" offers to apply compression reinforcement. However, compression reinforcement is only allowed if the reinforcement directions at the upper and lower side coincides. This is to guarantee that the full stiffness from the reinforcement at the opposite side can be accounted for. If additional compressive reinforcement is added, the internal lever arm should change due to a higher compression zone; however, this is not automatically adapted in "BEMESS" [12].

The shear control is performed by calculating the principal shear force, v_0, and controlling that it is less than the shear tension capacity, $V_{Rd,c}$, and the shear compression capacity $V_{Rd,max}$, from EC2. If the design shear force $v_0 > V_{Rd,c}$, the user can either add more longitudinal reinforcement, or add shear reinforcement. In the latter case, the required shear reinforcement, assuming perpendicular shear links, is calculated according to EC2 (or chosen code). The shear utilization degree determines the inclination, θ, of the fictive compression struts which is needed in the shear design calculation.

4.5.2   Serviceability Limit State (SLS)

The first SLS check "BEMESS" performs is a control of the minimum thickness of the compression zone. This control is performed in the directions of the principal moments. Since the calculation of the compression zone height requires that the reinforcement area is in the given direction, the reinforcement area gets converted from its original position to the principal direction. It is unclear in the User Manual why this test is performed.

"BEMESS" also offers to control the crack width, both with direct calculations, as in "FEM design", and without direct calculations, as in "DIANA". It is, however, recommended in the manual for "BEMESS" to normally use the crack control without direct calculations.

The SLS stresses, stress range, and fatigue can be controlled in three different ways with different level of simplifications and modifications. The simplest version uses the calculated internal forces directly without iterations. The more complex method finds equilibrium between all the forces, m_{xx}, m_{yy}, m_{xy}, n_{xx}, n_{yy}, n_{xy}, and the corresponding six strains in an iterative way to assure mechanical consistency. The manual doesn't get into detail about each method; hence, this thesis won't either.

Chapter 5

Simple beam example

5.1   Introduction

In order to show the difference between the different procedures in a simple way, a one meter wide plate strip of length 10m is subjected to two equal and symmetric edge moments, M_x=30 kNm. The plate strip is designed for ULS according to the different methods that have been presented in this thesis. For simplicity, all load factors are set to 1.0. An illustration of the beam is shown in Figure 5.1.

The input parameters are:

Concrete C30/37

h = 200 mm

$f_{cd} = 17$ MPa

$E_s = 200$ GPa

$f_{yd} = 434.8$ MPa

Ø = 10 mm (reinforcement diameter)

$c_x = 35$ mm (concrete cover)
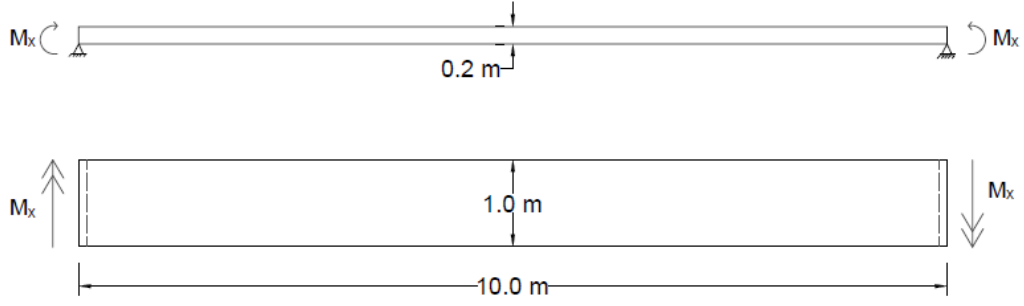
$d_x = 160$ mm (effective height)

Figure 5.1: Simply supported slab subjected to edge moments, M_x. Side view (top) and plan view (bottom)

5.2 Strain compatibility

The plate strip is initially designed using strain compatibility, which was explained in Section 3.2 for design based on the theory of elasticity. The moment capacity of the compression zone is calculated assuming normally reinforced cross section, see Eq. (5.1):

$$M_{Rd} = 0.275 f_{cd} b d^2 = 0.275 \times 17 MPa \times 1000mm \times (160mm)^2 = 119.7\,kNm \qquad (5.1)$$

As the next step, an approximate internal lever arm is calculated from the moment capacity utilization, see Eq. (5.2), where the design moment, M_{Ed}, is equal to the edge moment, $M_x = 30$ kNm.

$$z = \left(1 - 0.17\frac{M_{Ed}}{M_{Rd}}\right)d = \left(1 - 0.17\frac{30kNm}{119.7kNm}\right)160mm = 153.18\,mm \qquad (5.2)$$

Finally, the required reinforcement is found from moment equilibrium of the cross section:

$$A_s = \frac{M_{Ed}}{z \times f_{yd}} = \frac{30 \times 10^6\,Nmm}{153.8mm.8MPa} = \underline{450.4\,mm^2} \qquad (5.3)$$

5.3 The sandwich model

If the plate strip is calculated with the sandwich model, and the thickness of the layers are assumed to be two times the distance from the surface to the reinforcement centre, the in-plane design force in the bottom layer will be:

$$F_{sx} = n_x = \frac{m_x}{z} = \frac{m_x}{h - 2c} \tag{5.4}$$

$$F_{sx} = \frac{30 * 10^6 \, N/mm^2}{200mm - 2 \times 40mm} = 250000.0 \, N \tag{5.5}$$

The required bottom reinforcement in the longitudinal direction will then be:

$$A_s = \frac{F_{sx}}{f_{yd}} = \frac{250000.0 \, N}{434.8 \, MPa} = \underline{575.0 \, mm^2} \tag{5.6}$$

5.4 "FEM design"

The input moments for design in "FEM design" is as follows:

$$m_x = m_\xi = 30 \, kNm/m \tag{5.7}$$

$$m_y = m_\varphi = m_\eta = 0 \, kNm/m \tag{5.8}$$

$$m_{xy} = m_{\xi\varphi} = m_{\xi\eta} = 0 \, kNm/m \tag{5.9}$$

The four possible design moment pairs are then given as shown in Eqs.(5.10)-(5.17):

Case a)

$$\overline{m}_\xi = m_\xi - m_\vartheta \frac{cos\varphi}{1 + cos\varphi} + m_{\xi\vartheta} \frac{1 - 2 \, cos\varphi}{sin\varphi} = m_\xi = 30 \, kNm/m \tag{5.10}$$

$$\overline{m}_\eta = m_\vartheta \frac{1}{1 + cos\varphi} + m_{\xi\vartheta} \frac{1}{sin\varphi} = 0 \, kNm/m \tag{5.11}$$

Case b)

$$\overline{m}_\xi = m_\xi + m_\vartheta \frac{cos\varphi}{1 - cos\varphi} - m_{\xi\vartheta} \frac{1 + 2 \, cos\varphi}{sin\varphi} = m_\xi = 30 \, kNm/m \tag{5.12}$$

$$\overline{m}_\eta = m_\vartheta \frac{1}{1 - cos\varphi} - m_{\xi\vartheta} \frac{1}{sin\varphi} = 0 \, kNm/m \tag{5.13}$$

Case ξ)

$$\overline{m}_\xi = m_\xi - \frac{m_{\xi\vartheta}^2}{m_\vartheta} = 30\,kNm/m \tag{5.14}$$

$$\overline{m}_\eta = 0 \tag{5.15}$$

Case η)

$$\overline{m}_\xi = 0 \tag{5.16}$$

$$\overline{m}_\eta = \frac{m_\xi m_\varphi - m_{\xi\varphi}^2}{m_\xi (sin\varphi)^2 + m_\varphi (cos\varphi)^2 - m_{\xi\varphi} sin2\,\varphi} = 0\,kNm/m \tag{5.17}$$

It is clear that the only possible moment pair is $\overline{m}_\xi = 30$ kNm and $\overline{m}_\eta = 0$ kNm, resulting in reinforcement in the bottom of the plate.

The rest of the calculation of the required bottom reinforcement in ξ direction is shown in Eqs. (5.18)-(5.23):

$$\overline{m}_\xi = f_{cd} \times \lambda x (d - \frac{\lambda x}{2}) \tag{5.18}$$

$$30000\frac{Nmm}{mm} = 17\frac{N}{mm^2} \times \lambda x (160mm - \frac{\lambda x}{2}) \tag{5.19}$$

$$\lambda x = 11.44\,mm \tag{5.20}$$

$$a_{s\xi} = \frac{\lambda x \times \eta \times f_{cd}}{f_{yd}} \tag{5.21}$$

$$a_{s\xi} = \frac{11.44mm \times 1.0 \times 17N/mm^2}{434.8N/mm^2} \tag{5.22}$$

$$a_{s\xi} = 0.4473\,mm^2/mm = \underline{447.3\,mm^2/m} \tag{5.23}$$

The results calculated by the program are shown in Figure 5.2, and correlates well with the results calculated by hand.
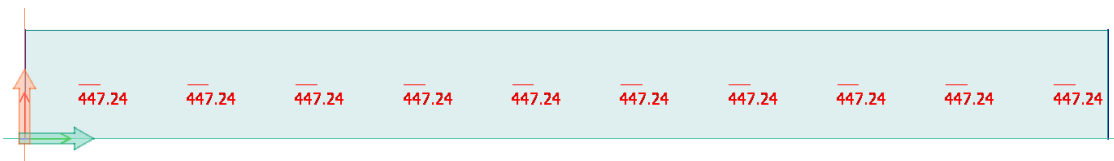

Figure 5.2: Required reinforcement from "FEM design"

5.5 "Robot Structural Analysis"

Since the reinforcement is orthogonal, and the loading is very simple, both the NEN method and the $Wood\&Armer$ method give the same design moment, m_{xd}^*=30 kNm, in the bottom. The stress distribution in the cross section, and hence the internal lever arm, is similar to that of "FEM-design"; consequently, the required bottom reinforcement in the longitudinal direction is also identical.

5.6 "DIANA"

The edge moment M_x=30 kNm gives an imaginary in-plane force of:

$$n_{xx,lo}^{'c} = \frac{m_{xx}^{'}}{z} = \frac{M_x}{0.9d} = \frac{30 * 10^6\,Nmm}{0.9 * 160\,mm} = 208333.3\,N = n_{1,lo}^{'c} \qquad (5.24)$$

This design force gives a required bottom reinforcement of:

$$A_{req,x} = \frac{n_{1,low}^{'c}}{f_{yd}} = \frac{208333.3\,N}{434.8\,N/mm^2} = \underline{479.1\,mm^2} \qquad (5.25)$$

The required reinforcement calculated by "DIANA" is shown in Figure 5.3, and correlates well with the hand calculated value.
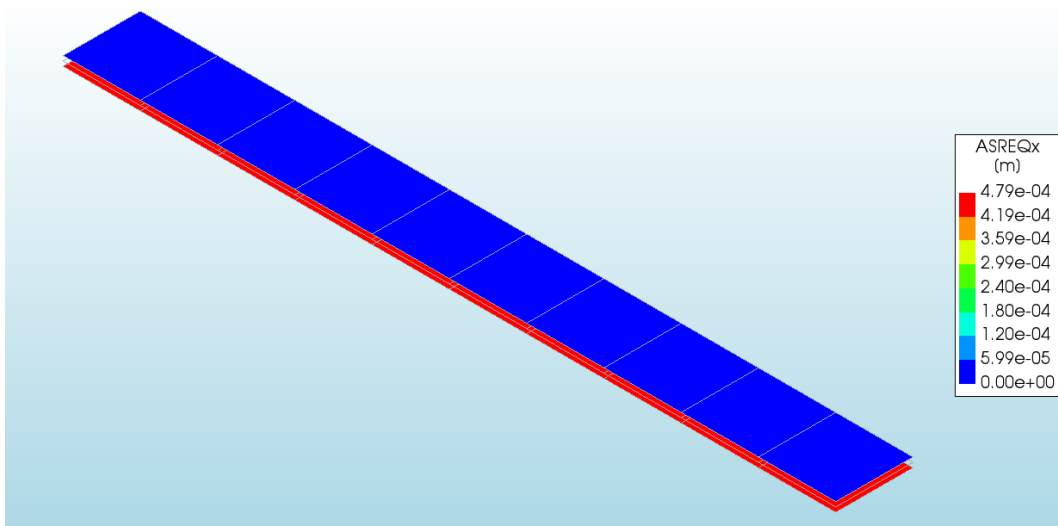

Figure 5.3: Required reinforcement in the longitudinal direction, designed with "DIANA"

5.7 Comparison of the different methods

The required amount of reinforcement for the different models and programs varies significantly. The lowest amount of reinforcement (447.3 mm^2) calculated by "FEM design", deviates more than 20% from the sandwich model (575.0 mm^2). The main reason for the difference is that the models have different values for the internal lever arms. While "FEM design" calculates the internal lever arm with the least possible compression zone height (14.3 mm), the sandwich model assumes the compression zone to be 80 mm, with uniformly distributed compression stress. In the sandwich model the compression stress can be lower than the compression strength, while "FEM design" assumes the compression zone to be fully utilized.

"FEM design" and "Robot" both assume a rectangular stress distribution according to Eurocode 2. Since the models have no restrictions for the steel strain, it might turn out to be very large, see Figure 5.4. With a compression zone height of x=14.3 mm, and the ultimate concrete strain set to 3.5‰, the steel strain in the model will be as high as 35.7‰. In reality, the compression stress would have been distributed over a longer compression zone, and the steel strain would be lower.

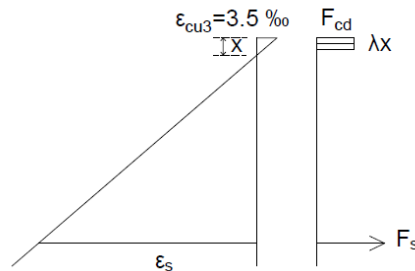Figure 5.4: Possible strain distribution with rectangular stress distribution

In a normally reinforced cross section, as shown in the example with strain compatibility, the maximum allowed steel strain is 5‰. For ULS, the programs and EC2 have no direct limit for the reinforcement strain. For SLS, however, the steel strain is restricted by the maximum allowed deflection of the plate, because large strains give large deflection.

Chapter 6

Discussion and conclusion

This thesis has described and compared several different methods for the modelling and design of concrete plates in finite-element programs. What is important to remember is that the results produced by a program are never of a higher quality than the input from the user ("garbage in – garbage out"). The structural engineer therefore needs to be fully aware of the simplifications that have been made in the modelling process, and the simplifications that have been made in the automatic design calculations in the program.

How the plate should be modelled depends on the given structure and loading, and whether the purpose is to design a new structure or to reproduce a structure that already exists. The parameters that varies are:

- The plate geometry

- The reinforcement directions

- The material parameters for both the concrete and the reinforcement

- The boundary conditions

- The load cases

- The element type

- The mesh

- The stress smoothing method

The most convenient way of modelling supports is normally with pin supports because it is easy, avoids unintended rotational restraints, and gives sufficiently accurate results in the critical section. If, however, the rotational restraint, or the vertical flexibility from the wall or column do have a significant effect on the stresses in the plate, for example on the plate edge, a more complex model should be used. One option is to apply spring supports, where the stiffness has to be carefully calculated. Another option is to simply model the whole wall or column. It is also possible to model the elements over a support as infinitely stiff in order to account for the rotational stiffness from the support. This might, however, lead to too much restraint.

Since linear-elastic material behaviour is assumed, the superposition principle is valid, but unreasonably high stresses may arise in regions where the concrete in reality acts highly non-linear. Such singularity zones are found over column supports, in re-entrant corners, in openings, and at points of concentrated loads. This is normally not a problem since the design forces are found outside of the singularity zone. However, if the actual stress behaviour is of interest, the singularities can often be solved with bedded supports around the singularity.

The automatic design procedures in the different programs mentioned in this thesis have many similarities. First the stress resultants are created and rotated to the directions of the reinforcement. Then, the design moments or imaginary in-plane forces, are calculated. Finally, the required reinforcement is found for the upper and lower plate layer. Whether the program allows the user to apply two or three reinforcement directions varies, and it also varies whether the program allows oblique reinforcement or only orthogonal.

An important difference between the programs is how the calculation procedures define the crack angle. When reinforcement is needed in both directions, an angle of $\frac{\pi}{4}$ gives a minimum amount of required reinforcement and is therefore what most of the programs use. If, however, reinforcement is necessary in only one direction, a crack angle of $\frac{\pi}{4}$ is no longer optimal, and some of the programs (i.e., "FEM design" and "Robot") recalculate the angle in order to minimize the required reinforcement amount. With this approach, the amount of reinforcement decreases compared to an analysis that keep the crack angle

constant at $\frac{\pi}{4}$. To illustrate this, an example was done on a plate element subjected to pure moments (m_x= 20 kNm/m, m_y= -10 kNm/m, and m_{xy}= 5 kNm/m) such that only one reinforcement direction in each layer was necessary. The required reinforcement was calculated according to both "FEM design" and the NEN-method in "Robot". The only important difference in the two methods is that while the NEN-method assumes the crack angle to be $\frac{\pi}{4}$, "FEM design" calculates the optimal crack angle to minimize the reinforcement. The increase in reinforcement amount, for a crack angle of $\frac{\pi}{4}$ compared to an optimal crack angle, for the lower and upper plate layer, was as much as 11% and 34%, respectively. It should be noted that a crack angle that gives a minimum amount of reinforcement isn't necessarily desired if the first cracks develop in an angle far from the design crack angle. The rotation of the crack in such situations involve large deformation; hence, the cracks become large.

Another difference that highly influences the results is the difference in internal lever arms which affects the efficiency of the reinforcement. A longer internal lever arm will give a more efficient reinforcement. If rectangular stress distribution is assumed (as in "FEM design" and "Robot"), a long internal lever arm is possible, provided the compression zone is very small. If a simply supported, 200 mm high beam is subjected to an edge moment of 30 kNm, the internal lever arm is 154.3 mm (assuming rectangular stress distribution). If, however, the steel strain is limited to a maximum value of 5‰, the internal lever arm is 153.2 mm. In "DIANA", the lever arm is the effective height, d, multiplied by a relative compression zone height of 0.9 (as default). Applied to the beam example, "DIANA" gives a lever arm of 144.0 mm. The shortest lever arm (140 mm) is obtained with the sandwich model assuming cracked concrete in the outer layers. In the beam example, the lowest lever arm gives about 20 % more reinforcement than the longest one. Figure 6.1 gives an overview of the different stress distributions, and the internal lever arms that are used by the different models. All of the models from the commercial software have in common that there is no direct limit for the reinforcement strain for the Ultimate Limit State (ULS). The deflection criteria in the Serviceability Limit State (SLS) will, however, limit the steel strain. Which of the models that give the most accurate results depend on the loading and the real compression stress distribution for each case.
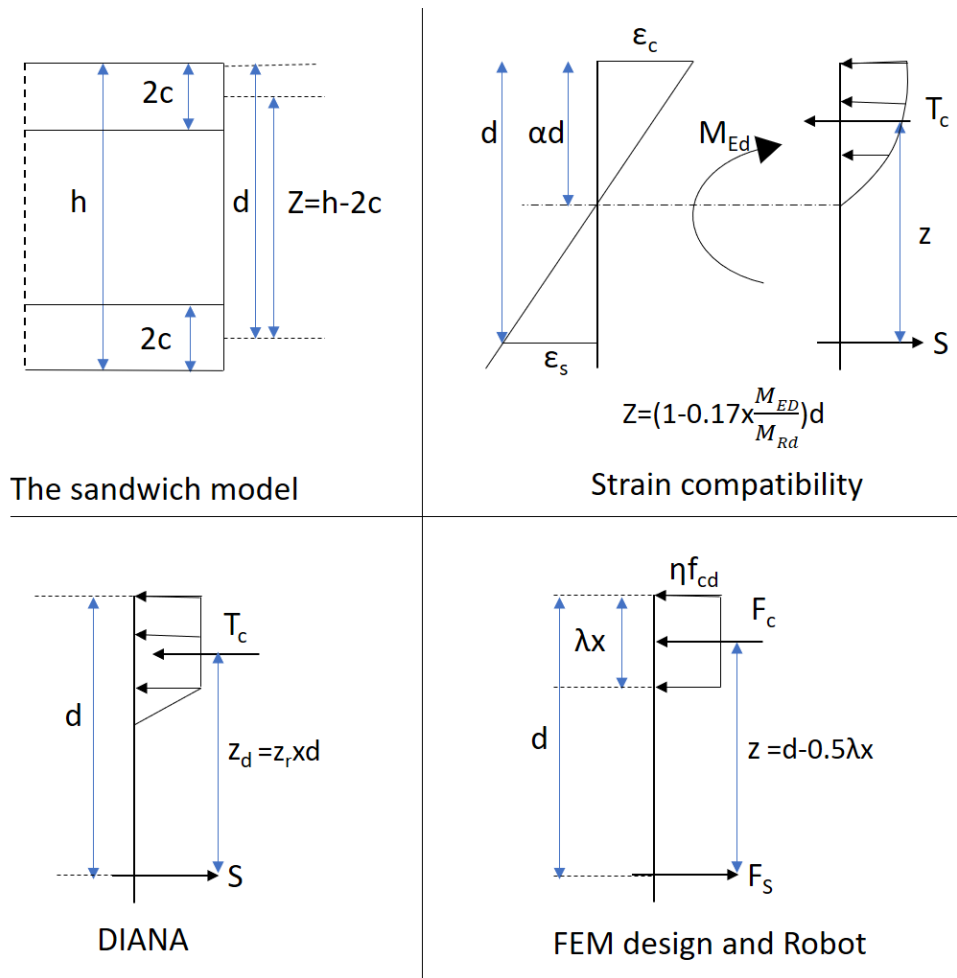
$$Z=(1-0.17x\frac{M_{ED}}{M_{Rd}})d$$

Figure 6.1: Different models for stress distribution give different internal lever arms

In SLS it is important to account for the cracking of concrete. This is done either by changing the stiffness locally for elements with too high stresses, or changing the stiffness of the entire plate in order to obtain a smooth displacement field. The crack width control is done with one of the following two methods:

- Direct calculation: The actual crack width is calculated, and controlled against the maximum allowed value from the design code

- Indirect calculation: The reinforcement diameter and spacing is controlled according to maximum values from tables in the design code.

While direct calculation gives more accurate results, indirect calculation saves computational time, and is usually a sufficiently accurate estimate.

Bibliography

[1] Concrete bridge - Lutjegast (Holland). `http://www.bartels-global.com/projects/concrete-bridge-lutjegast-holland`. [Online; accessed 29.04.2017].

[2] `http://en.grupogic.mx/precast-concrete-slabs/`. [Online; accessed 23.05.2017].

[3] Blaauwendraad, J. *Plates and FEM: Surprises and Pitfalls.* Springer, 2010.

[4] Mathisen, K.M. Lecture notes from the course "The Finite Element Method Introduction and Fundamental Concepts" at NTNU, 2015.

[5] Rombach, G.A. *Finite-element Design of conrete structures. Practical problems and their solutions.* ICE Publishing, second edition, 2004.

[6] Pacoste, C., Plos, M., and Johansson, M. Recommendations for finite element analysis for the design of reinforced concrete slabs. Technical report, KTH Royal Institute of Tchnology, 2012. 52.

[7] Engen, M. Lecture notes from the course "Concrete structures 3" at NTNU , 2016.

[8] *EN 1992-1-1 Eurocode 2: Design of concrete structures - Part 1-1: General rules and rules for buildings*, Brussels, 2004. CEN.

[9] FEM-Design, Applied Theory and Design. `http://download.strusoft.com/FEM-Design/inst110x/theory.pdf`. [Online; accessed 13.03.2017].

[10] DIANA - Finite Element Analysis User's Manual release 10.1 Theory . `https://dianafea.com/manuals/d101/Diana.html`. [Online; accessed 15.03.2017].

[11] User's guide-robot structural analysis professional software. `http://help.autodesk.com/view/RSAPRO/2017/ENU/?guid=` `GUID-FF347447-519A-4A03-B3DC-2CDB5A6BE028`. [Online; accessed 05.04.2017].

[12] SOFiSTiK AG. *BEMESS-Design of Plates and Shells, SOFiSTiK 2016*, 2016.

[13] Hughes, T.J.R. *The Finite Element Method*. Englewood Cliffs, 1987.

[14] Nielsen, M.P. and Hoang, L.C. *Limit Analysis and Concrete Plasticity*. CRC Press, third edition, 2011.

[15] FEM Modeling: Mesh, Loads and BCs. `http://www.colorado.edu/` `engineering/CAS/courses.d/IFEM.d/IFEM.Ch07.d/IFEM.Ch07.pdf`. [Online; accessed 07.03.2017].

[16] Øverli, J.A. Formula sheet from the course "Concrete structures 1" at NTNU , 2015.

[17] Katili, I. A new discrete kirchhoff-mindlin element based on mindlin–reissner plate theory and assumed shear strain fields—part ii: An extended dkq element for thick-plate bending analysis. *International Journal for Numerical Methods in Engineering*, 136, 1993.

[18] Wood, R.H. *The reinforcement of slabs in accordance with a pre-determined field of moments*. Garston, Eng. : Building Research Station, 1968.

[19] Vecchio, F. J. and Collins, M. P. . Compression response of cracked reinforced concrete. *Journal of Structural Engineering*, 119, 1993.

[20] JSCE. Standard specifications for concrete structures - 2012 "design". Technical report, Japan Society of Civil Engineers, 2012.

Appendices

Appendix A

Design with "DIANA"

In 2016, "DIANA" introduced "DIANA Interactive Environment" ("DIANA IE"), a new graphical user interface where it is possible to do the modelling, design, and post-processing without programming. Because the program is relatively new, there is limited information, forums and tutorials online, and few colleagues to ask. This appendix is therefore going to describe the main steps for performing the design of a simple beam/plate strip. The same plate strip as was used in the example in Chapter 5 will be used here.

First, the geometry of the beam is defined, and assigned material and geometrical properties. This includes defining the element type, which should be set to Q20SH for design analysis. The Q20SH element, shown in Figure 1.1, is a four-node quadrilateral isoparametric curved shell element [10].
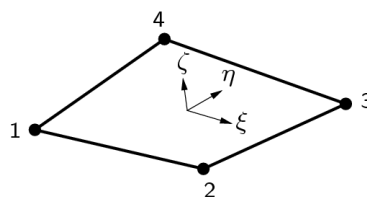
Figure 1.1: Q20SH element [10]

After the concrete beam is assigned properties, the reinforcement layers should be defined with the same corner coordinates as the beam, but with z-coordinates corresponding to the height of the top- and bottom reinforcement layer. For a beam in bending, one reinforcement layer is sufficient, but for the sake of illustration, both the top- and

bottom layer is included here. When the layers are assigned reinforcement properties, it is important that both the element geometry, and the material property for the reinforcement is marked for design as illustrated in Figure 1.2; otherwise, the design check analysis is unable to run.
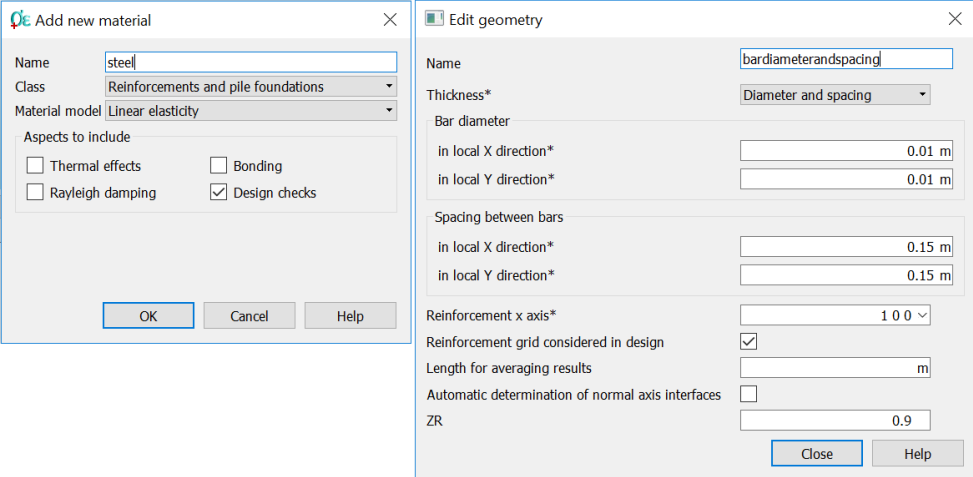

Figure 1.2: Material and geometrical properties for the reinforcement

After this, the geometry tool bar at the left side of the display window should look like Figure 1.3- 1.5.
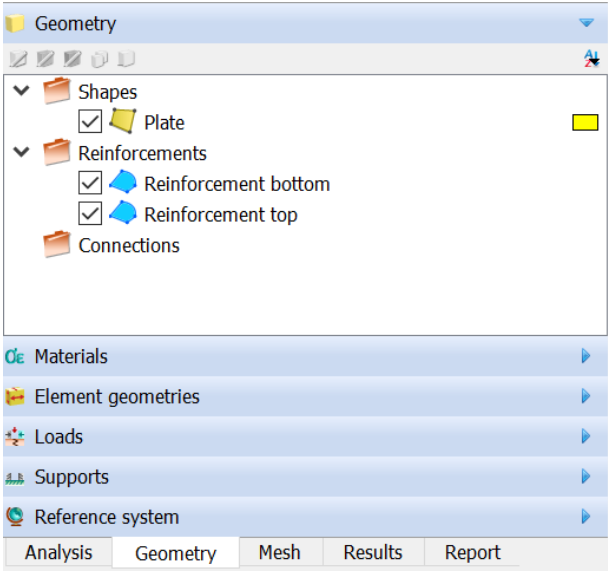

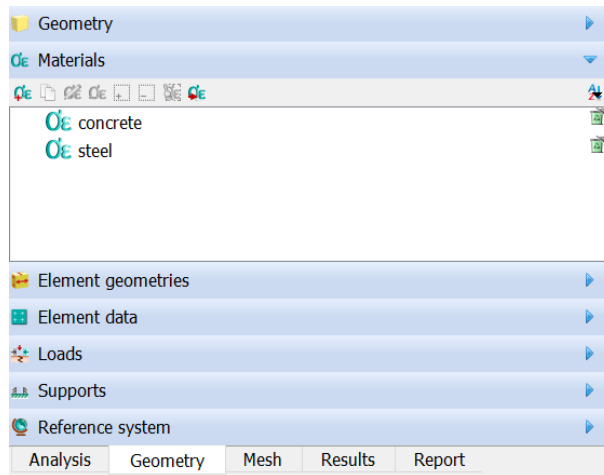
Figure 1.3: The geometry tool bar: Geometry
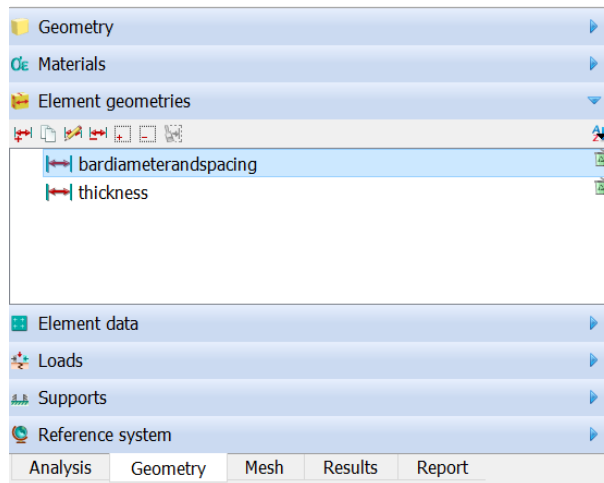
Figure 1.4: The geometry tool bar: Materials

Figure 1.5: The geometry tool bar: Element geometries

The loads, supports, and units can be defined straight forward, and the geometry tool bar should look like Figure 1.6-1.8. The final model can be seen in Figure 1.9.
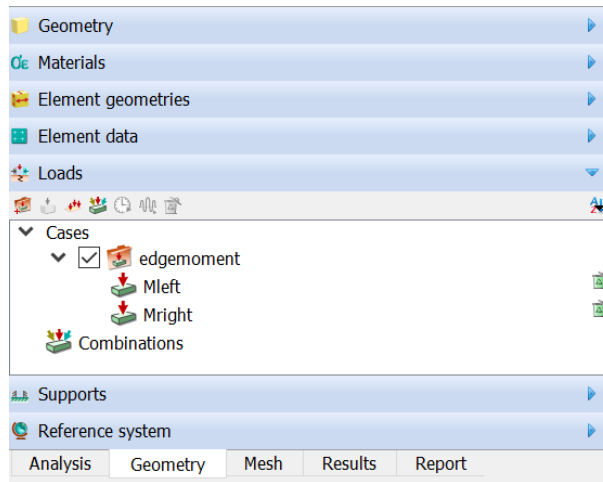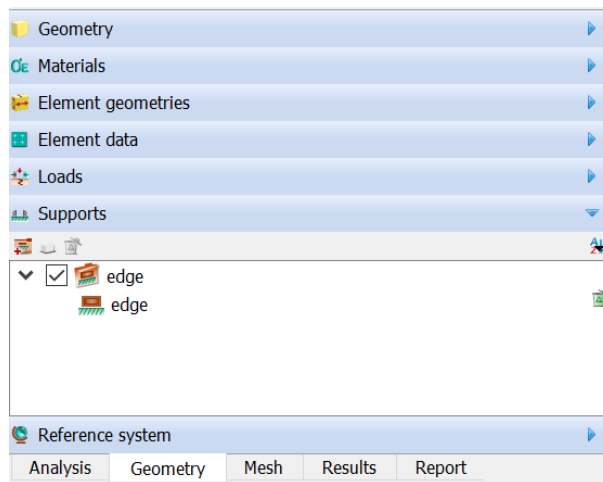
Figure 1.6: The geometry tool bar: Loads

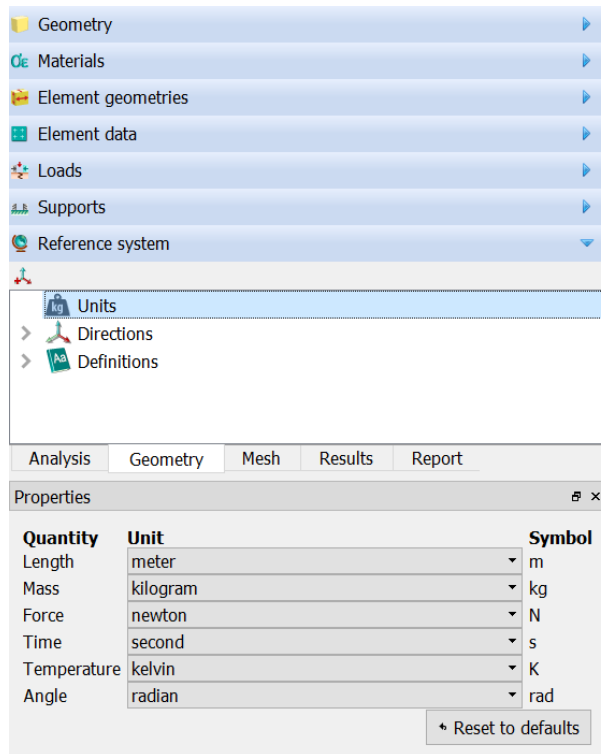Figure 1.7: The geometry tool bar: Supports

Figure 1.8: The geometry tool bar: Reference systems
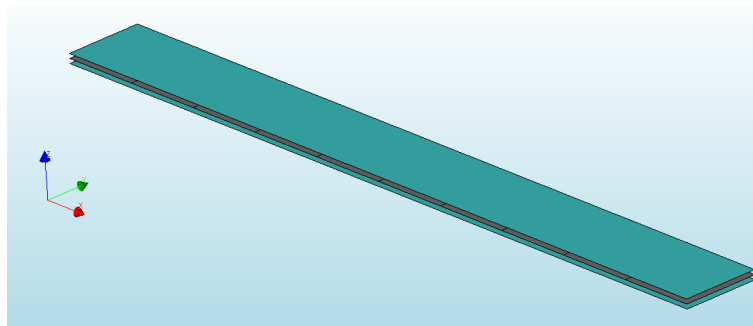
Figure 1.9: Final model of the simple beam

The model is now ready for the analysis. First, a new analysis has to be created. Then, the commands "Structural Linear Static", and "Design check" have to be selected, as illustrated in Figure 1.10.
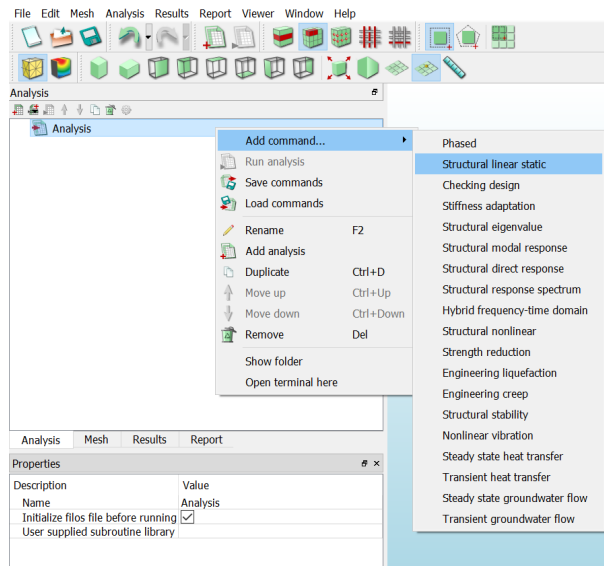
Figure 1.10: Add a new analysis

The final step is to define the required reinforcement as output for the design check. In the properties for the output, a load set and a limit state needs to be defined. This is illustrated in Figure 1.11- 1.13.
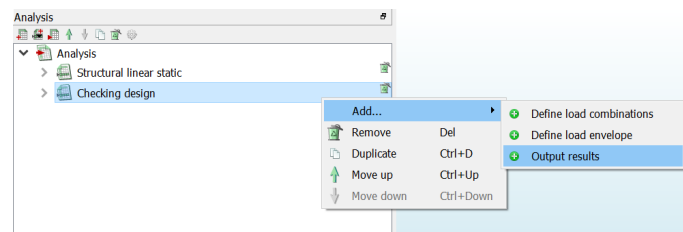
Figure 1.11: Add a new output
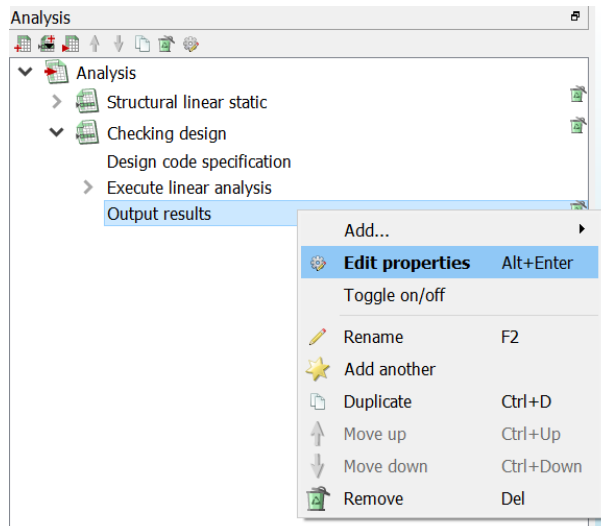
Figure 1.12: Edit properties of the output
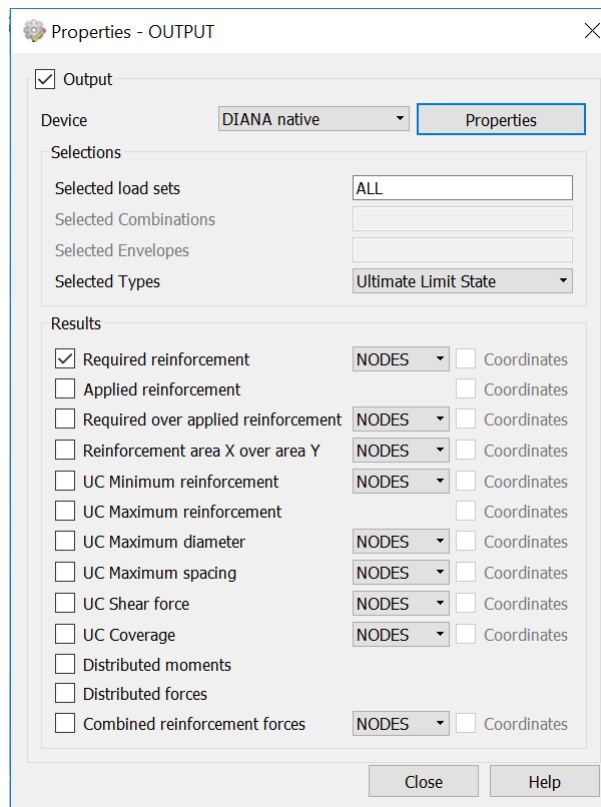
Figure 1.13: Output properties

When "DIANA 10.1" was used in this master thesis, the software failed to export some of the commands, like the units-table, from the "DIANA IE" to the actual code, so it had to be inserted manually. The final code for the model is therefore attached below:

```
: Diana Datafile written by Diana 10.1
'UNITS'
        LENGTH M
        MASS KG
        FORCE N
        TEMPER CELSIU
        ANGLE RAD
'DIRECTIONS'
   1   1.00000E+00   0.00000E+00   0.00000E+00
   2   0.00000E+00   1.00000E+00   0.00000E+00
   3   0.00000E+00   0.00000E+00   1.00000E+00
'MODEL'
  GRAVDI 3
  GRAVAC  -9.81000E+00
'COORDINATES'
   1   1.00000E+01   1.00000E+00   0.00000E+00
   2   1.00000E+01   0.00000E+00   0.00000E+00
   3   0.00000E+00   0.00000E+00   0.00000E+00
   4   0.00000E+00   1.00000E+00   0.00000E+00
   5   1.00000E+00   0.00000E+00   0.00000E+00
   6   2.00000E+00   0.00000E+00   0.00000E+00
   7   3.00000E+00   0.00000E+00   0.00000E+00
   8   4.00000E+00   0.00000E+00   0.00000E+00
   9   5.00000E+00   0.00000E+00   0.00000E+00
  10   6.00000E+00   0.00000E+00   0.00000E+00
  11   7.00000E+00   0.00000E+00   0.00000E+00
  12   8.00000E+00   0.00000E+00   0.00000E+00
  13   9.00000E+00   0.00000E+00   0.00000E+00
  14   9.00000E+00   1.00000E+00   0.00000E+00
  15   8.00000E+00   1.00000E+00   0.00000E+00
  16   7.00000E+00   1.00000E+00   0.00000E+00
  17   6.00000E+00   1.00000E+00   0.00000E+00
  18   5.00000E+00   1.00000E+00   0.00000E+00
  19   4.00000E+00   1.00000E+00   0.00000E+00
  20   3.00000E+00   1.00000E+00   0.00000E+00
  21   2.00000E+00   1.00000E+00   0.00000E+00
  22   1.00000E+00   1.00000E+00   0.00000E+00
  23   1.00000E+01   1.00000E+00   6.00000E-02
  24   1.00000E+01   0.00000E+00   6.00000E-02
  25   0.00000E+00   0.00000E+00   6.00000E-02
  26   0.00000E+00   1.00000E+00   6.00000E-02
  27   1.00000E+01   1.00000E+00  -6.00000E-02
  28   1.00000E+01   0.00000E+00  -6.00000E-02
  29   0.00000E+00   0.00000E+00  -6.00000E-02
  30   0.00000E+00   1.00000E+00  -6.00000E-02
'MATERI'
   1 NAME    "concrete"
     MCNAME CONCDC
     MATMDL EN1992
     ASPECT TOTCRK
     CONCRE EN1992
     WEIGCC NORMAL
     CLASS  "C30/37"
     AGGTYP QUARTZ
```

```
      CEMTYP N
      CRACKN
      PLASTN
      TOTCRK ROTATE
      TENCRV BRITTL
      COMCRV EC2
      POIRED DAMAGE
      YOUN28    3.28366E+10
      POISON    2.00000E-01
      THERMX    1.00000E-05
      DENSIT    2.40000E+03
      TENSTR    2.89647E+06
      COMSTR    3.80000E+07
    2 NAME    "steel"
      MCNAME REINFO
      MATMDL LINEAR
      YOUNG     2.10000E+11
      ASPECT DESIGN
      YLDSTR    4.34800E+08
'GEOMET'
    1 NAME    "thickness"
      GCNAME SHEET
      GEOMDL FLASHL
      KFAC      1.50000E+00
      XAXIS     1.00000E+00    0.00000E+00    0.00000E+00
      THICK     2.00000E-01
    2 NAME    "diameterandspacing"
      GCNAME RSHEET
      GEOMDL REGRID
      XAXIS     1.00000E+00    0.00000E+00    0.00000E+00
      DESIGN
      PHI       1.00000E-02    1.00000E-02
      SPACIN    1.50000E-01    1.50000E-01
      ZR        9.00000E-01
'DATA'
    1 NAME    "Element data 1"
'ELEMENTS'
 SET   "Plate"
  CONNECT
    1 Q20SH  2 1 14 13
    2 Q20SH  13 14 15 12
    3 Q20SH  12 15 16 11
    4 Q20SH  11 16 17 10
    5 Q20SH  10 17 18 9
    6 Q20SH  9 18 19 8
    7 Q20SH  8 19 20 7
    8 Q20SH  7 20 21 6
    9 Q20SH  6 21 22 5
   10 Q20SH  5 22 4 3
  MATERIAL 1
  GEOMETRY 1
  DATA 1
'REINFORCEMENTS'
  SET   "Reinforcement top"
```

109

```
   LOCATI
    1 GRID
      PLANE  24 23 26 25
   MATERIAL 2
   GEOMETRY 2
   DATA 1
   SET  "Reinforcement bottom"
   LOCATI
    2 GRID
      PLANE  28 27 30 29
   MATERIAL 2
   GEOMETRY 2
   DATA 1
'LOADS'
   CASE 1
   NAME "edgemoment"
   ELEMEN
   10   EDGE   ETA2
        MOMENT   3.00000E+04
        DIRECT 2
   1    EDGE   ETA1
        MOMENT  -3.00000E+04
        DIRECT 2
'SUPPOR'
   NAME "edge"
   / 1-4 / TR 3
'END'
```